GEORGIA DOT RESEARCH PROJECT 16-11

FINAL REPORT

DEVELOPMENT OF GEOSYNTHETIC DESIGN AND CONSTRUCTION GUIDELINES FOR PAVEMENT EMBANKMENT CONSTRUCTION IN NORTH GEORGIA

OFFICE OF PERFORMANCE-BASED MANAGEMENT AND RESEARCH
15 KENNEDY DRIVE
FOREST PARK, GA 30297-2534

1. Report No.: FHWA-GA-19-1611	2. Government Accession No.:	3. Recipient's Catalog No.:
4. Title and Subtitle: Development of Geosynthetic Design and Construction Guidelines for Pavement Embankment Construction in North Georgia		5. Report Date: January 2019 6. Performing Organization Code:
7. Author(s): S. Sonny Kim, Ph.D., P.E., J. David Frost, Ph.D., P.E., Stephan A. Durham, Ph.D., P.E., Mi G. Chorzepa, Ph.D., P.E., Jason Wright, and Sangy S. Hanumasagar		8. Performing Organization Report No.: 16-11
9. Performing Organization Name and Address: University of Georgia, College of Engineering Driftmier Engineering Center, Athens, GA 30602 Phone: (706) 542-9804, Email: kims@uga.edu		10. Work Unit No.: 11. Contract or Grant No.: PI# 0015117
12. Sponsoring Agency Name and Address: Georgia Department of Transportation Office of Performance-Based Management and Research 15 Kennedy Drive, Forest Park, GA 30297-2534		13. Type of Report and Period Covered: Final; May 2016 – Jan. 2019 14. Sponsoring Agency Code:
15. Supplementary Notes: Prepared in cooperation with the U.S. Department of Transportation, Federal Highway Administration.		

16. Abstract:

Geosynthetics are becoming a popular alternative for soil improvement in highway construction to achieve enhanced performance in regions with soft problematic soils or to reduce aggregate base layer thickness to decrease construction costs. Subgrade soil improvement in a geosynthetic-reinforced pavement system is achieved by lateral distribution of vertical stresses at the reinforcing layer, through the tensile properties of the geosynthetic material, which is hard to measure with small-scale triaxial tests. Therefore, it is desirable to conduct large-scale testing to more accurately monitor the behavior of aggregate and soils under rolling wheel loadings when geosynthetic is present.

The current study seeks to verify the behavior of geosynthetic-reinforced pavement systems through large-scale and bench-scale rolling wheel tests performed with problematic subgrade soils found in North Georgia. Large-scale and bench-scale specimens that mimic an aggregate base–geosynthetics–subgrade system were constructed at different subgrade soil conditions. Subgrades were constructed at a moisture content to produce a low California bearing ratio (CBR) or at optimum moisture content (OMC) during specimen preparation. Both an extruded biaxial geogrid and woven geotextile were placed at various locations in the aggregate base layer to investigate the optimal placement location for the different subgrade conditions. Pressure sensors were installed near the bottom of the aggregate base layer and near the top of the subgrade layer to monitor the vertical stress variations within the pavement system during trafficking. For large-scale testing, light weight deflectometer (LWD) and dynamic cone penetrometer (DCP) measurements were taken post-trafficking to determine the effects of the geosynthetics on the stiffness increase of pavement foundation layers.

The results of this research indicate the effects of different subgrade conditions, geosynthetic reinforcement type, and geosynthetic placement location on the pressure experienced by pavement layers and the changes in stiffness of the aggregate base course.

17. Keywords: Continuously Reinforced Concrete Pavement, Ground Penetration Radar, Eddy Current Technique, Condition Assessment	18. Distribution Statement:		
19. Security Classif. (of this report): Unclassified	20. Security Classification (of this page): Unclassified	21. No. of Pages: 174	22. Price:

Form DOT 1700.7 (8-69)

GDOT Research Project No. 16-11

Final Report

Development of Geosynthetic Design and Construction Guidelines for Pavement Embankment Construction in North Georgia

By

S. Sonny Kim, Ph.D., P.E., F.ASCE
Associate Professor

J. David Frost, Ph.D., P.E., F.ASCE
Eliz. and Bill Higginbotham Professor

Stephan A. Durham, Ph.D., P.E.
Associate Professor

Sangy S. Hanumasagar
Graduate Research Assistant

Mi G. Chorzepa, Ph.D., P.E.
Associate Professor

School of Civil & Envir. Engineering
Georgia Institute of Technology

Jason Wright
Graduate Research Assistant

Civil Engineering, College of Engineering
University of Georgia

Contract with

Georgia Department of Transportation
In cooperation with
U.S. Department of Transportation
Federal Highway Administration

January 2019

TABLE OF CONTENTS

Page

LIST OF TABLES

LIST OF FIGURES

EXECUTIVE SUMMARY

Geosynthetics are becoming a popular alternative for soil improvement in highway construction to achieve enhanced performance in regions with soft, problematic soils or to reduce aggregate base layer thickness in order to decrease construction costs. Subgrade soil improvement in a geosynthetic-reinforced pavement system is achieved by lateral distribution of vertical stresses at the reinforcing layer, through the tensile properties of the geosynthetic material, which are hard to measure with small-scale triaxial tests. Therefore, it is desirable to conduct large-scale testing to more accurately monitor the behavior of aggregate and soils under rolling wheel loadings when geosynthetic is present.

This study seeks to verify the behavior of geosynthetic-reinforced pavement systems through large-scale and bench-scale rolling wheel tests performed with problematic subgrade soils found in North Georgia. Large-scale and bench-scale specimens that mimic an aggregate base–geosynthetics–subgrade system were constructed at different subgrade soil conditions. Subgrades were constructed at a moisture content to produce a low California bearing ratio (CBR) or at optimum moisture content (OMC) during specimen preparation. Both an extruded biaxial geogrid and woven geotextile were placed at various locations in the aggregate base layer to investigate the optimal placement location for the different subgrade conditions. Pressure sensors were installed near the bottom of the aggregate base layer and near the top of the subgrade layer to monitor the vertical stress variations within the pavement system during trafficking. For large-scale testing, light weight deflectometer (LWD) and dynamic cone penetrometer (DCP) measurements were taken post-trafficking to determine the effects of the geosynthetics on the stiffness increase of pavement foundation layers. From a matched t-test statistical

analysis, with a 95% confidence, the mean pressure experienced at the bottom of the aggregate layer and at the top of the subgrade layer is expected to decrease between (6.63%, 23.94%) and (6.07%, 31.61%), respectively, when using a geosynthetic. The results of this research indicate the effects of different subgrade conditions, geosynthetic reinforcement type, and geosynthetic placement location on the pressure experienced by pavement layers and the changes in stiffness of the aggregate base course.

ACKNOWLEDGEMENTS

The research team gratefully acknowledges the financial support for this work provided by the Georgia Department of Transportation (GDOT). The authors thank the many GDOT personnel who assisted with this study, particularly Mr. David Jared, P.E.; Mr. Binh Bui; Dr. Moussa Issa; and Mr. Ian Rish, P.E., for their research support and valuable input. Special thanks to Mr. Brennan Roney, who advised the research team in successfully performing the study. Finally, the authors thank Mr. Bruce Lacina from Tencate Geosynthetics Americas and Dr. Mark Wayne from Tensar International Corporation for their technical assistance and geosynthetics materials support.

1. INTRODUCTION

1.1 Background and Problem Statement

The soil support value (SSV) is currently used by the Georgia Department of Transportation (GDOT) as a design parameter that serves as an index of the relative ability of a soil to support the applied traffic loads. The SSV is a normalized parameter correlated with the resilient modulus or California bearing ratio (CBR) of a soil and is obtained from historical research of similar projects in the region, field visits, soil borings, and/or laboratory tests and analysis. GDOT uses a chart correlating soil CBR to SSV. Typical SSV values in Georgia range from 2.0 to 4.5. Higher SSVs indicate stronger subgrade soils with higher support characteristics, while lower SSVs are expected to have lower support capabilities.

Areas in North Georgia are well-known for having subgrade soil with SSVs ranging from 2.0 to 3.0, which commonly consist of fine-grained soils. In general, soil found above the fall line (an imaginary line running from Augusta to Columbus, Georgia, separating the coastal plain from the Piedmont region) typically has soil support values from 2.0 to 3.0. Below the fall line, SSVs range from 3.0 to 4.5. Because of the differences in the geological formation of the areas, North Georgia soils are typically weaker. Figure 1.1 shows GDOT's SSV map.

GDOT currently uses the AASHTO *Interim Guide for the Design of Pavement Structures 1972* to design flexible pavements across the state. The SSV is an input to calculate design traffic loadings (W_{18}) in the 1972 AASHTO flexible pavement design equation. This SSV is influential on the calculation of support capabilities for the flexible pavement. For larger construction projects, GDOT typically performs testing in order to

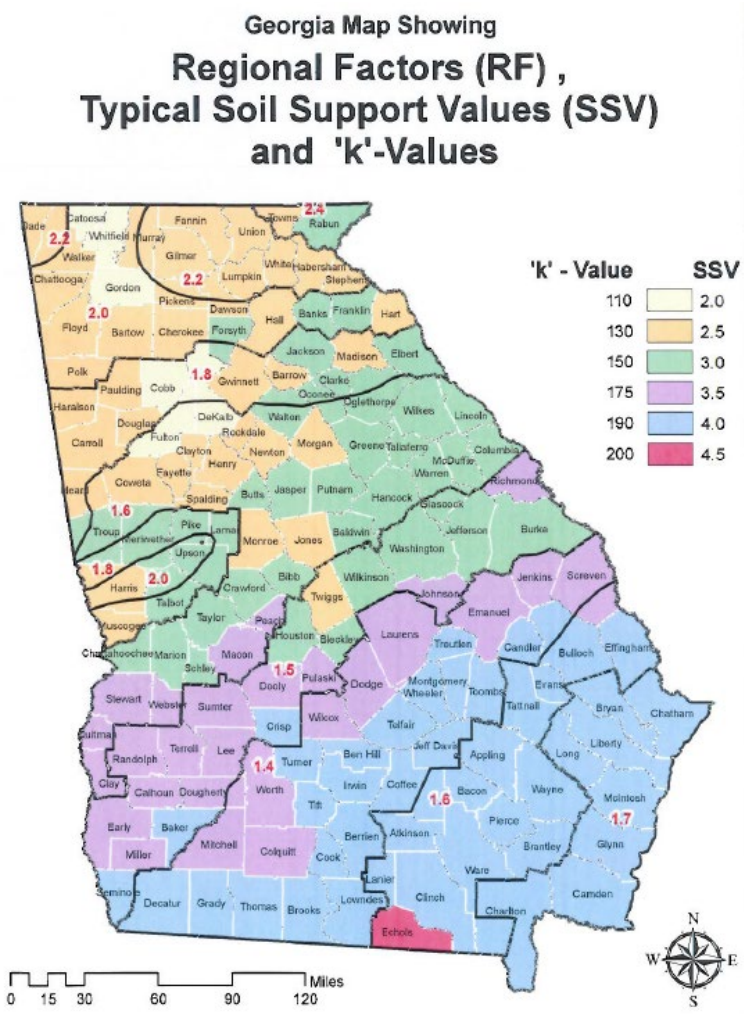

FIGURE 1.1

GDOT Soil Support Value Map (GDOT, 2013)

confirm historical data of SSVs. For smaller projects, designers usually determine values from a map that delineates SSV and regional factors across the state, shown in Figure 1.1.

Subgrade soil is the topmost material underneath pavement structures. Pavement strength is dependent on the subgrade soil properties; therefore, it is vital to maintain a good subgrade condition to ensure stability. In order for prepared subgrade to be stable, it must have particular strength and deformation characteristics. Specific subgrade properties such as high moisture and high silt content are more likely to be unstable and exhibit

excessive rutting (IDOT, 2005). In order for pavements to have a long and effective design life, they must have a stable subgrade. Different solutions have been developed to combat weak subgrades, including removal of unsuitable soils, remediation techniques such as mixing of soil and cement for strength, and placement of geosynthetics in the pavement system.

It is known that geosynthetics reinforcement is a viable alternative to stabilize subgrade in highway pavement construction in regions with soft, problematic subgrade soils. Geosynthetics are typically marketed as having the ability to either increase the pavement design life through an enhanced load distribution over underlying weak subgrade or as a cost-saver to reduce the aggregate base thickness while maintaining the same number of design equivalent single axle loads (ESALs) as traditional pavement systems. Geosynthetics can provide these benefits through reinforcing pavement layers that help prevent excessive rutting. Another benefit is their ability to provide separation between the base and subgrade layers. Most of the native soils in North Georgia contain high silt or clay percentages that increase the potential for localized bearing failures due to the fines migration from the subgrade into the base course layers when no separation exists. As the fine material migrates and mixes with the base course, a decrease in the structurally sound base course thickness occurs, in addition to a lowered density of the subgrade, and thereby decreases the pavement structural number (SN). A 19% loss of base course results in a 50% reduction in load-carrying capacity when using the AASHTO 1993 flexible pavement design method (Lacina et al., 2015).

There have been various studies investigating the effects of adding geosynthetics to flexible pavements with varying results. In 2008, the Federal Highway Administration

(FHWA) published an updated reference manual for geosynthetic design and construction guidelines (Holtz et al., 2008). Guidelines are provided in that manual for geosynthetic applications for soil with different CBR values. The manual provides a general procedure for using a geosynthetic in roadway design and is used as a template for engineers to input region-specific material properties and geosynthetic product types to calibrate the design process.

Three different soil samples from North Georgia (i.e., from Coweta, Hall, and Gordon Counties) with SSVs ranging from 2.0 to 2.5 are evaluated in this study with two different types of geosynthetics placed in pavement systems in order to calibrate and validate the FHWA method to determine the benefits of using geosynthetics in GDOT roadways. To quantify the reduction in vertical soil pressure distribution in geosynthetics-reinforced pavement systems over problematic soils, a large-scale testing apparatus was fabricated and installed at the University of Georgia's STRuctural ENGineering Testing Hub (STRENGTH Laboratory). In addition, a bench scale laboratory rutting test apparatus has been developed at the Sustainable Geosystems Systems Laboratory at the Georgia Institute of Technology. The information obtained with the large-scale and bench-scale systems were used to investigate potential correlations between the soil behavior and physical properties including liquid limit, percentage fines, and undrained shear strength. These correlations will ultimately aid the Georgia Department of Transportation (GDOT) in improving design guidelines and incorporating geogrids in pavements. This report highlights efforts in the development of rutting simulator systems at both universities and presents test results from the large-scale and bench-scale systems.

1.2 Objectives

This study uses both large-scale and bench-scale rolling wheel testing apparatus to assess the benefits of using geosynthetics in pavement foundation. The results of the experimental testings performed through this study are used to:

1) properly identify and evaluate potential applications of geosynthetics in problematic soils; and
2) assist roadway engineers in determining ideal locations and types of geosynthetics by providing a geosynthetic selection guide suitable for Georgia's soil conditions, which results in extended service life of pavements and future cost savings.

This study investigates the performance of geosynthetic-reinforced pavement foundations with strong and weak subgrade conditions. Since the effectiveness of the geosynthetics is dependent on subgrade strength, it was advantageous to provide a range of subgrade conditions to investigate their effects on load distribution. Three different soil types were obtained from areas in North Georgia.

Additionally, the subgrade was prepared at different moisture conditions (optimum and high moisture contents) to investigate the effects of the geosynthetics on the behavior of pavement foundation under moving wheel loadings. The placement location of the geosynthetic was varied to analyze its influence on load distribution. Ultimately, the research findings provide practical guidelines for the application of geosynthetics to state agencies and practitioners. This report includes guidance on the use of geosynthetics for

pavement embankment construction in order to extend the service life and reduce the maintenance and rehabilitation costs of pavements.

2. LITERATURE REVIEW

2.1 Behavior and Load Distribution Mechanism of Pavement Foundations under Traffic Loadings

Flexible pavement provides support for traffic loadings through several structural layers of selected materials to gradually distribute loads from the pavement surface to the underlying layers. A suitable pavement design allows the expected traffic loading to be transmitted and dispersed downward so that each successive layer's load-bearing capacity is not exceeded (Mishra, 2016). Flexible pavement systems generally consist of a top layer of hot mix asphalt (HMA) ranging from 3 to 6 in. (76 to 152 mm), a base course layer typically ranging from 4 to 12 in. (102 to 305 mm), and a bottom subgrade layer (Mishra, 2016). Typically, flexible pavement layers are stronger on top where the intensity of stress is high and weaker near the bottom where the intensity has decreased. The use of each layer of flexible pavement can be modified or omitted based on necessity or economic purpose (Huang, 2012). The stress distributed to a given subgrade can be decreased by increasing the thickness of overlying layers. Figure 2.1 shows the difference in stress induced on the subgrade layer with thick and thin pavement layers. It shows that the thicker the overlying materials in a pavement system, the higher the area of stress distribution to the subgrade layer, which decreases the strength required to prevent failures.

The HMA layer typically is made up of two different lifts and occasionally a seal coat on the surface. The seal coat is the surficial treatment to prevent water from penetrating into the surface. The top lift is a surface course or wearing course and consists of a densely graded HMA, which is generally 9.5 mm (3/8 in.) or 12.5 mm (1/2 in.) nominal maximum aggregate size (NMAS). Its purpose is to prevent distortion or deformation under traffic

while providing a smooth riding quality. The intermediate lift of the HMA mixture is the binder mixture, which is composed of 19 mm (¾ in.) NMAS, while the bottom lift is referred to as the base mixture and consists of larger aggregates and less asphalt (i.e., 25 mm or 1 in. NMAS) resulting in a more economical design (Huang, 2012).

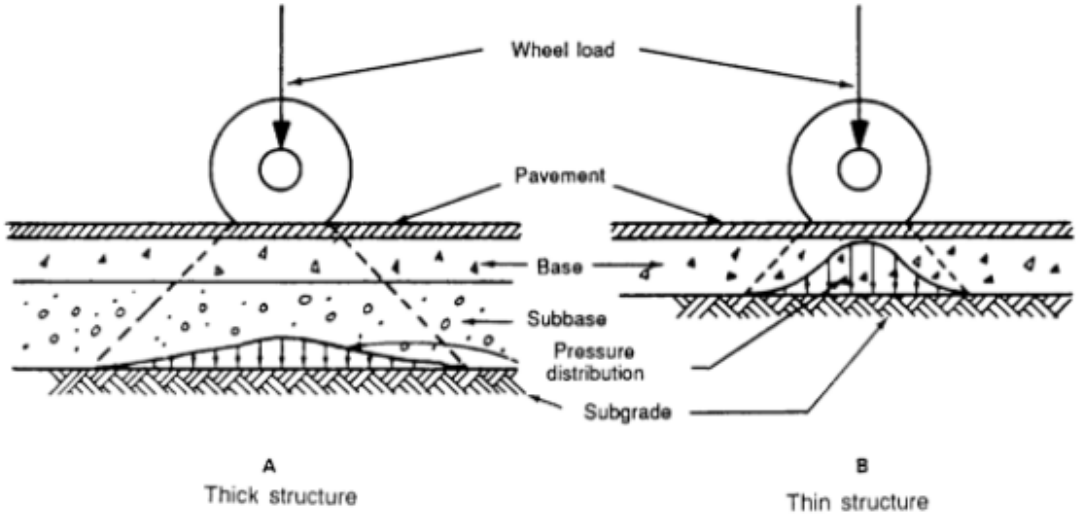

FIGURE 2.1

Distribution of Pressures Under Single-Wheel Load (Department of the Army, 1994)

The aggregate base course is the second layer of flexible pavements and is located underneath the HMA. It serves as a principal structural component of the pavement system and distributes the wheel load to the subgrade. The layer must have sufficient strength and thickness to prevent failure of the subgrade, and prevent volume changes due to fluctuations in moisture content. Typically, lower strength subgrades require thicker base course layers to reduce a higher percentage of load transfer from the surface traffic loading. Figure 2.2 shows the distribution of stress for both a weak and a firm subgrade with the required thickness of the base. The low-bearing-ratio subgrade requires a thicker base course to distribute stress over a greater area of the subgrade. Base course layers usually

consist of crushed or uncrushed granular aggregate. An additional subbase layer is sometimes included in pavement systems where frost action is severe. Subbase layers are optional and similar to base course layers but have less strict requirements due to the lower loaded stress expected. For this study, a subbase layer is not used due to its infrequent use in GDOT roadways.

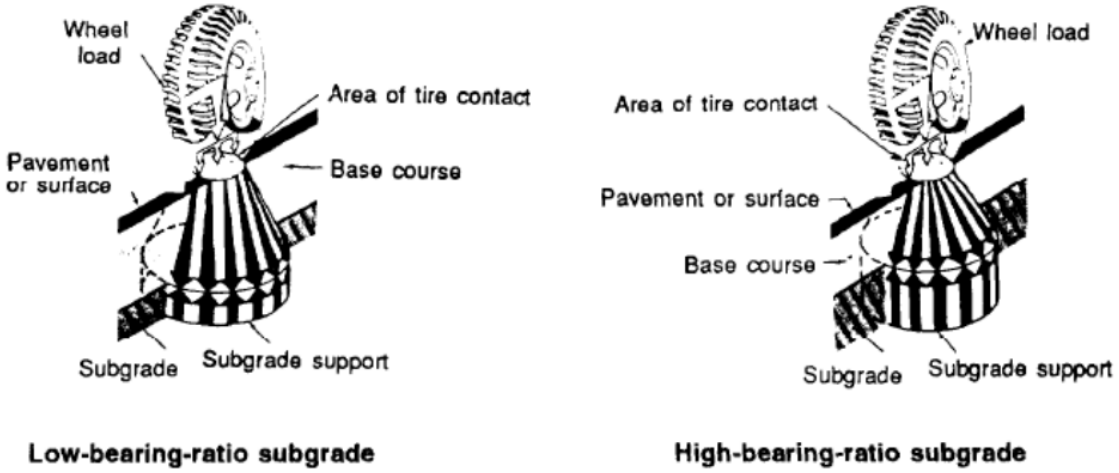

FIGURE 2.2

Stress in Base Course and Effects of Subgrade Strength on Base Thickness (Department of the Army, 1994)

The final layer of the pavement system is the subgrade layer, which is a compacted soil layer considered to be the foundation of the pavement system. During construction, the top 6 in. (15.2 cm) of subgrade should be scarified to allow optimum moisture content to be reached. After scarification, compaction to maximum dry density is completed. This compacted subgrade may be the in situ soil on the construction site or selected replacement for exceedingly weak subgrades (Huang, 2012). Subgrade soils are subjected to the smallest stresses of pavement layers. Figure 2.3 shows a typically constructed flexible pavement layer system with each of the above-described three layers.

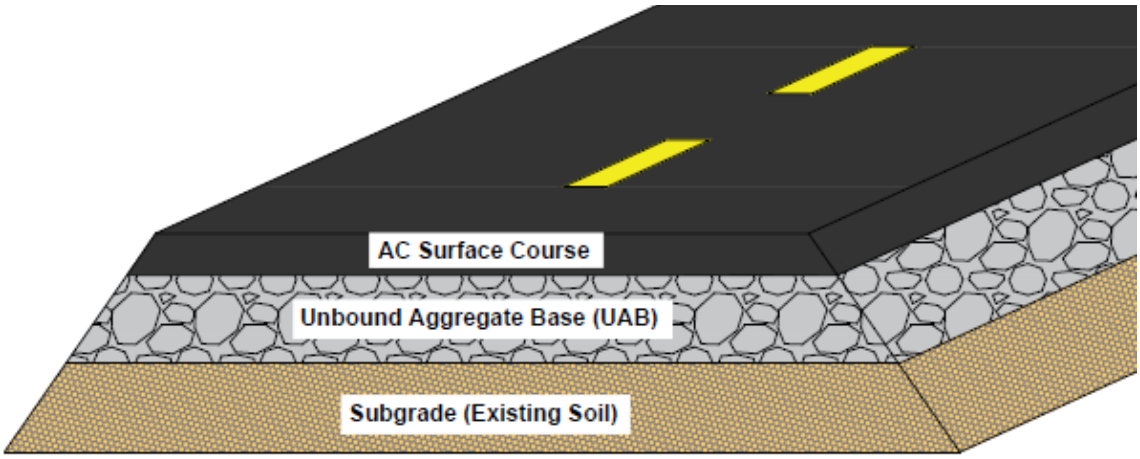

FIGURE 2.3

Typical AC System Layers

The stress distribution of surface traffic loads is of great interest to both geotechnical and pavement engineers. The easiest way to characterize the behavior of flexible pavements under traffic loading is to consider it a homogenous mass. Before layered-system theories were developed, Boussinesq's theory was commonly used to determine the stress, strain, and deflection of pavement systems under a concentrated load condition (Boussinesq, 1885). Vertical stresses under concentrated loads on horizontal planes are displayed with a bell-shaped surface with the most substantial stresses directly under the load. Pressures are highest at shallow depths, practically approaching zero at a finite depth. For pavement, the load at the surface is not a point load because it is distributed over an ellipse area by the tire, but does follow the point load pattern for the variation of stress with depth (Yoder and Witczak, 1975). In reality, flexible pavements are layered systems and are unable to be represented by a homogenous mass accurately. In 1945, Burmister developed solutions for a three-layer system to predict stresses in pavement systems (Burmister, 1945). With the advent of computers, new models are capable of calculating the stresses of a multilayer system with any number of layers. Figure 2.4 shows

this difference between Boussinesq's single mass and Burmister's two-layer system with their respective pressure distributions.

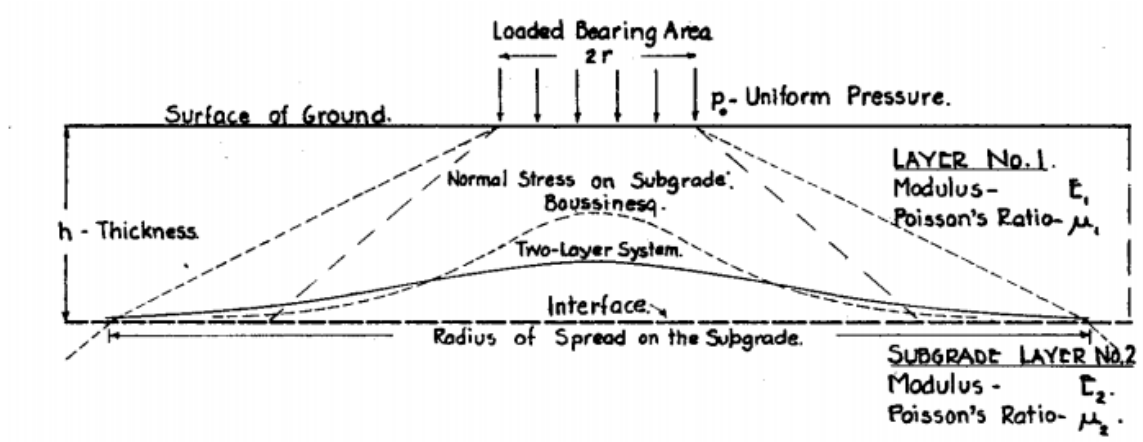

FIGURE 2.4

Stress Distribution on Subgrade Soil (Burmister, 1945)

For weak subgrades, the stress transferred from the asphalt concrete (AC) and base layers needs to be minimized in the design process. From a multi-layer analysis, it can be found that for a given load with a constant contact area, a decrease in subgrade stress can be accomplished by an increase of the base course thickness and increase of the AC surface course thickness. Another efficient method of reducing the vertical compressive subgrade stress is to increase the rigidity of the upper pavement layers. In a layered system, the majority influence upon stress in the subgrade is usually exerted by the stiffness of the layer directly above the subgrade (Burmister, 1945). Consequently, the subgrade stress is more dependent on the stiffness of the aggregate base layer than the AC layer in a three-layer system.

2.1.1 Effect of Unbound Aggregate Base Material Properties on Load Transfer

Unbound aggregate base layer properties are highly influential on the load transfer from the bottom of the AC layer to the subgrade layer. ASTM D 8-11 defines an aggregate base layer as "a granular material of mineral composition such as sand, gravel, shell, slag, or crushed stone, used with a cementing medium to form mortars or concrete, or alone as in base courses, railroad ballasts, etc." This layer is commonly included in pavement systems because it provides a working platform, a structural layer, a drainage layer, and a frost-free layer. More specifically, densely graded unbound aggregate base (UAB) layers provide load distribution by dissipating high wheel-load stresses with depth and ensuring adequate support and stability for the asphalt surface. Using a granular base layer in pavement projects is cost-effective and more sustainable as it allows for utilizing materials that can be acquired near construction sites, increasing the practical use of recycled aggregate products, and improving the lifespan and pavement performance (Tutumluer, 2013).

GDOT specifies the use of a graded aggregate base (GAB) as the UAB layer. GAB plays a critical role in the overall integrity of the concrete slab or bituminous pavement layer (Kim et al., 2015). For the remainder of this report, GAB and UAB will be used interchangeably. GDOT specifies that the GAB is placed between the prepared subgrade and the AC layer. The GAB course serves a variety of purposes depending on the construction practices and the environment, including the provision of structural capacity to the AC layer and low susceptibility to soil frost.

The strength of the GAB and its ability to provide support to overlying pavement systems is dependent on several different factors, including aggregate type, aggregate grading, moisture content, and aggregate compaction (Kim et al., 2015). The base course layer is a matrix of different-sized aggregates compacted together forming a continuous

system. This matrix is created by the inter-particular friction and interlock creating a stable system. Confining stresses in the matrix are produced from the surrounding base material as the particles are compacted together. The purpose of the geosynthetics is to augment the matrix and stress paths by stabilizing through friction and interlock of the base material.

Dantu (1957) revealed that the load transfer in granular materials is not uniformly distributed as previously believed and is instead concentrated along load-carrying particle chains. These continuous columns of particles are laterally supported by the surrounding material and at a critical load will fail, which rearranges the internal structure. Therefore, the deformation pattern of a GAB layer is directly related to load transfer by shear in the columns of particles supported under confinement (Tutumluer, 2013). As roadways are trafficked, the GAB layers undergo both elastic and plastic deformation. Figure 2.5 shows the GAB behavior under repeated loading.

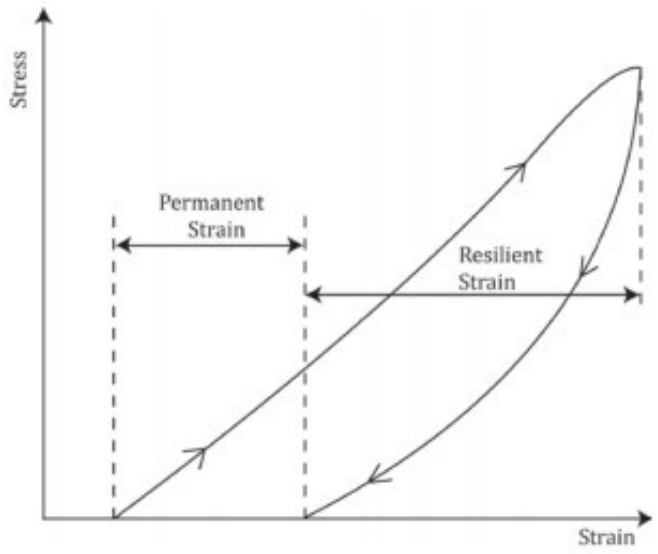

FIGURE 2.5

Strains in a Granular Material During One Cycle of Load Application (Tutumluer, 2013)

2.1.1.1 Unbound Aggregate Base Deformation

For thinly surfaced flexible pavement, rut formation in pavement systems can be attributed to deformation in the underlying layers (i.e., subgrade and base course material). Base course deformation usually occurs due to aggregate breakdown and the movement of aggregate particles, which lower the density, causing failures (Bagshaw, Herrington, and Kathirgamanathan, 2015). One of the common failure types of flexible pavement systems is permanent deformation due to deformation of the GAB layer. In the GAB layer, the accumulation of permanent deformation gradually declines with the increase in load applications. Once this layer has been compacted, there should be a densely compacted matrix in which all load applications result in resilient, elastic deformations. Compaction of this layer ensures the majority of deformations from vehicle loading are resilient in nature to prevent significant permanent deformation (Kim et al., 2007). The total permanent deformation is a critical design parameter of the GAB layer. Permanent deformation has been established as a direct indicator of pavement performance compared to the resilient modulus test. Despite this, there is no standard test procedure for the testing of aggregates for permanent deformation. Although there have been several attempts to develop devices to simulate stress conditions to predict pavement behavior, they are not feasible because of equipment cost and personnel training requirements (Tutumluer, 2013).

2.1.1.2 Unbound Aggregate Base Gradation

It is noted that gradation of the GAB is a critical factor in the success of aggregate as a base course. Since the gradation of the aggregate can affect structural capacity, drainage, and frost susceptibility, control of gradation is a principal concern for most engineers. Three types of gradations are common for roadway projects across the country: 1) aggregate with

no fines; 2) fines just filling the voids of the aggregate fraction, and 3) fines overfilling the voids of the aggregate fraction. In GDOT construction, GAB having a specified gradation and consisting of particle sizes ranging from 1.5 in. (37.5 mm) to No. 200 sieve size (75 μm) is the generally accepted material. The gradations specified for silicate aggregates, granite, granitic gneiss, quartzite, and other similar type aggregates are called Group II aggregates, while the gradations specified for carbonate aggregates, limestone, dolostone, and marbles are classified as Group I aggregates. Two possible gradations are specified for Group I base due to the tendency of some carbonate rocks to produce inadequate amounts of fines when crushed (GDOT *Pavement Design Manual*, Section 5.1).

In the first type of gradation, the aggregate derives its strength from the interlocking of the aggregate particles. Therefore, the base course material should be confined in order to ensure the layer is stable. However, this type of aggregate gradation provides excellent drainage and is completely non-frost-susceptible. In the second type, the aggregate still derives its strength from interlocking of the aggregate particles. However, due to the cohesiveness of the fine particles, the structural integrity of the aggregate is not compromised if unconfined. In addition, the drainage is adequate and can be non-frost-susceptible. In the third type, the strength of the aggregate is primarily derived from the interlocking effect of the fine particles rather than the larger particles. Therefore, a strength reduction occurs. The drainage characteristic of these types of aggregate would be poor and would cause high frost susceptibility.

In order to design and maintain long-lasting roadways, transportation agencies have developed requirements for specific aggregate properties. Aggregate gradation influences its behavior because of the packing order and void distributions that can vary. Aggregate

gradation influences not only the mechanical response behavior characterized by the resilient modulus, shear strength, and permanent deformation, but also permeability, frost susceptibility, erosion susceptibility, and so forth (Bilodeau et al., 2009). It is important to determine the gradation of the aggregate base in pavement systems in order to ensure a sufficiently strong base material.

Excessive fines (particles passing the No. 200 sieve) deteriorate aggregate layer performance and are especially sensitive to moisture (Kim et al., 2007). The maximum amount of fines allowed in the GAB layer is limited to 12%. Maximum particle sizes of 1.5 in. (37.5 mm) are best to ease the effort needed for satisfactory compaction. The presence of plastic fines, usually from silty or clay subgrade layers, is best limited and can be accomplished through a specific gradation or the use of a geosynthetic as a separator between base–subgrade layers.

Resilient behavior of GAB is dependent on the percentage of fines in the aggregate base materials. Increasing the percentage of fines reduces the permanent deformation resistance. GDOT has set the requirements for GAB used for pavement construction (GDOT *Standard Specifications*, Section 815, 2013). Table 2.1 is taken from the specification and shows the required gradation for GAB materials.

TABLE 2.1
GDOT GAB Gradation Requirements
(GDOT *Standard Specifications*, Section 815, 2013)

Sieve Size	Percent Passing By Weight
Group I Aggregates	
2 in (50 mm)	100
1-1/2 in (37.5 mm)	95-100
3/4 in (19.0 mm)	60-95
No. 10 (2 mm)	25-50 (Note 1, 2 and 3)
No. 60 (250 µm)	10-35
No. 200 (75 µm)	7-15
Group II Aggregates	
2 in (50 mm)	100
1-1/2 in (37.5 mm)	95-100
3/4 in (19 mm)	60-90
No. 10 (2 mm)	25-45 (Note 2 and 4)
No. 60 (250 µm)	5-30
No. 200 (75 µm)	4-11
NOTE 1: Group I aggregates having less than 37% passing the No. 10 (2 mm) sieve, shall have at least 9 percent passing the No. 200 (75 µm) sieve.	
NOTE 2: For graded aggregate stabilized with Portland Cement, 30-50 percent by weight shall pass the No. 10 (2 mm) sieve. All other requirements remain the same.	
NOTE 3: Material passing the No. 10 (2 mm) sieve shall have a sand equivalent of at least 20 for Group I aggregates.	

2.1.1.3 Unbound Aggregate Base Compaction

Unbound aggregate layers function primarily through interparticle load transmission through aggregate contact with other particles. Compaction of the layer is vital to avoid excessive shear deformation. The degree of compaction is one of the primary factors that affect the performance of the GAB layer. Compacting the GAB layer reduces the thickness by approximately one-third of its loose placement depth. The maximum lift thickness stated by governmental agencies is typically on the conservative side, and adequately constructed surfaces can have single lift depths up to 10 to 12 in. (254 to 308 mm) (Saunders, 1997). In the state of Georgia, GDOT allows GAB "to be placed in a single or multiple layers

depending on its thickness; layers are not to exceed 8 in. (203 mm) and not to exceed two layers" (GDOT *Standard Specifications*, Section 815, 2013). Compaction of GAB layers results in preferential orientation of individual aggregate particles, which causes cross-anisotropic behavior in the layer (Tutumluer et al., 2003).

According to a study by Tutumluer et al. (2003), increasing the density of a granular material makes the aggregate layer stiffer and reduces the magnitude of the resilient and permanent deformation response to both static and dynamic loads. The density of the aggregate base is more influential on permanent deformation behavior than the resilient modulus. The primary objectives of compaction are to 1) reduce and prevent detrimental settlements by creating a denser packing of individual particles; 2) increase shear strength; 3) improve bearing capacity of pavement subgrade; and 4) control undesirable volume changes. Although compaction increases the density of the layer, the true objective of compaction is found in other mechanical properties like shear strength and a decreased likelihood of permanent deformation accumulation. The compatibility of the GAB depends on the compaction energy, the moisture content, and the aggregate physical and morphological properties. A decrease of the degree of compaction from 100% to 95% of maximum dry density increases permanent axial strain by an average of 185% (Barksdale, 1972). The degree of compaction is the most influential factor in controlling the permanent deformation. Aggregate base moisture content can cause an increase in strength in the pavement structure due to capillary suction, or it can cause a decrease in strength due to lubrication between particles; it also can reduce effective stress between particle contact points, decreasing strength.

To achieve sufficient compaction, several laboratory tests are needed to determine optimal compaction densities and moisture content. Commonly, an impact-type compaction effort is applied to aggregate samples using the methods specified in the AASHTO T 99 Standard and AASHTO T 180 Modified test procedures (also ASTM D 698 and D 1557). The maximum dry density (MDD) values obtained from impact hammer–based methods, such as the AASHTO T 99 and AASHTO T 180, are subsequently corrected, as per AASHTO T 224, to compensate for particles larger than ¾ in. (19 mm). Pavement layers in the field are compacted to specified percentages of their MDD. This MDD is achieved at the optimum moisture content (OMC). The Proctor compaction test results delineate these values for the materials tested. When the material is compacted, material strength and bearing capacity can be increased, and deformation tendencies and undesirable volume changes can be reduced. A study by Kaya et al. (2012) revealed that impact compaction caused a change in aggregate gradation due to a crushing and breaking of the material. Alternatively, vibratory compaction caused no such damage and no change in gradation, which was optimal for this study. Vibratory compaction on aggregate base materials tends to produce higher CBR values but lower resilient modulus values than impact compaction.

2.1.2 Effect of Subgrade Material Properties on Load Transfer

The structural integrity of flexible pavement is dependent on the subgrade soil strength and its maintenance is vital to ensure stability. For a finished subgrade to be stable, it must have a certain strength and deformation properties that affect flexible pavement construction activities. Subgrade soil properties are directly influential on the performance of pavement and load transfer. Subgrade performance in roadways is dependent on its load-bearing

capacity and volume change. The subgrade must be able to support loads transmitted through the pavement structure. Subgrades also must resist volume changes when exposed to excessive moisture or freezing conditions (Pavement Interactive, 2012).

The moisture content in subgrade soil is a major factor affecting the soil resilient modulus in addition to its dry weight and coefficient of uniformity. If the seasonal water table level reaches the top of the subgrade level, then pavements are susceptible to heaving during winter and losing bearing capacity, causing pavement failures (Abdalla, 2008).

According to the Illinois Department of Transportation's *Subgrade Stability Manual*, subgrade material must not have a rut depth greater than 0.5 in. (1.3 cm) under all construction traffic before pavement construction, and it must provide adequate support for placement and compaction of pavement layers, and have a minimum immediate bearing value (IBV) of 6.0 (IDOT, 2005). Subgrade that does not meet these characteristics must be treated prior to pavement construction. Certain subgrade classifications and characteristics, such as high moisture and high silt content, are more likely to be unstable and exhibit excessive rutting. Subgrades with high silt contents, i.e., 60–80% silt, can be problematic because there is a likelihood of pumping silt into aggregate base layer materials from repeated loads drawing moisture from high groundwater into the surface) and they are frost-susceptible, impacting long-term performance (IDOT, 2005).

According to the GDOT *Standard Specifications*, subgrade soil must have certain soil class requirements for use as subgrade material. If Class IIB3 and better soils are available, contractors are required to distribute and compact these soils in 8-in. (200 mm) uniform layers over the entire width of the embankment. If enough Class IIB3 soils are available, they should be used in the top 12 in. (300 mm) of the roadbed. If Class IIB4 soils

are present at the construction site, contractors should distribute and compact these soils in 8-in. (200 mm) layers over the entire width of the embankment unless Class IIB3 or better soils are available in borrow pits, in which case contractors should use these soils in the top 12 in. (300 mm) of subgrade. Class IIB4 soils may be used in the top 12 in. (300 mm) of subgrade if approved by the Office of Materials, Geotechnical Engineering Bureau (GDOT *Standard Specifications*, Section 814, 2013).

The GDOT *Standard Specifications* states that "weak subgrades can be stabilized mechanically (by adding granular materials), chemically (by adding chemical admixtures), or with a stabilization expedient (sand grid, matting, or geosynthetics). Stabilization with chemical admixtures (lime, portland cement, fly ash, and such) is generally costly but may prove to be economically feasible, depending on the availability of the chemical stabilization agent in comparison with the availability of granular material" (GDOT *Standard Specifications*, Section 814, 2013).

A stabilization expedient may provide significant time and cost savings as a substitute to other means of stabilization or low strength fill. The most popular of the man-made stabilizers are sand grid, roll-matting, and various types of geosynthetics, especially geotextiles. Matting and sand grid are expedient methods of stabilizing cohesionless soils such as sand for unsurfaced road construction. Geotextiles and other geosynthetics (i.e., geogrid) are primarily used to reinforce weak subgrades, maintain the separation of soil layers, or control drainage through the road or airfield design. The availability of these materials must be weighed with the considerable time savings for use of expedients in combat construction.

The treatment of weak subgrade is a common practice in roadway construction and is primarily focused on providing a temporary stable platform for construction vehicles. Geotechnical reports often indicate problematic subgrade areas for pavement designers found from soil investigations and provide a general subgrade treatment recommendation. If subgrade problems are not identified and treated, subgrade can easily be damaged and require lengthy and expensive repair.

If a subgrade is determined to be inadequate from the strength tests, then soil modification may be required to increase the subgrade strength. Soil-modification efforts include the addition of modifiers like lime, fly ash, or cement to enhance strength. If soil modification is not feasible due to its gradation, time, and weather restrictions, then removal and replacement with a granular material is an alternative option. Figure 2.6 is a collection of procedures developed for the use of pavement maintenance and construction. The soil stabilization index system (SSIS) developed by Nelson and Miller (1997) can be used to determine the most appropriate method to be used for stabilization based on the plasticity index (PI) of the soil.

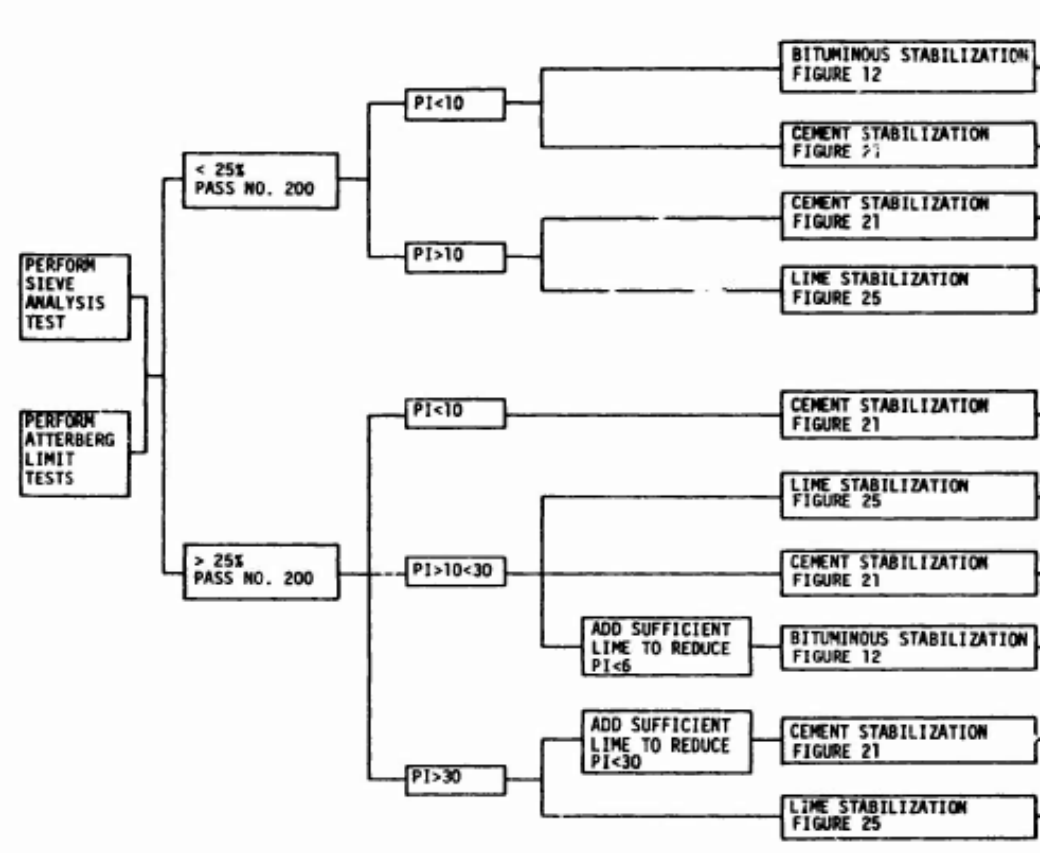

FIGURE 2.6

Selection of Stabilization Technique – SSIS Method
(Nelson and Miller, 1997)

An alternative stabilization technique includes the use of geosynthetics. Geosynthetics are used for subgrade restraint to increase the support of construction equipment over a weak subgrade. Geosynthetics work by providing a tensile resistance and lateral restraint as wheel loads attempt to cause rutting in the subgrade. When placing a geosynthetic, it is essential to place it in a taut or stretched condition. This will require less excessive rutting to develop the tension that provides the restraint (IDOT, 2005).

Weak subgrades can be the result of expansive soil. Expansive soil is defined as any soil or rock material that has a potential for shrinking or swelling under changing moisture conditions likely causing settlement to occur (Nelson and Miller, 1997). The

primary problem that expansive soils pose is that the deformations are significantly larger than elastic deformation and therefore cannot be predicted with classical elastic or plastic theory. This settlement usually takes place in an uneven pattern and often causes extensive damage to the structures and pavements resting on them. The damage expansive soils cause on structures is more extensive than that of any other natural hazard, including earthquakes and flooding.

Two major factors must be identified in the characterization of a site for highway construction. The first is the expansive shrink or swell potential of the soil. The second is the environmental conditions that influence the moisture conditions of the soil that cause expansion. Nelson and Miller (1997) described that expansion of the soils is a result of changes in the soil water system that disturb the internal stress equilibrium. Clay particles generally are platelets having negative electrical charges on their surfaces and positively charged edges. They have a unique molecular structure that is sensitive to variances in the amount of water or the chemical composition. When this occurs, the particle spacing changes and causes shrinkage or swelling. The factors influencing the shrink–swell potential of soil are environmental factors, soil characteristics, and the state of stress.

The soil plasticity is a property that is influential to shrink–swell potential. In general, soils that exhibit plastic behavior and have high liquid limits have greater potential for swelling and shrinking. In other works, plasticity is an indicator of swell potential. In addition to the plasticity, the dry density can be used as an indicator of swelling potential. A higher density of a soil indicates closer particle spacing, which may mean greater repulsive forces between particles, which cause a higher likelihood of swelling.

Expansive soil problems can typically be caused by seasonal fluctuations of the water table level. Water contents in the upper few yards of the soil are highly influential to subgrade support capabilities, and the area is called the zone of seasonal fluctuation or the active zone (Nelson and Miller, 1997). Figure 2.7 shows an example of the fluctuation of water content causing extreme swelling potential.

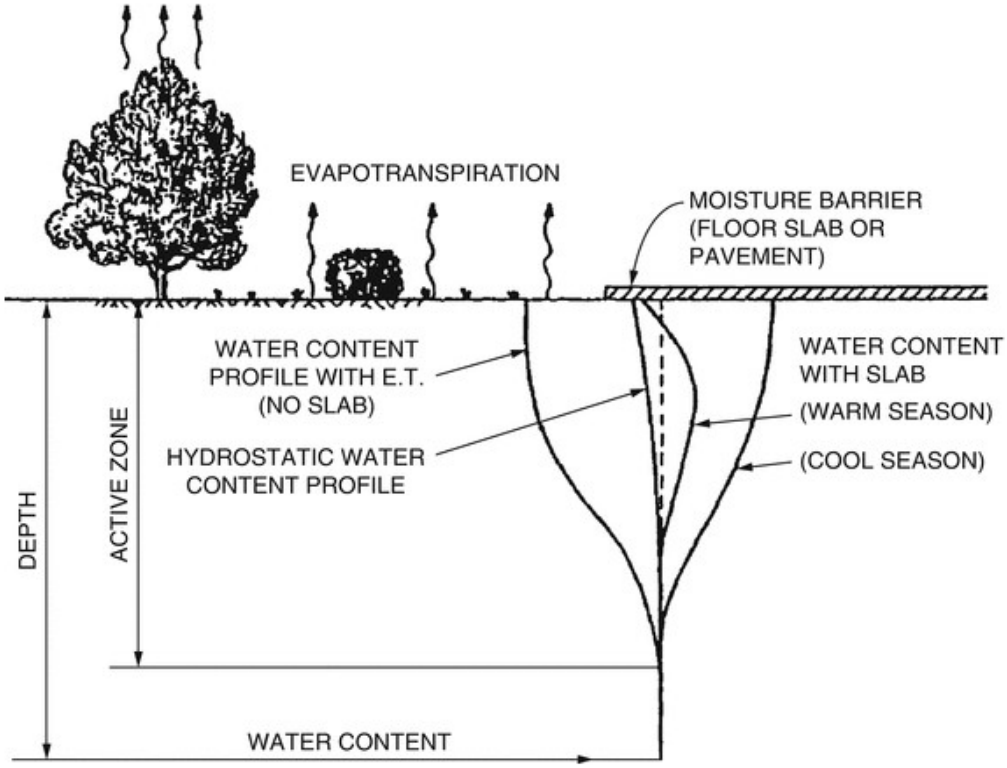

FIGURE 2.7

Water Content Profiles in the Active Zone
(Nelson and Miller, 1997)

Specific soil properties can be used to predict the degree of expansion of a soil. The use of Atterberg limits to predict the swell potential of a soil is the most popular approach. Several different methods have been developed to predict the degree of expansion expected

in subgrade using different soil properties and measurements. Table 2.2 presents a single index method for identifying an expansive soil solely by its plasticity index (Chen, 1973).

TABLE 2.2
Expansive Soil Classification
Based on Plasticity Index
(Chen, 1973)

Swelling Potential	Plasticity Index
Low	0–15
Medium	10–35
High	20–55
Very high	35 and above

Flexible pavement is highly susceptible to damage in subgrade soil. Damage to pavements on expansive clays appear in the following forms: severe unevenness along a significant length of pavement with or without cracking or visible damage, longitudinal cracking, significant localized deformation, and localized pavement failure. Pavements cannot be isolated from the soil and it is uneconomical to make the subgrade stiff enough to resist differential movements. Instead, soil subgrade treatments are commonly employed to stabilize or minimize soil movements (Nelson and Miller, 1997).

2.1.3 Summary of Load Distribution Mechanism in Pavement Foundation

Traffic loading is distributed downward through flexible pavement layers that are typically composed of an asphalt concrete layer on top, base course layer in the middle, and subgrade layer for the foundation. The modulus of the layers decreases as the loading travels downward because as the loading is disbursed, less strength and stiffness are needed to prevent functional failures such as permanent deformation and cracking. The GAB's ability to disperse loading to the subgrade and prevent permanent deformation is dependent on its

compaction, gradation, and material properties. The subgrade soil must have a certain strength and deformation properties, which are usually defined as its load-bearing capacity, resilient modulus, and volume change. The gradation, soil classification, and moisture content are all influential in the CBR value, which is commonly used in pavement design. Lower CBR values indicate a lower resilient modulus and lower bearing capacity, which ultimately require some form of stabilization or thicker overlying layers.

2.2 Geosynthetics

A geosynthetic is a planar product manufactured from a polymeric material used with soil, rock, earth, or other geotechnical-related material as an integral part of a civil engineering project, structure, or system according to ASTM D 4439. As an unconventional construction material, geosynthetics have been used in roadways in the United States since the 1970s and have seen steady growth over the years. As of 2001, the geosynthetic market in the U.S. was estimated to be $1.1 billion, among which the geosynthetic used for reinforcement applications in roadways is worth about $200 million per year (Perkins et al., 2005).

2.2.1 Types of Geosynthetics

There are many different types of geosynthetics, including geotextiles, geogrids, geomembranes, and geocomposites. Geotextiles and geogrids have been widely used in pavement applications and regarded as having several beneficial functions. ASTM 4439-18 defines a geotextile as a permeable geosynthetic comprised entirely of textiles. Geogrids are defined as a geosynthetic formed by a regular network of integrally connected elements with apertures greater than ¼ in. (6.4 mm) to allow interlocking with surrounding soil, rock,

earth, and other materials to function primarily as reinforcement. Figure 2.8 shows a biaxial extruded geogrid and a woven geotextile.

FIGURE 2.8

Biaxial Geogrid and Woven Geotextile
(Holtz et al., 2008)

Geogrids and geotextiles are manufactured with similar processes. Geotextiles are manufactured with either long, continuous filaments of polymer or short, staple fibers between ¾- and 6-in. (19.0–152.4 mm) length. The combination method of the fibers determines their type. Woven geotextiles are produced with monofilament, multifilament,

or silt film tapes. The other classification of geotextiles is of the nonwoven type. Geogrids can be classified as extruded (integral), woven or flexible, or welded, depending on their production process (Holtz et al., 2008).

Pavement can fail either structurally where a collapse of the structure as a whole causes the pavement to be effectively unable to sustain loading, or functionally where the pavement roughness is too uncomfortable for drivers or causing distress on vehicles traveling over the pavement. A one- to two-year extension of pavement life from the use of a geosynthetic can cover the cost of the purchase and installation, which can range from $1 to $3 per yard (Holtz et al., 2008). Geosynthetics are deemed most effective for reinforcement in flexible asphalt concrete pavements in comparison with rigid pavements. Using geosynthetics has negligible influence on the critical stresses in rigid pavements for predicting transverse cracking. However, there is a strong likelihood of geogrids reducing permanent deformation in the base course layers and improving pavement performance by reducing joint faulting and roughness in rigid pavements (Luo et al., 2017).

Geosynthetics are most commonly used for filtration, drainage, separation, reinforcement, as a fluid barrier, and for protection, and their properties are varied depending on the primary function driving their use in the pavement system. A standard classification for the function of the geosynthetic is dependent on the subgrade soil condition. For soft subgrades with CBR values less than 3, the primary function of the geosynthetic is for reinforcement, and the use of geosynthetic can significantly lower the aggregate base thickness required for adequate support (Korner, 2005). For intermediate-strength subgrade with a CBR in the range of 3 to 8, the primary function is stabilization, which allows for a smaller stone base in addition to a longer lasting structure. For firm

subgrades with a CBR greater than 8, separation is the primary function, which increases the lifespan of the roadway. Visual techniques and falling weight deflectometers (FWD) help monitor the long-term performance of the geosynthetic-reinforced pavement foundation (Korner, 2005). For separation between the soft subgrades and aggregate base layers, geotextiles are most commonly used because they prevent pumping of fine material from the subgrade into the base course during changes in water table elevation commonly experienced by roadways during their lifespan. Table 2.3 below shows the status of different geosynthetics used by industry in pavement applications. It shows situations where the use of geosynthetics is being realized fully (i.e., unpaved, paved, and asphalt overlays) and areas in which research and application may grow (i.e., paved vertical and horizontal stress reductions).

The poor performance of geosynthetics for pavement projects is often attributed to poor product acceptance, poor construction monitoring procedures, and improper installation of the geosynthetic. When a geosynthetic is not placed properly in the roadway structure or is significantly damaged, the full functional benefits are not realized. Often, the failure or underperformance of roadways is blamed on the geosynthetic, which limits its widespread use throughout the nation.

The installation process is critical to maximize the benefits of geosynthetics. Roadways are often wider than one roll of geosynthetic; therefore, in order to have a satisfactory geosynthetic seam, a minimum overlap of 12 in. (300 mm) is needed. Some situations require unreasonable overlap of geosynthetic rolls. In this situation, sewing is a practical alternative, most commonly used with geotextiles (Holtz et al., 2008). Figure 2.9 shows a step-by-step installation procedure for geosynthetic placement.

TABLE 2.3
Status of Geosynthetics in Pavement Applications (Korner, 2005)

Application Category (recall Figure 4)	Type of Geosynthetic	Function of Geosynthetic	Commentary by Author on Current Status			Recommendation
			Theory	Experiment	Verification	
(i) Unpaved	GT or GG	reinforcement	excellent	excellent	excellent	use it!
(ii) Paved or unpaved	GT	separation	poor	possible	good	under utilized
(iii) Paved						
(a) vertical stresses	GG	reinforcement	complex	available	lagging	needs acceptance
(b) horizontal stresses	GG	reinforcement	poor	excellent	doable	great opportunity
(iv) Asphalt overlay						
(a) full-width	GT	reinforcement	reasonable	available	mixed	questionable
(b) full-width	GT	waterproofing	reasonable	available	good	ongoing
(c) over cracks	GT or GG	reinforcement	reasonable	reasonable	good	ongoing

a. Prepare the ground by removing stumps, boulders, etc.; fill in low spots.

PREPARE THE GROUND

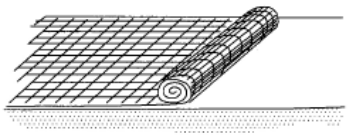

b. Unroll the geosynthetic directly over the ground to be stabilized. If more than one roll is required, overlap rolls. Inspect geosynthetic.

UNROLL THE GEOSYNTHETIC

c. Back dump aggregate onto previously place aggregate. Do not drive on the geosynthetic. Maintain 6 to 12 inches (150 – 300 mm) cover between truck tires and geosynthetic.

BACK DUMP AGGREGATE

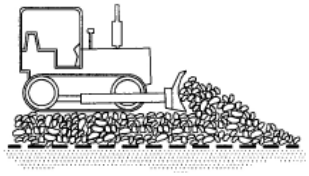

d. Spread the aggregate over the geosynthetic to the design thickness.

SPREAD THE AGGREGATE

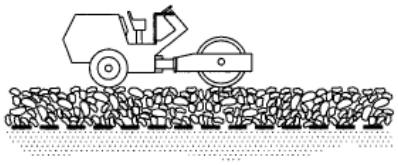

e. Compact the aggregate using dozer tracks or smooth drum vibratory roller.

COMPACT THE AGGREGATE

FIGURE 2.9

Installation Procedure of the Geosynthetic (Holtz et al. 2008)

2.2.2 Role of Geosynthetics for Load Transfer

Geosynthetics have several different functions that dictate their use in different construction conditions. The most common functions of geosynthetics are stabilization, reinforcement, and separation. Reinforcement refers to the strength addition from the geogrid or geotextile. On the other hand, stabilization is the strength retention through locking particles in place. The mechanisms and results of both stabilization and reinforcement are discussed in this section. One mechanism that geogrids and geotextiles use to provide strength to roadways is through friction or interlock between base course materials and the geosynthetic, as shown in Figure 2.10. These benefits ultimately combine in the form of mechanical stabilization for weak subgrade soils. A study by Luo et al. (2017) investigated two other mechanisms caused by the geosynthetic: stiffening of the base course, and more efficient distribution of tire load. Benefits from using a geosynthetic in asphalt pavements depend on the thickness of the aggregate base layer and location of geosynthetic in the layer. For thin base layers of 6 in. (152 mm) or less, geosynthetics are

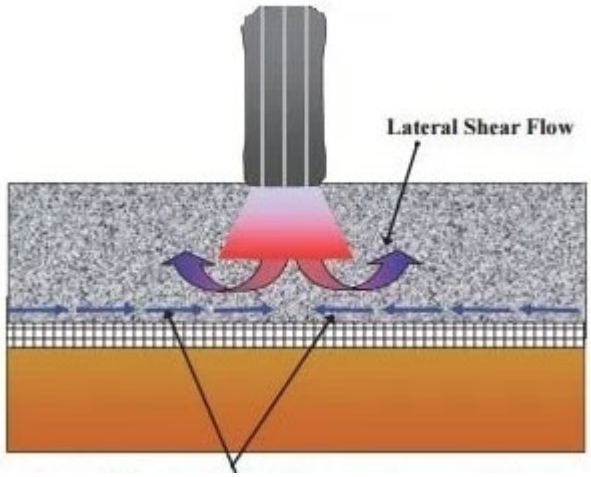

FIGURE 2.10

Lateral Restraint Due to Friction and Aggregate Interlock (Luo et al., 2017)

more effective at the base–subgrade interface. For thicker layers, 10 in. (254 mm) or more, geosynthetics are more useful at the midpoint of the base layer.

For CBR values of 3 to 6, the subgrade material can support a majority of the load transferred from the base course layer, but a stabilization geosynthetic can be used for some additional support and ensure separation between the layers. Geosynthetics vary in their strength properties. For design, the required strength is dependent on the following characteristics: the drop height of base course materials on top of the geosynthetic, the maximum aggregate size (MAS), and finally the strength of the subgrade beneath the interface. An increased drop height of base course materials requires higher strength geotextile, a larger MAS requires higher strength geotextile, and weaker subgrade strength requires higher strength geosynthetics.

Design strength of the geosynthetic is based on two factors. First, the geosynthetic strength should be high enough that the stress at the top of the subgrade due to the weight of the aggregate and traffic is less than the bearing capacity of the soil plus a safety factor from the geosynthetic. Secondly, the strength of the geotextile should be designed for the stress expected during construction, which may be greater than its service life. The geosynthetic must have enough strength to survive construction operations in order to provide its intended function. Geotextiles are rated in classes depending on their ability to survive different construction practices. Class 1 geotextiles are designed to survive severe construction practices, while Class 2 geotextiles are more suited for normal construction methods.

Geosynthetics used on soft subgrades provide both cost and performance benefits due to the reinforcing properties of the geosynthetic. Geosynthetics reduce stress intensity

on the subgrade, which reduces the depth of excavation required of unsuitable subgrades. This decreases the thickness of aggregate required to stabilize subgrades, lessening the disturbance of soft subgrade during construction. A reduction in disturbance provides uniform support for the base course layer by decreasing differential settlement and minimizing variations of subgrade strength.

The reinforcing properties of geogrids and geotextiles are based on several mechanisms. Friction produced by geotextiles, and interlock produced by geogrids produce lateral restraint of base and subgrade materials. An increase in bearing capacity can be expected due to the higher shear strength surfaces ultimately changing the potential bearing capacity failure surface. Lastly, membrane support of wheel loads is commonly realized as a reinforcing property of geosynthetics, but it is only experienced with wheel path rutting greater than 4 in. (102 mm) (Holtz et al., 2008).

Some geosynthetics can be used at the bottom of base course layers to provide lateral confinement of the aggregate layer, effectively working as a reinforcement layer. Shear stresses between the aggregate and the geosynthetic reinforcement cause lateral confinement during the forces experienced during loading, compaction, and placement. Lateral confinement increases with each load application due to the ever-increasing residual restrain after load applications (Holtz et al., 2008).

Vertical loading applied on the surface of the granular fill layer, either directly or indirectly through a pavement layer induces high horizontal and vertical stresses under the loaded area. The horizontal thrust due to this loading is resisted by horizontal stresses in the fill outside the loaded area, but also results in outward shear stresses on the surface of the subgrade below as the load is transferred downward. These outward shear stresses on

the subgrade reduce the bearing capacity factor for the clay by as much as half the value expected from vertical loading. When a geosynthetic is used, the shear stresses are picked up by reinforcement and only vertical forces are transmitted into the subgrade, allowing for the utilization of the full bearing capacity. This reduction in shear stress explains why reinforcement provides an improvement in road performance at small rut depths (Milligan et al., 1989).

Several soil types are classified as poor soils and can often benefit from a geosynthetic in roadway construction: SC, CL. CH, ML, MH, OL, OH, and PT based on Unified Soil Classification System (USCS). In addition to the soil type, in situ properties of undrained shear strength conditions, such as CBR less than 3, can also benefit from geosynthetics. Geosynthetics can serve multiple functions under these weak soil conditions. Because flexible asphalt pavement design is highly dependent on subgrade strength, geosynthetics used as reinforcement provide lateral restraint and reduce the stress on the subgrade, which improves its bearing capacity due to its stress-softening characteristic. Table 2.4 shows the applications of geosynthetics for different CBR conditions.

In addition, geosynthetics are used to reduce construction costs by limiting the amount of base course required for adequate pavement support when designed as a reinforcement. Table 2.5 shows the available benefits of using geosynthetics. In order to use this benefit of the geosynthetic in design methods, several large-scale experiments have been created to calibrate the performance compared to control sections. For the design process of unpaved roadways, the benefit of using a geosynthetic is usually realized through a higher bearing capacity factor (Nc) of the subgrade soil (Holtz et al., 2008).

TABLE 2.4
Application and Associated Functions of Geosynthetics in Roadway Systems (Holtz et al., 2008)

Application	Function	Subgrade Strength
Separator	Separation & filtration	$3 \leq CBR \leq 8$
Stabilization	Separation, filtration & some reinforcement	$CBR < 3$
Base Reinforcement	Reinforcement & separation	$3 \leq CBR \leq 8$

TABLE 2.5
Reinforcement Benefits (Berg et al., 2000)

Benefit	General Anticipated Magnitude	Applicability
Reducing Under Cut (i.e., the depth of excavation required for the removal of unsuitable subgrade materials)	Reduced up to 50%	CBR <3 (M_R < 30 MPa)
Reducing the thickness of aggregate required to stabilize the subgrade	Reduced up to 50%	CBR <3 (M_R < 30 MPa)
Reducing disturbance of the subgrade during construction	Allows construction of relatively thin base (subbase)	CBR <3 (M_R < 30 MPa)
Reinforcement of the subbase aggregate in a roadway to reduce the section	Reduced up to 250 mm with 75 mm typical	Depends on depth of base and initial depth of base/subbase
Reinforcement of the base aggregate in a roadway to reduce the section	Reduced up to 150 mm with 75 mm typical (20 to 50%)	Strong potential benefit
Reinforcement of the subbase aggregate in a roadway to increase its design life	TBR = 1 to 3.8	Depends on depth of base and initial depth of base and subbase
Reinforcement of the base aggregate in a roadway to increase its design life	TBR = 1 to 10	Strong potential benefit
Improved reliability	Improves performance during overload and/or seasonally weak subgrade conditions	Always a benefit

Though there have been numerous studies to investigate what properties of geosynthetics influence pavement performance, the current practice of using geosynthetics for subgrade stabilization is based on empirical evidence from constructed test sections.

Studies utilizing natural subgrades have difficulty in achieving uniform conditions throughout the project. Alternatively, studies involving artificially placed subgrade soils usually demonstrate better consistency. Historically, laboratory studies can be completed in less time and with more conditions than full-scale pavement test sections, but often lack similar results to the more accurate large-scale field tests. The large-scale testing apparatus attempts to bring the benefits of small-scale laboratory testing and large-scale field testing together (Cuelho and Perkins, 2009).

2.2.3 Role of Geosynthetics for Separation and Their Impact

Geotextiles have been used for decades in the separation between soft subgrade soil and the aggregate base course in roadway construction. For separation design, the base course thickness is required to adequately carry the design traffic loads of the pavement. On the other hand, in stabilization and reinforcement design, geosynthetics may reduce base course thickness required to adequately carry design traffic load (Holtz et al., 2008). Geotextiles used for long-term roadway applications can be especially beneficial due to their layer separation and prevention of the pumping of fines from the subgrade into the base course material. Significant fines migration has been found in some subgrades with a CBR up to 8. AASHTO M 288 states that with a CBR > 3, geotextile application is identified as separation, drainage, and filtration, and not as much reinforcement (Holtz et al., 2008). Soils with a CBR < 3 are typically wet and close to saturation and benefit from a geosynthetic because of its filtration capabilities. The filter allows water to pass through into the aggregate and ultimately decreases pore pressure over time while maintaining separation of the two layers (Holtz et al., 2008). Figure 2.11 shows this separation and mixing of the subgrade and aggregate base course. Geotextiles are

considered the simplest and most cost-efficient way to separate the base course materials (Lacina, 2011).

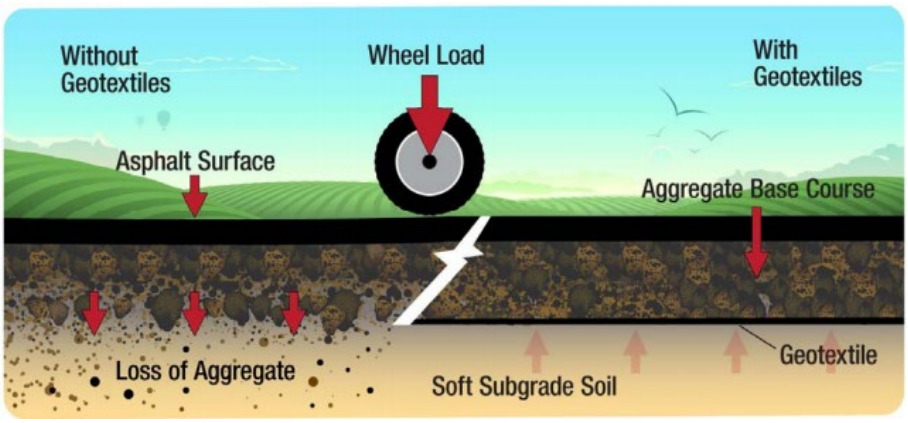

FIGURE 2.11

Separation Effect of Geotextile between Subgrade and Base Course (Lacina, 2011)

2.2.3.1 Pore Water Pressure Reduction with Geotextiles

Water in the base and subgrade can cause severe problems in roadways. A saturated subgrade can develop pore water pressure (PWP), which softens the subgrade. Saturated soils with fine-grained soils are typically considered some of the weakest subgrades. PWP is generated in these soils when traffic loads are applied, and it increases as load repetitions continue. Geosynthetics reduce PWP development by a reduction of stress in the subgrade, a reduction of point stress and corresponding pore pressure developed by gravel penetrating subgrade layers, and PWP dissipation in the plane of some geosynthetics. To investigate this effect, Christopher et al. (2009) conducted laboratory tests with a pavement-testing box. The pavement-testing box was used to observe the performance of a weak saturated subgrade with and without different geosynthetics used for base course reinforcement and stabilization. Their results showed that for some conditions, the reduction of excess pore

water pressure in a geotextile-reinforced test section accounted for 80% of the reduced rutting, while the remaining 20% was attributed to the reinforcement compared to a control test specimen. This signifies the importance of geotextiles in the reduction of PWP. Figure 2.12 shows the results of that study and the benefit that using a geosynthetic has on reducing PWP in soft subgrades.

Subgrade strength properties like resilient modulus or undrained shear strength are highly dependent on water content. For most of the current empirical design models, field measurements of these subgrade characteristics are taken from untrafficked and partially saturated soil conditions. After repeated traffic loads and an increase in pore water pressure, the initial measurements used in the design process can be overestimated for the actual field conditions over the lifespan of the roadway because of this, empirical models may not

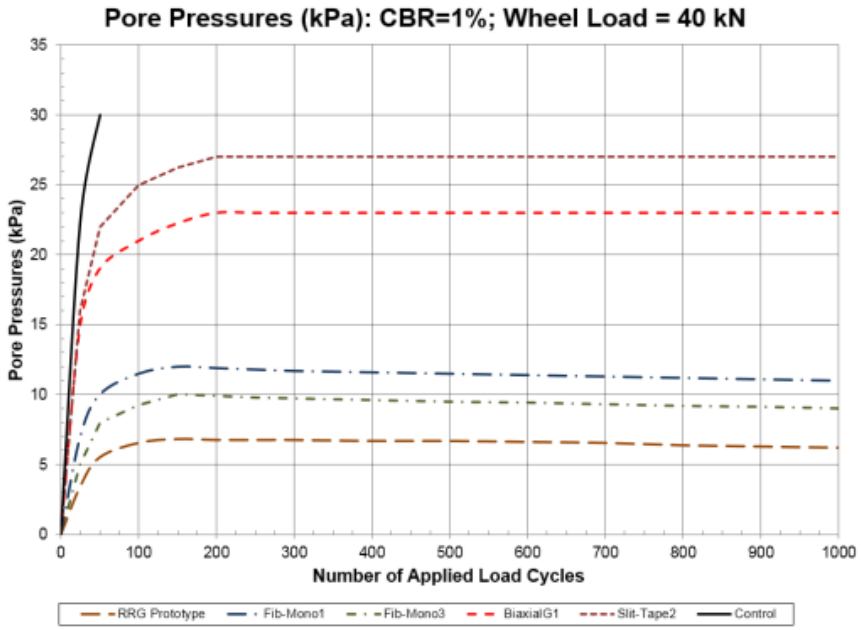

FIGURE 2.12

Pore Water Pressure Due to Use of Different Geotextiles (Lacina et al., 2015)

match measurements taken in the field. Accounting for the pore water pressure can help adjust the models to more accurately the reactions of the roadway in the field.

2.2.3.2 Separation Effect

Using a geotextile as a separator between base course material and subgrade is strongly suggested if there are more than 15% fines in the subgrade (Lacina et al., 2015). To prevent migrations of fine material in the subgrade upward into the base layer, a separator is highly recommended. If the subgrade soil has less than 50% passing the No. 200 sieve, a separator is not needed. On the contrary, for any subgrade soil with more than 50% passing the No. 200 sieve, a geotextile is needed to prevent migration (Bagshaw et al., 2015).

Over time without this separation, a mixing of the two layers occurs and eventually leads to aggregate base course loss. Depending on the CBR of the subgrade, large percentages of the base course thickness can be lost into a soft subgrade layer. At a CBR value of 2.5, up to 30 percent of the thickness can be lost, which proves the importance of using a geotextile for separation in soft subgrade soils (Lacina, 2011). A 19% loss of base course can cause up to a 50% reduction in load-carrying capacity according to *AASHTO 1993 Flexible Pavement Design Method* (Lacina et al., 2015).

Long-term stability of roadways is greatly affected by water. When water is introduced to the pavement foundation, it can reduce the shear strength of the subgrade soil by increasing the pore water pressure within the soil. This reduces the ability of a subgrade to support a roadway and can cause the merging of aggregate base layer with the subgrade soil, decreasing the effectiveness of the pavement system. One of the benefits of using a geotextile is that it provides a border between the base course and subgrade that prevents the mixing of the two (subgrade fines traveling into the base course material defined as

pumping) but also allows water to drain downward. This prevention of mixing of the two layers is vital in the maintenance of the design thickness of each layer (Lacina, 2011).

Load distribution of saturated roadways differs from that of a dry roadway in that the traffic load is transferred nearly fully downward into the subgrade soil instead of being distributed through the base course material. Using a geotextile in this situation keeps subgrade soils intact and distributes the vertical load over a larger area, essentially decreasing the load realized by the subgrade directly under the wheel path of the traveling vehicles (Lacina, 2011).

Woven geotextiles are useful for separation because of the multiple planes in their structure, which allow water to easily flow through the surface while remaining impenetrable by fines from the subgrade. Figure 2.13 shows the individual woven yarns in a geotextile.

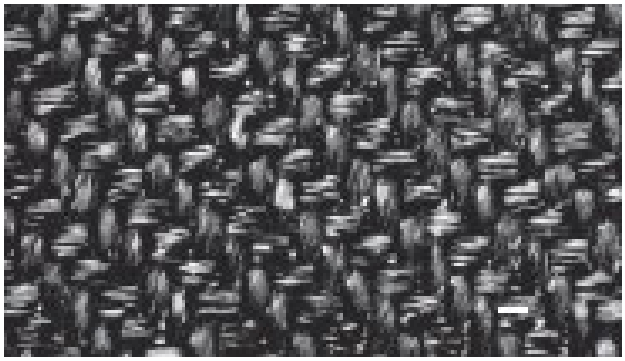

FIGURE 2.13

Woven Geotextile (Lacina, 2011)

Geotextiles used for separation must be designed with enough strength to provide satisfactory performance after installation damage and expected stresses throughout their lifespan. There are other methods to decrease water damage to a roadway, including using a free-draining aggregate and asphalt layer that essentially create a permeable pavement.

Though this method can have the same beneficial effect as using a geotextile, it is usually more expensive and has a shorter lifespan of effectiveness (Lacina, 2011).

AASHTO M 288, "Standard Specification for Geotextile Specification for Highway Applications," allows users to determine the usefulness of geotextiles for separation and stabilization. This separation effect helps increase the number of loads that a roadway is capable of handling before failure. Research has been conducted to determine the pavement design life extension by comparing the increase in the number of simulated traffic loads that a geotextile-included cross-section can withstand versus a control unreinforced section. Results of these experiments have shown that the benefit ratio varies from 1.5 to 4. A recommended value of 2 is used for most designs. This benefit value is the ratio of the number of load cycles of a geosynthetic-reinforced section to the number of load cycles of an unreinforced section for a given level of performance.

In addition to the design life extension due to the geotextile's separation function, an additional benefit can be expected in the design process by increasing the drainage coefficient in the *AASHTO Flexible Pavement Design Method*. In rare cases where a drainage layer of roadway is not available, geotextiles with lateral drainage capability can be placed between the subgrade and aggregate base layer to allow drainage when a densely graded base course is used and allow for quicker drainage (Holtz et al., 2008).

AASHTO M 288 addresses geotextiles utilized as a material for separation of soil subgrades, stabilization of soft subgrades, and prevention of reflective cracking. Separation of soil subgrades is accomplished by placing a flexible porous geotextile between different layers so that the integrity and function of both layers can remain intact. Stabilization (reinforcement) is accomplished by the improvement of a system's total strength created

by the introduction of a geotextile (good in tension) into a soil (good in compression but poor in tension) or other disjointed and separated materials. The filtration function of a geotextile involves the movement of liquid through the fabric. In AASHTO M288-96, the classifications are essentially a list of strength properties meant to withstand varying degrees of installation survivability stresses. Provided below are the classifications:

- Class 1 – for severe or harsh survivability conditions where there is a greater potential for geotextile damage
- Class 2 – for typical survivability conditions; this is the default classification to be used in the absence of site-specific information
- Class 3 – for mild survivability conditions

In general, class 1 geotextiles are utilized for stabilization of subgrades, class 2 geotextiles are used for separating soil subgrades, and class 3 geotextiles are recommended for prevention of reflective cracking unless harsh survivability conditions are anticipated. Hydraulic conductivity (i.e., permeability, subsurface filtration, or drainage) must be considered in problematic soil environments (i.e., fine-grained soils, silts, and clays). The soil-to-geotextile system must allow for adequate fluid flow with limited soil loss across the plane of the geotextiles over its service life. Minimum fabric properties, woven or nonwoven, should be based on minimum average roll values (MARV) and not average lot values. MARV is a term commonly used in the geosynthetic industry to establish expected strength and survivability properties used for the design with geosynthetics. MARV are based on a statistical analysis of the specific geosynthetic and quoted as the lowest possible value that could be produced and pass through the quality assurance tests of the manufacturer. Average lot values are considerably higher than the minimum value because

MARV are based on the lower extremity of possible strength values to be conservative. This value is two standard deviations lower than the average lot value (GDOT Office of Materials and Research, 2013).

Geotextiles as separators in a pavement between the base course layer and subgrade layers are underutilized due to the lack of public knowledge of the cost-to-benefit ratio provided by using a geotextile. Though a large amount of research has been done on soft subgrades, there are limited long-term studies on the benefits of using geosynthetics (Perkins et al., 1999; Luo et al., 2017; Al-Qadi et al., 2008; Cuelho and Perkins, 2009; and Cuelho et al., 2011).

2.2.4 Effect of Placement and Location of Geosynthetics

Geosynthetics are typically placed at the interface between aggregate base and subgrade layers. Geotextiles should always be placed at this location due to their effectiveness in the prevention of the migration of fines. The possible benefit of enhanced reinforcement from geotextile placed within the base course is unable to surmount the functional separation of pavement layers. Therefore, geotextile should only be placed at the base–subgrade layer. Alternately, several recent studies have investigated the optimal placement of geogrid within pavement foundations. Al-Qadi et al. (2008) constructed nine low-volume pavement design sections to investigate the optimal location for the installation of geogrid in pavements. Testing was conducted using an accelerated loading facility utilizing heavily instrumented test specimens built on a subgrade at CBR 4%. The study found that for thick granular base materials, a single geogrid installed in the upper third of the layer was able to improve the performance. Additionally, for thinner pavement sections geogrid placed at

the upper third of the base material performed similarly to specimens with the geogrid placed at the base–subgrade interface.

Luo et al. (2017) performed large-scale testing on flexible pavements using an 8-ft-diameter by 6-ft-high circular steel tank. They found that geogrids are more effective when placed at the center of thick aggregate base layers exceeding 10 in. (254 mm) in depth, and at the bottom (interface of subgrade and base course) for thinner base course layers, 6 to 10 in. (152 to 254 mm) in depth. Results from the study suggest that the placement of geogrid at the interlayer of the subgrade and base course will influence pressure reduction below the geosynthetic (Luo et al., 2017).

Perkins et al. (1999) conducted large-scale laboratory tests investigating reinforced geogrid pavement roadways in a large concrete box in which field-scale pavement layers were placed. A cyclic 40-kN load was applied through a circular plate to the pavement surface to measure pavement distress results. The test results demonstrated significant improvement in pavement performance on a soft clay prepared at CBR 1.5. Geogrid was tested at both the subgrade–base interface and 4 in. (100 mm) up in the 12-in.-thick (300 mm) base layer. They found that the geogrid placed higher up in the base performed significantly better (Perkins et al., 1999).

2.3 Use of Large-Scale Testing in Geosynthetics-Reinforced Pavement Foundations

Pavement engineers are faced with a critical problem in the design of heavy-duty pavements where loading conditions differ significantly from previous experiences. Traditionally, a test section would be built, and the in-service traffic would be measured, but these results are often lengthy and may not provide sufficient results. Even if this test section is built on a major route, it is still possible that the traffic growth over the

pavement's lifespan will exceed the loading accumulated on the experimental pavement, which would invalidate any conclusions drawn from the study. Engineers must be able to evaluate new materials in order to advance the practice of civil engineering. Because of this, a methodology is required to allow for the exploration of new pavement configurations with controlled traffic load parameters accumulated quicker than traditional test sections (Metcalf, 1996).

Difficulties in conducting reliable field performance comparisons of open roadways exist for several reasons. The high costs of reconstruction of test pavements after failure cause a disincentive to experiment with new methods and materials for pavement systems. When test results from field tests are compared, there is a high likelihood of variance in quality of construction from region to region. In addition, long testing periods of pavement systems likely have personnel reassignments, resulting in a discontinuity of interest and assessments for the evaluation period. For roadway sections, the uncertainty in the number and weight of axle loadings causes problems in the comparison of test sections. Finally, the environmental effects can vary from region to region, making comparisons difficult (Powell, 2012).

2.3.1 Accelerated Pavement Testing

Accelerated pavement testing (APT) is a specific type of research utilized by several programs around the world to produce comparative results between test sections. These controlled testing conditions permit results that can reveal differences in long-term performance potential within relatively short periods of time. APT is defined as "the controlled application of a prototype wheel loading, at or above the appropriate legal load limit to a prototype or actual, layered, structural pavement system to determine pavement

response and performance under a controlled, accelerated accumulation of damage in a compressed time period. The acceleration of damage is achieved by increased repetitions, modified loading conditions, imposed climatic conditions, the use of thinner pavements with a decreased structural capacity and thus shorter design lives, or a combination of these factors" (Metcalf, 1996). Figure 2.14 shows the APT apparatus at the Civil Infrastructure Systems Laboratory of Kansas State University, which has been used for 12 different experiments since 1996.

FIGURE 2.14

APT Testing Facility at Kansas State University
(Metcalf, 1996)

APT is highly useful in that it can reveal how pavements will predict future loading conditions. The United States' total truck tonnage is expected to increase by about 50% by 2020 (Powell, 2012), and the prediction of future pavement performance under this traffic condition cannot be done by existing performance-testing devices. Because of the multitude of benefits that APT provides, there has been significant national and

international interest in supporting APT efforts in the past few decades. One contributing factor for the emergence of APT is the 1986 planning document of the Strategic Highway Research Program (SHRP) listing APT as a potential study type in long-term pavement performance (LTPP) research (TRB-SHRP, 1986).

There are about 28 APT facilities currently operational around the world with about 15 located in the United States. These numbers are most likely an underestimation due to the results being provided by known facilities with APT testing capabilities. Most tests are at fixed sites, but some are focused on field studies due to the belief that there is improved vehicle–pavement–environment interaction. The coordinating organization in the U.S. is the Transportation Research Board (TRB) Committee AFD40: Full-Scale and Accelerated Pavement Testing, which was transitionally formed in 2000 from Task Force A2B52. The committee is concerned with APT conducted in either the laboratory or the field with mobile or fixed equipment. The purpose of the group is to assimilate significant worldwide accomplishments from the past and present and recommend approaches for future practice (Powell, 2012).

APT is a vital tool used for innovations in pavement technologies due to its ability to accurately measure mechanical performance in comparison with real situations. Over the past five decades, traffic load simulators have been effectively used to help minimize the risk of expensive development failures and to adopt quality standards for pavement applications. APT allows simulated roadways to be built and tested under laboratory conditions that accurately represent traffic loadings expected in a pavement's life. APT allows researchers to determine the influence of the ever-changing motor vehicle construction and evaluate the effect of changing loads on the structural behavior of

pavement systems in an accelerated way. In addition to the accelerated testing aspect, APT allows for reproducible and clearly defined testing procedures, which are vital for testing new materials and their influence on pavement systems (Partl et al., 2015). APT does have its limitations in that only the effect of mechanical loading can be evaluated in an accelerated manner. Time-lapse, climate influences, and the aging process are cumbersome to simulate with this technology. Most APT devices are prototypes and only exist in limited numbers. Because of this, there are relatively high acquisition, operation, and maintenance costs, and requirements for significant human resources and well-trained researchers to use the system.

APT systems are grouped into two different classifications. Full-scale systems are those in which a standard truck tire or combination of tires is used for applying the loads to the pavement. Small-scale systems are those in which a scaled-down version of a truck tire and tire load is applied to the pavement. Program costs of APT typically exceed the initial price of the facility and initial construction cost of the experimental pavements. This drawback is often combated with the benefits derived from using the system. APT systems typically make use of the standard types of measurements, including permanent deformation, pressure sensors, and elastic deformation in some form, as well as basic environmental data, such as moisture content (Steyn, 2012). Though theoretical analyses can be effective in predicting pavement response to loading (critical stresses and strains in each pavement layer), the current state of the practice is not advanced enough to produce accurate predictions for all properties of a pavement. Because of this, large-scale testing is needed to produce actual measurements of pavement response to vehicular loading (Al-Qadi et al., 2008).

APT is commonly used for several pavement materials and structural evaluations. A majority of APT testing facilities use HMA for the surfacing material, granular materials for base layers, and unstabilized materials for subgrade layers. Structural cracking and permanent deformation are most commonly evaluated as the structural distress type of the pavement. Most programs use wheel loading as the load characteristics, and more commonly report tire-related properties, such as inflation pressure and contact stress, as playing a prominent role. The vehicle–pavement interaction is the specific interaction between the loading device and pavement structure, focusing on simulating real traffic loading (Steyn et al., 2012). APT aims to evaluate pavement sections under a range of loading and environmental conditions in order to improve the knowledge of the potential performance of pavement layers. Having the different loading conditions allows engineers to predict pavement responses under all expected loading conditions, allowing for a more economical, long-lasting design. APT is effective for evaluating the influence of using geosynthetics in pavement systems. A multitude of studies has been completed with various APT methods to determine the influence of geosynthetics on rut formation and pressure distribution compared to non-reinforced test sections (Saghebfar et al., 2013; Greene et al., 2011; Bagshaw et al., 2015; Tang et al., 2014). Though APT methodologies are implemented differently, they are deemed valuable to the geosynthetic industry due to their ability to test roadways under different loading conditions in an abbreviated manner.

2.3.2 Large-Scale Test Case Studies

Several large-scale case studies provide useful insight into results, test procedures, and methodologies adopted for this study. Five large-scale study results are summarized in this literature review to show previous results of the use of geosynthetics in pavement

applications. The large-scale testing results found various conclusions that promote one geosynthetic over another, but with no consistent findings of a superior product. While no consensus of the optimal geosynthetic type has been found, there is a general trend reported of the benefit of all geosynthetic products for weak subgrade conditions.

Case Study 1: Geosynthetic Reinforcement of Flexible Pavements – Laboratory-based Pavement Test Sections

Perkins et al. (1999) investigated an extruded biaxial geogrid and a woven geotextile on pavement performance, as defined by surface rutting. They found that with a base thickness of 12 in. (300 mm) the test sections with geogrid performed better than the sections using the geotextile product, while an improvement from the geotextile was still appreciable. In addition, they determined that the geotextile-reinforced specimens deformed more than the unreinforced sections during the early portion of loading. The reinforced sections had traffic benefit ratios (TBR) that led to at least a 20% reduction of base thickness.

Case Study 2: Flexible Pavement Performance With and Without Geosynthetics, Nine-Year Follow-Up.

This study was completed to evaluate the differential performance of asphalt pavement sections close to Raleigh, North Carolina. An area with mica present in silty or clayey sands, causing typically weak subgrade strength, was required to install a geotextile in addition to 2 in. (51 mm) of extra aggregate base material for pavement support. After four years of service, the roadways that were built with geotextile exhibited much less pavement distress than other areas of asphalt roadways built six months prior during a previous phase of the project, even though the geosynthetically reinforced roadways had higher traffic counts than the unreinforced roadways. In addition to less pavement deterioration, the

roadways that were constructed with geotextile exhibited less road noise when traversed and were smoother than the unreinforced counterparts. It was theorized that this reduction of road noise was due to the separation of the subgrade and GAB layers causing less permanent deformation and therefore a smoother riding surface.

Several destructive and nondestructive pavement calculation methods were performed on the similar roadways to evaluate the performance of the geotextile in the roadway. The repair of the roadway included a lightweight, slit-tape, woven geotextile that was placed near the bottom of the repair undercut. In addition to the geotextile, a biaxial geogrid was installed under 9 in. (229 mm) of aggregate and 4 in. (102 mm) of hot mix asphalt. This repair technique is common for flexible pavement systems. Another nondestructive testing technique was surface roughness testing. The Internal Roughness Index (IRI) is used to measure pavement smoothness, where lower IRI values indicate a smoother ride of traversing vehicles. This roughness testing was completed on three sections of the roadways in the study. The two sections that had reinforcement between aggregate and subgrade layers had lower IRI results, indicating smoother rides (Lacina and Dull, 2013).

Case Study 3: Geosynthetics in Basecourse Reinforcement – NZ Agency

This study investigated the stabilization of unbound granular pavements with the use of geosynthetics. A large-scale testing apparatus was constructed so that a specimen was traversed in a reciprocating manner beneath a standard truck tire pressed down onto the sample. Figure 2.15 shows the testing setup.

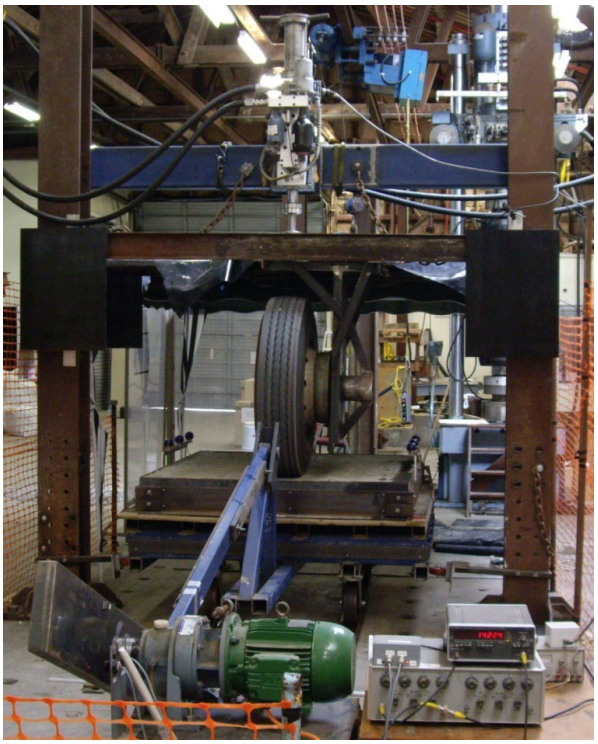

FIGURE 2.15

Large-Scale Pavement Testing Apparatus
(Bagshaw et al., 2015)

The results of this study show that the rate of rutting can be decreased by as much as 50% when geogrids are placed at the subbase–base course layer interface. Little difference was found between the rate of rut formation with geogrid placed at the base or the mid-height of the sample. The study also demonstrated that pavement stabilization is more effective for low bearing-strength subgrades. When the California Bearing Ratio approaches a value of 8 and above, the benefit of using geosynthetics decreases. It was found that a triaxial geogrid performed better than a biaxial geogrid. No geotextile was used in this study. Rut formation in pavement systems can sometimes be attributed to deformation in the underlying layers (i.e., subgrade and base course material). Base course deformation usually occurs due to aggregate breakdown and the movement of aggregate particles, which lowers the density and causes failures (Bagshaw et al, 2015).

Case Study 4: Field Investigation of Geosynthetics Used for Subgrade Stabilization, Part 1

This study used large-scale field testing to investigate the use of reinforcement geosynthetics in unsurfaced roads built of a soft subgrade. An 8-in.-thick (200 mm) aggregate layer was prepared on top of a subgrade of CBR strength of 1.8 and trafficked with a fully loaded tandem-axle dump truck. The study determined that welded geogrids, woven geogrids, and integrally formed (extruded) geogrids provided the best overall performance when compared to the two geotextile products. The study determined that test specimens failed under a small number of traffic passes. Because of this, a recommendation was made to increase base thickness during construction so it is less likely to fail as rapidly (Cuelho and Perkins, 2009).

Case Study 5: Full-Scale Field Study of Geosynthetics Used as Subgrade Stabilization, Part 2

This study was performed as part 2 to the "Field Investigation of Geosynthetics used for Subgrade Stabilization" by Cuelho and Perkins (2009). For that study, a thicker base course of 11 in. (279 mm) was used per the recommendations of Part 1 to investigate the performance of geosynthetics under less severe conditions. Test specimens were built with subgrade prepared at a CBR of 1.8. Geosynthetics were evaluated by their accumulation of rut formation. They found that woven geotextile performed the best followed by BX geogrid. The base course reduction analysis found that the most significant reduction in base thickness was 27% from a woven geotextile. The nonwoven geotextile also performed better than many of the geogrid products (Cuelho et al., 2011).

3. MATERIALS AND PRELIMINARY TEST

As shown in the literature review, the material properties of subgrade, GAB, and the geosynthetic are highly influential on the load transfer through pavements and their ability to support traffic loading. It is important for pavement engineers to identify these properties prior to construction and design to ensure the best and most cost-efficient design available. To determine soil properties, several soil tests are needed. Sieve and hydrometer analyses are commonly used to determine the particle size distribution of a soil and are ultimately used in determining the soil classification according to AASHTO or USCS publications. Results from the Proctor test, including the maximum dry density of soil and optimum moisture content, are commonly used by engineers to define compaction requirements during construction.

3.1 Material Usage

Because of the large number of test specimens required to complete the testing plan, the aggregate base materials were recycled and reused for four test specimens before acquiring new material. While using new material for every test was unpractical due to the limited space at the testing facility and logistics of transportation of the material, fresh material was needed periodically because of the separation of particles that occurred after several testing sequences and the material loss during the construction and deconstruction processes.

Approximately 4 yd^3 (3 m^3) of subgrade soils were acquired from each material location. This soil was reused for each test and dried out to a predetermined moisture content for each testing condition. New material was not required for the subgrade material

due to the absence of large granite particles that are crushed during compaction techniques, and a smaller occurrence of separation of larger and smaller particles of the subgrade. For this testing procedure, subgrade samples were uninstalled and mixed with the remainder of the sample to ensure similar conditions of the soil when the material was first acquired and when the soil testing was completed.

3.2 Material Physical Properties

Soil is often separated into classes or groups with each having similar characteristics and potentially similar behavior. Two simple tests are routinely used to classify soils:

1) Gradation – accomplished by a sieve and hydrometer analysis, and
2) Atterberg limits – accomplished by a liquid limit and plastic limit test.

There are two commonly used soil classifications. The AASHTO classification is used mainly for subgrade rating for highway purposes and requires the gradation, liquid limit, and plasticity index of a given soil. The USCS, which is used mainly for geotechnical purposes, requires also the gradation, liquid limit, and plasticity index of the soil.

3.2.1 Subgrade Soil and GAB

3.2.1.1 Particle Size Distribution

Particle size distribution is usually completed by a combination of two tests: the sieve test and the hydrometer test. These tests are vital for the classification of a soil and the determination of the percent of fines in a material, which is highly related to its ability to function as a foundation. Sieve analysis was completed following ASTM D422 for four soil samples (i.e., GAB, and Coweta, Hall, and Gordon County soils). For the GAB material, the particle size distribution was then compared to GDOT standard specifications. It was determined that the base course material was sufficient for this study. The particle

size distribution for the subgrade materials was completed and the results are shown in Figure 3.1.

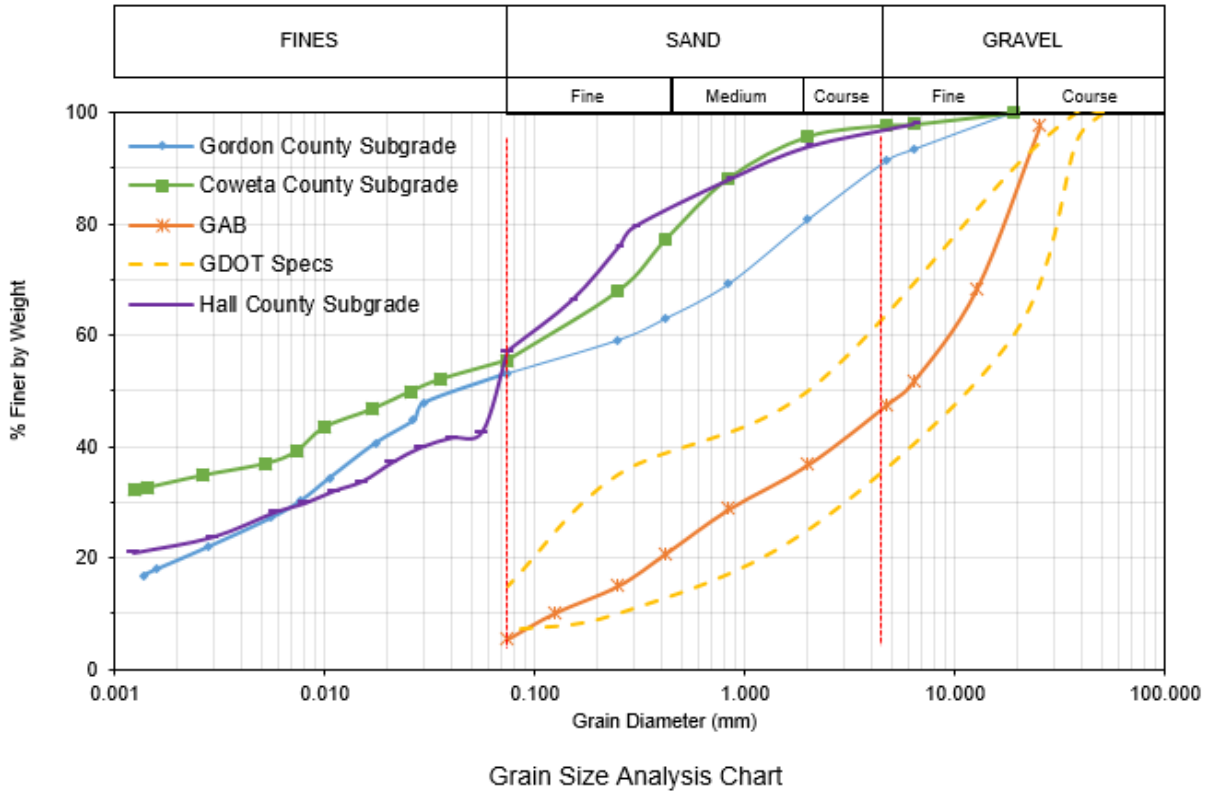

FIGURE 3.1

Particle Size Distribution Chart of Materials

3.2.1.2 Atterberg Limits

The Atterberg limits testing procedure is defined in ASTM D4318-17, Standard Test Methods for Liquid Limit, Plastic Limit, and Plasticity Index of Soils. These tests were performed on each type of soil, along with other soil characterization tests and are summarized in Table 3.1. Using these Atterberg limits tests and gradation results, the four materials are classified in Table 3.2.

TABLE 3.1
Properties of Granular Materials

Test Results	Soils Tested			
	Gordon County	Coweta County	Hall County	GAB
Specific Gravity	2.76	2.79	2.76	NA
Fines (%)	53	55	57	5.45
Plastic Limit	42	41	37	NA
Liquid Limit	63	64	57	NA
Plasticity Index	22	23	20	NA

TABLE 3.2
Soil Classifications

Soil Type	AASHTO Classification	USCS Classification	GDOT Classification
GAB	A-1-a	GW	NA
Coweta County	A-7-5	MH	IIB3
Gordon County	A-7-5	MH	IIB3
Hall County	A-7-5	MH	IIB3

As described in the literature review, some properties cause the subgrade's ability to support pavements to be insufficient under certain moisture contents and compaction levels. GDOT uses Figure 3.2 to generalize specific subgrade conditions and support values for pavement construction. Frequently, soils with SSVs of 2.0 or 2.5 are commonly excavated and replaced with a select material, as stated in GDOT standard specifications. This study focuses on two subgrade soils from areas with SSV of 2.5 (Coweta and Hall Counties) and one area with SSV of 2.0 (Gordon County). These North Georgia soils are

well-known for their weaker soil strength. Figure 3.2 shows the locations where the subgrade was acquired from and the respective SSVs of the counties' soils.

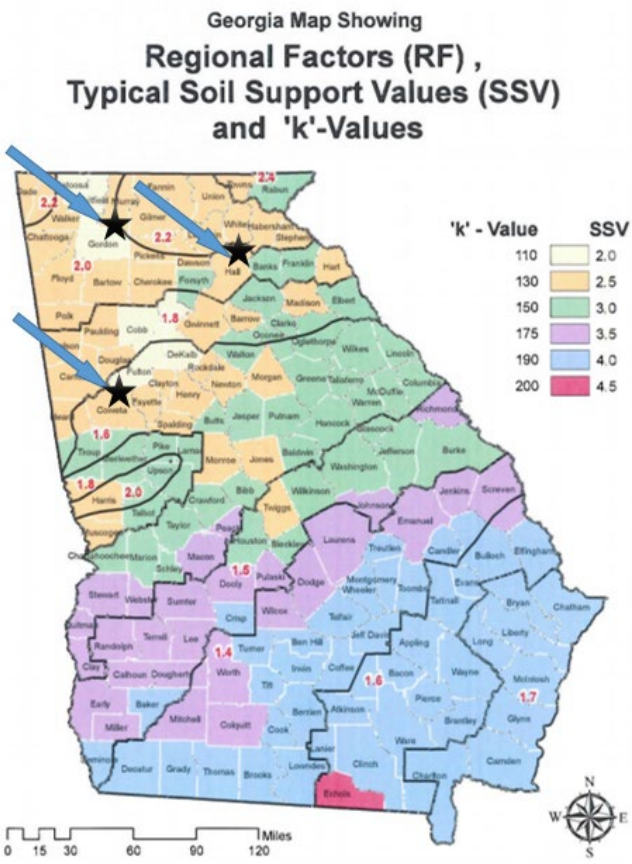

FIGURE 3.2

Locations of Subgrade Soil Investigated (GDOT, 2013)

3.2.2 Geogrid

The geogrid used in the study was Tensar® BX1200, a high density, extruded, and stretched polypropylene material. This geogrid was selected based on a geogrid aperture size that met the requirement that the gradation of the base course material lies between D50 and 2×(D85) of the aggregate fill, as recommended by Holtz et al. (2008). A biaxial geogrid with an aperture size of 1-in. (25.4 mm) × 1.3-in. (33 mm) fulfilled these characteristics

and was chosen for this study. BX1200 Geogrid specifications are shown in Table 3.3. These values are minimum average roll values determined in accordance with ASTM D4759-02.

TABLE 3.3
Geogrid Specifications

Index Properties	Units	Minimum Average Roll Value	
		MD	CD
Aperture Dimensions	in. (mm)	1.0 (25)	1.3 (33)
Minimum Rib Thickness	in. (mm)	0.05 (1.27)	0.05 (1.27)
Tensile Strength @ 2% Strain	lb/ft (kN/m)	410 (6.0)	620 (9.0)
Tensile Strength @ 5% Strain	lb/ft (kN/m)	810 (11.8)	1,340 (19.6)
Ultimate Tensile Strength	lb/ft (kN/m)	1,310 (19.2)	1,970 (28.8)

Note: MD = machine direction and CD = cross-machine direction

3.2.3 Geotextile

As discussed in the literature review, there are many different types of geotextiles. The individual properties of geotextiles dictate their performance and functions for use in different applications. The geosynthetic used for this study was a woven geotextile. More specifically, the Mirafi® HP270 geotextile was selected and is composed of high-tenacity polypropylene yarns that are woven into a network such that the yarns retain their relative position. Mirafi HP270 geotextile is inert to biological degradation and resistant to naturally encountered chemicals, alkalis, and acids. The specifications published for HP270 woven geotextile are shown in Table 3.4.

TABLE 3.4
Geotextile Properties

Mechanical Properties	Test Method	Unit	Minimum Average Roll Value	
			MD	CD
Tensile Strength (at Ultimate)	ASTM D4595	lb/ft (kN/m)	2,640 (38.5)	2,460 (35.9)
Tensile Strength (at 2% Strain)	ASTM D4595	lb/ft (kN/m)	504 (7.4)	600 (8.8)
Tensile Strength (at 5% Strain)	ASTM D4595	lb/ft (kN/m)	1,272 (18.6)	1,440 (21.0)
			Minimum Roll Value	
Flow Rate	ASTM D4491	gal/min/ft^2(l/min/m^2)	40 (1, 630)	
Permittivity	ASTM D4491	sec^{-1}	0.6	
			Maximum Opening Size	
Apparent Opening Size (AOS)	ASTM D4751	U.S. Sieve (mm)	30 (0.60)	

Note: MD = machine direction and CD = cross-machine direction

Values are listed for both the machine direction (MD) and the cross-machine direction (CD) in the table. These values are the tensile capacity for the geotextile in the parallel direction of the roadway (MD) and the perpendicular direction of the roadway (CD) and are different due to the specific weaving pattern during the manufacturing process. This specific geotextile was selected for several reasons.

Functionally, it acts as a filter between the subgrade and base layers, it acts as a separation, and it provides soil reinforcement. Most of the native soils in North Georgia contain high silt or clay percentages with the potential for localized bearing failures due to the fines migration from the subgrade into the base course layers when no separation exists. As the fine material migrates and mixes with the base course, a decrease in the structurally sound base course thickness occurs in addition to a lower density of the subgrade and

thereby decreasing the pavement structural number. For this study, the other selection criteria fulfilled by HP270 was for the product to be non-proprietary because of the governmental funding.

4. LARGE-SCALE TEST

4.1 Testing Matrix and Geosynthetic Placement Design

For this study, a large-scale Accelerated Testing Facility (ATF) was built at the University of Georgia's Structural Engineering Testing Hub (STRENGTH) laboratory in Athens, Georgia. The testing program consisted of 16 different individually constructed test specimens. Three subgrade samples were obtained from areas in North Georgia. The subgrade county locations were selected due to their low GDOT soil support value classification. GDOT uses SSV ranging from 2.0 to 4.5 to classify support capabilities of the subgrade for pavement construction, with lower SSVs indicating a weaker subgrade.

Subgrade moisture content is highly influential on the performance of the roadway and the stiffness of the layer; therefore, two different subgrade conditions were evaluated. The first condition was high moisture, weak condition (low CBR) of the subgrade. The second condition investigated was subgrade placed at its optimum moisture content, which explains how geosynthetics benefit roadways in relatively new, post-construction conditions.

The location of the geosynthetic in the region-specific base material, graded aggregate base layer was also varied. Geosynthetics are usually placed at the interface between the subgrade and the aggregate base because they help function as a separator and filter between the two materials, which maintains thickness and support to the overlying structure. However, other studies have found that for thicker base course layers a geosynthetic installed within the base course layer helps to improve the pavement performance (Al-Qadi et al., 2012). GDOT typically prepares a 12-in.-thick (305 mm) GAB layer with two 6-in. (152 mm) lifts. Therefore, the mid-height of the GAB layer was

studied also as a possible location for geosynthetic installment. Similar to all scientific experiments, control cases were also needed for a baseline to compare the effects of geosynthetics. Table 4.1 shows the summarized testing plan for this study in conjunction with a naming convention.

Large-scale rolling wheel test sections are labeled in a way to allow users to determine the controlling properties of each test. The first term of the test designation is the test number out of all large-scale testing performed within this study. The second term in the designation is the geosynthetic specification. This study includes results for control (C), geotextile (GT), geogrid (GG), and geotextile and geogrid combination (GC) reinforced test specimens. The third term is the soil strength condition, which includes "LCBR" for test sections with the subgrade prepared at a high moisture content creating a low CBR and "OMC" where the subgrade was prepared at its optimum moisture content. The fourth term indicates the location from where the subgrade was obtained. CA, GN, and HL are abbreviated from Coweta, Gordon, and Hall Counties. The fifth term stands for the location of the geosynthetic. "INT" represents the geosynthetic at the base–subgrade interface, "MH" indicates the geosynthetic at the mid-height of the base course, and "COM" indicates specimens that had both a geotextile at the interface and geogrid at the mid-height of the base course. The final term indicates which testing series the specimen is used in for load comparisons.

TABLE 4.1
Testing Plan

Testing Sequence	Test Designation	Soil Type	Soil SSV	Soil Condition	Geosynthetic Type	Location of Geosynthetic
1	T6-CL-LCBR-CA-INT-S1	Coweta	2.5	Low CBR	Control	NA
	T7-GT-LCBR-CA-INT-S1	Coweta		Low CBR	Geotextile	Interface
	T5-GG-LCBR-CA-INT-S1	Coweta		Low CBR	Geogrid	Interface
2	T4-CL-LCBR-GN-INT-S2	Gordon	2.0	Low CBR	Control	NA
	T8-GT-LCBR-GN-INT-S2	Gordon		Low CBR	Geotextile	Interface
	T3-GG-LCBR-GN-INT-S2	Gordon		Low CBR	Geogrid	Interface
3	T12-CL-OMC-GN-MH-S3	Gordon	2.0	OMC	Control	NA
	T14-GT-OMC-GN-MH-S3	Gordon		OMC	Geotextile	Mid-Height GAB
	T13-GG-OMC-GN-MH-S3	Gordon		OMC	Geogrid	Mid-Height GAB
4	T12-CL-OMC-GN-INT-S4	Gordon	2.0	OMC	Control	NA
	T17-GT-OMC-GN-INT-S4	Gordon		OMC	Geotextile	Interface
	T16-GG-OMC-GN-INT-S4	Gordon		OMC	Geogrid	Interface
5	T23-CL-OMC-HL-INT-S5	Hall	2.5	OMC	Control	NA
	T21-GT-OMC-HL-INT-S5	Hall		OMC	Geotextile	Interface
	T18-GG-OMC-HL-INT-S5	Hall		OMC	Geogrid	Interface
6	T23-CL-OMC-HL-INT-S6	Hall	2.5	OMC	Control	NA
	T22-GC-OMC-HL-COM-S6	Hall		OMC	Combined	Interface & Mid-Height
	T20-GG-OMC-HL-MH-S6	Hall		OMC	Geogrid	Mid-Height GAB

4.2 Large-Scale Testing Setup

The Accelerated Testing Facility was designed and fabricated based on a study described in the NZ Transport Agency Research Report 574 (Bagshaw et al., 2015). For the study, a large-scale rolling wheel testing apparatus was designed and built by the University of Georgia's Instrument Design and Fabrication Shop. The experimental testing configuration used a similar design to the NZ Transport Agency due to its large size and its ability to fit in an area shared with other structural and geotechnical research apparatus.

The testing apparatus consists of a 6-ft × 6-ft × 2-ft-deep (1.83 m × 1.83 m × 0.61 m) steel box with removable walls, which promotes easier construction and removal of samples post-testing. The box is welded onto four wheels, which allows for unidirectional movement during testing. Once the specimen is fully constructed and ready for testing, the specimen's wheels are placed in a 6-ft-long track under an MTS hydraulic actuator used to apply the wheel load during testing. A rotating motor is then used to track the testing apparatus back and forth under the constant loading at a speed of approximately 1 mph (0.447 m/s), which is similar to the speed of the sample in the NZ Transport study. This speed was determined to be conservative, as the subgrade soil experiences stress over an extended period of time. After testing, the motor is then removed, and the test specimen is deconstructed and prepared for future testing. The installed large-scale testing apparatus is shown in Figure 4.1. Further testing procedures are described in later portions of this document.

FIGURE 4.1

Large-Scale Testing Apparatus

4.2.1 Sample Fabrications and Compaction

Pavement layer thickness was selected to replicate the typical roadway conditions found in North Georgia. In North Georgia, due to the weak subgrade conditions of the area, a 12-in. (305 mm) aggregate base course is typically used regardless of the expected number of design ESALS. Therefore, for this study, 12 in. (305 mm) of GAB was prepared on top of a 12-in. (305 mm) underlying subgrade layer. Figure 4.2 shows the layer configuration. The testing apparatus allowed for relatively rapid test preparation and installation as compared to building a comparable highway test section in the field.

FIGURE 4.2

Layer Configuration

The subgrade material was hydrated or dried to the desired moisture content before being placed into the steel testing apparatus to start the construction process. The metal box was filled with loose subgrade material while ensuring a constant moisture content (according to ASTM D4643) after each bucketload was placed. The subgrade material was then compacted with a vibratory plate compactor.

After compaction of the subgrade, several preliminary, quality-control soil tests were performed to determine its condition. Four dynamic cone penetration strength measurements were taken according to ASTM D6951 (one from each quadrant), and one sand cone density measurement was taken according to ASTM D1556 near the middle of the specimen. Finally, a LWD test was performed at the center of the subgrade area to determine the layer stiffness. The LWD was acquired from GDOT near the end of the project period to help measure subgrade soils' stiffness. Therefore, LWD testing results are limited to three specimens. These pretesting results were then evaluated and compared to

the objective soil properties for the test. The subgrade layer was then instrumented with the sensors described in Section 4.2.2 – Large-Scale Testing Instrumentation of this report.

The second 12-in. (305 mm) layer of steel walls was then attached to the test specimen in preparation for the placement of the GAB material. If a geosynthetic was specified at the interface of the specimen, it was placed with the machined direction parallel to the wheel path, as it would be in the field. A 4-in.-thick (102 mm) memory foam was placed vertically alongside the walls to minimize boundary effects from the borders of the apparatus. Further, it was confirmed through trial testing that the metal box walls do not exert any boundary confining effects at the stated 2,250-lb (10 kN) wheel testing load with the use of the foam. A thin layer of GAB was then distributed over the geosynthetic, as shown in Figure 4.3, and the remaining pressure cells were then entrenched in the wheel path at their specified heights.

FIGURE 4.3

GAB Placed on Geogrid

When the instrumentation was sufficiently placed and protected, GAB was placed in the container with a first lift thickness of about 8 in. (203 mm). This GAB layer was then compacted with the vibratory plate compactor until it reached approximately 6 in. (152 mm). This method of placing two lifts is common for GDOT roadways for layer thicknesses greater than 8 in. (203 mm) in total depth. An additional 7 to 8 in. (178 to 203 mm) of GAB was then added to the test specimen to fill the box. The material was then compacted to a total GAB thickness of 12 in. (305 mm) and leveled to obtain a flat testing surface. The aforementioned quality assurance tests were then performed on the surface of the material similar to the subgrade layer. After the soil specimen was prepared, it was installed in the testing tracks under the hydraulic force transducer attached to the rotatable wheel, covered with plastic to prevent evaporation, and left for about 48 hours to allow the moisture to equalize throughout the specimen.

4.2.2 Large-Scale Testing Instrumentation

Several instruments were required to monitor the effects of geosynthetics in the pavement systems. Post-test forensic investigations revealed that a majority of the permanent deformation was found in the top 4 in. of the aggregate base course. Due to the thick base course layer, it was deemed that the deformation was not a good indicator of geosynthetic performance and thus, this study focuses on the stress reduction at the bottom of the aggregate base and top of the subgrade layers.

4.2.2.1 Pressure Cells

Pressure cells were installed in each specimen to measure in-ground total stresses during trafficking. The pressure cells used in this experiment are manufactured by Tokyo Sokki Kenkyujo Co., Ltd. and consist of stainless steel, with excellent corrosion resistance. They

measure minute displacement of pressure-sensitive areas due to their dual-diaphragm structure. The cells have a 2-in. (51 mm) outside diameter with a 1.4-in.-diameter (35.6 mm) pressure-sensing area and an ability to measure up to 29 psi (200 kPa) loading during testing. This smaller diameter pressure cell was selected to minimize the interruption of load distribution through the pavement layers to produce accurate results. In the testing specimen, the pressure cells were horizontally offset approximately 2 in. (51 mm) from each other to reduce the effect of higher pressure cells on the lower pressure cells.

Pressure Cell Setup and Calibration

The pressure cells were attached to a data logger and programmed with the instruNet World (iW) software with proper calibration factors provided by the pressure cell manufacturer. During wheel-load testing, each pressure cell was programmed to record a reading every 0.2 sec (5 Hz) to determine the maximum pressure experienced on each pass. The software provides output text files of the pressure readings, which were then analyzed using Microsoft Excel.

Before running large-scale rolling wheel testing experiments, the pressure cells were calibrated to determine the required factors to apply to the testing results acquired from the pressure cells. To do this, known weights in increments of 0.50 lb (0.23 kg) were placed on each cell starting with 0 lb and reaching to a maximum of 30.0 lb (13.6 kg). The output readings were then recorded for each weight and graphed in Excel versus the true weight. Figure 4.4 shows the calibration process used for pressure cell 4 of the true weight versus the output reading from the iW file.

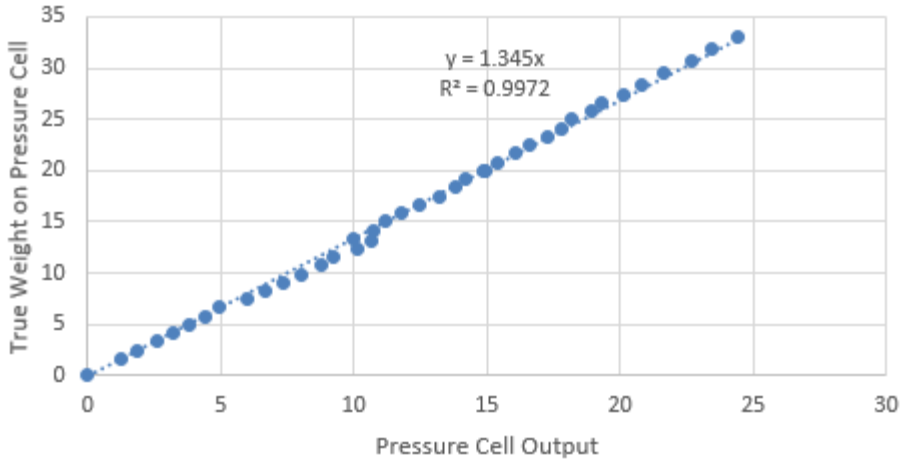

FIGURE 4.4

Calibration Data for Pressure Cell 4

A linear trend line was established that determined an average relationship between the actual weight on the pressure cell versus the pressure cell reading and an R^2 error estimation value. The R^2 values ranged from 0.988–0.999, demonstrating the accuracy in readings of pressures in the range of 0–30 lb (0–13.61 kg). The slope of the trend line was then divided by the area of the pressure cell–sensing surface, 1.49 in. (3.77 cm), to give a calibration factor in units of psi. Table 4.2 shows the calibration factors for each of the four pressure cells used in the experiments, alongside the error estimation.

TABLE 4.2
Pressure Cell Calibration Factors

Pressure Cell #	Calibration Factor	R^2
1	1.025118	.999
2	1.026195	.996
3	1.196229	.988
4	0.905724	.997

Pressure Cell Installation

Pressure cells were installed carefully in the soil specimens to prevent damage to the thin wire connecting to the data acquisition system. The cells were placed and surrounded by a poorly graded sand to create bedding to ensure constant accurate pressures over the cell area. In addition, cells were wrapped in a thin plastic covering to prevent water penetrating into the cells, which would render them unusable. Cell wires were wrapped in duct tape at the junction of the wire and pressure cell. Figure 4.5 shows a pressure cell installed in the GAB layer with the sand bedding.

FIGURE 4.5

Pressure Cell Installed in GAB Layer

Figure 4.6 shows the elevation view of the pressure cell configuration for the large-scale tests.

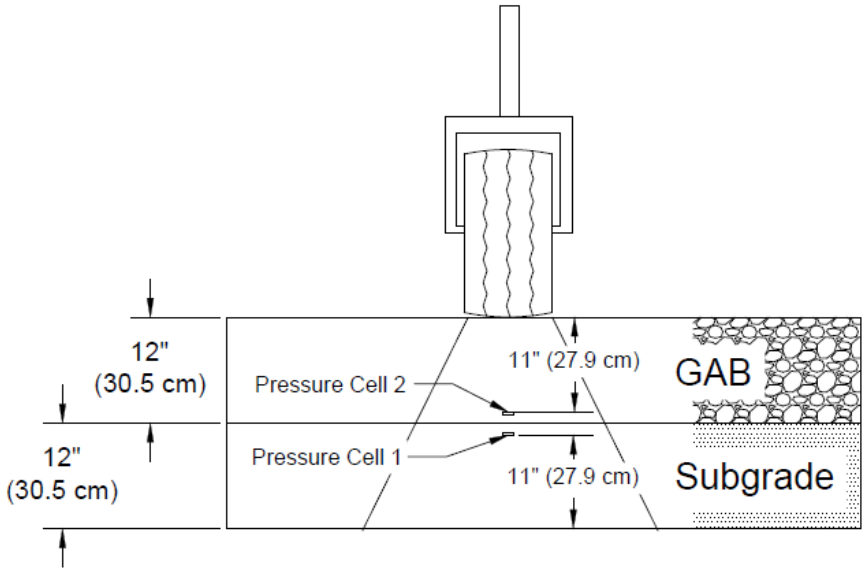

FIGURE 4.6

Pressure Cell Layout

4.2.2.2 Strain Gages

The geogrid was instrumented with foil strain gages on the underside of the geosynthetic (facing the subgrade) in both the machine direction parallel to the wheel path and the cross-machine direction perpendicular to the wheel path. Several attempts were made to attach strain gages to the geotextile. Initial geotextile strain measurements were deemed unreasonable and therefore were not included in this research.

The tensile strength of the geosynthetic can only be utilized when strain is introduced in the material from the vertical loading. The geosynthetic is then able to distribute that force laterally over its area instead of distributing it directly downward on the pavement foundation. Bauer and Abd El Halim (1987) utilized strain gages on a biaxial geogrid with 3 in. (76 mm) of granular aggregate placed over the geogrid. In that study, they found maximum strain encountered during the test was about 1.2%, which was three times smaller than the elastic limit of the geogrid used of 3.6%. This indicated that the

geosynthetic strength was not fully activated. A follow-up study was prepared with a weaker subgrade and found that the geogrid was forced to mobilize a higher strain, indicating more beneficial effects of the geogrid reinforcement than the stronger subgrade (Bauer and Abd El Halmin, 1987). A more recent study by Tingle and Jersey (2009) found that strain gage data showed that geogrid strain magnitude was much less than the geotextile. The geotextile exhibited strain ranging from 1.0–4.5%, while the geogrid experienced 0.1–2.1%. All strain was localized along the wheel path area and was highest in the longitudinal direction.

4.2.2.3 Piezometer

A vibrating wire (VW) piezometer was used to measure pore water pressure throughout testing. The piezometer was installed approximately at the mid-height of the subgrade under the wheel path of the specimen to determine the PWP during rolling wheel load trafficking. Piezometer results indicate that no PWP was developed during the large-scale rolling wheel tests.

4.2.3 Moving Wheel Load Applications

A typical semi-truck tire with a 40-in. (102 cm) diameter and a load application area diameter of 10 in. (254 mm) was attached to the bottom of the actuator to transfer the load onto the tracking test specimen. A finite element analysis (FEA) in ANSYS v18.2 was simulated to determine the load transferred from a 9,000-lb (4082 kg) tire load through an 8-in.-thick (203 mm) asphalt layer. It was determined that approximately 25% or 2,250 lb (1021 kg) were transferred from the bottom of the AC layer to the top of the GAB layer. During the testing, this 2,250-lb (1021 kg) load was then applied to the stationary testing specimen, and all instrumentation is checked to ensure functionality. When deemed

successful, the motor to the crank arm was started and moved the specimen at approximately 1 mph (1.61 km/h). After 5400 total passes were completed, the motor was disconnected, and data were then exported from the acquisition system for analysis.

4.3 Preliminary Tests

The use of a large-scale rolling wheel testing apparatus allows for the rapid construction and testing of different test section properties. The construction of the test sections in this study was completed with a defined procedure to minimize the differences of subgrade and GAB strength and support conditions between specimens, which is often difficult to accomplish in full-scale field testing over artificial and in situ subgrade conditions. To ensure similar conditions between tests, several quality assurance (QA) / quality control (QC) measurements of the subgrade and GAB layer are needed, including the measurement of density, moisture content, stiffness, and resilient modulus. In addition to the quality control measurements, several different measures were taken to simulate accurate traffic conditions and reduce boundary effects of the walls of the apparatus. Several measurements were performed pre-construction, during testing, and post-construction to determine the effect of the geosynthetic on pavements. These tests allow for the complete effect of geosynthetics on the stress distribution, PWP formation, and stress stiffening or softening effect of the GAB and subgrade layers.

4.3.1 Sand Cone Test

To produce testing results that simulate conditions in the field, test specimens must be constructed to similar standards as those required in the field by GDOT specifications. Pavements are constructed on compacted subgrade and GAB layers. Construction requirements usually require a certain level of compaction of a material compared to its

maximum dry density property. In order to measure a level of compaction, several apparatus can be used. The most prevalent measurement of density in the field is with the nuclear gauge, although there is a growing interest in moving to non-nuclear–based testing for a variety of reasons. For this study, the sand cone test method was determined to be the most viable option due to the availability of the apparatus and the research personnel's experience with testing using the apparatus.

The sand cone test method is used to determine the density and water content of compacted soils placed during the construction of earth embankments, road fill, and structural backfill. It is often used as a basis of acceptance for soils compacted to a specified density or percentage of a maximum density. For this study, a sand cone test was performed on each layer of subgrade and GAB after compaction.

4.3.2 Dynamic Cone Penetration Test

Historically, many of the QA/QC measurements of GAB and subgrade layers have been based on target density values with respect to the theoretical maximum density values determined in the lab. Recently, with the rise in popularity and implementation of mechanistic–empirical (M-E) design, which does not use density as an input value, new measurements such as resilient modulus values are needed and determined from QC tests. This increase in interest in modulus-based compaction control procedures requires new colorations and testing procedures to determine the inputs into the M-E software. Though the density tests and moisture content tests of GAB layers are straightforward and practical, they do not provide any direct colorations about layer modulus or shear strength of the system.

For quality control, most states use the density of both the unbound base and in-place subgrade even though density is not a load-bearing indicator. Due to the high costs of repairing roadways that failed due to poor base or subgrade quality, it is imperative to monitor and improve materials before finishing pavement placement with paving. The pavement performance is highly influenced by the material quality and thickness of pavement layers and uniformity. One technique commonly used by state highway agencies is proof rolling, which is a process that verifies the quality of the unbound material. The downside of proof rolling is that it does not accurately measure the subgrade and base course materials' modulus and stiffness. Additionally, proof rolling does not indicate the profile through the depths of the pavement. The stiffness of subgrade and base layers are dependent on several different factors, including moisture, density, soil type, and the magnitude of stress level. One factor commonly measured for field testing verification is the density of the material using a nuclear density gauge. However, this measure is not sufficient as a standalone method because it fails to give a representative stiffness value and can only test shallow layers. Dynamic cone penetration tests defined in ASTM D6951 allow users to evaluate the in situ stiffness of the base course and subgrade layers quickly and in a straightforward manner.

Engineers commonly modify or correct soil characteristics using the DCP test in the field before paving occurs by evaluating the stiffness and uniformity of the subgrade and base course layer. DCP testing is a simple process in which a free-falling hammer strikes the cone of the apparatus causing the cone to penetrate the base course or subgrade material. Each blow is measured and denoted as a penetration index with a unit of mm/blow.

This measurement indicates the stiffness and uniformity of the material, with a larger penetration index indicating a weaker material.

The DCP can be used to estimate the strength characteristics of fine- and coarse-grained soils, granular construction materials, and weak stabilized or modified materials. It is important to note that DCP measurement results in a field or in situ CBR and will not typically correlate with the laboratory or soaked CBR of the same material. The test is, thus, intended to evaluate the in situ strength of a material under existing field conditions.

For this study, eight DCP tests were performed on each specimen. A DCP test was run in each of the four corners of the testing specimen approximately 12 in. (305 mm) from each side on both the subgrade and GAB layers. These tests ensured a consistent level of compaction and stiffness throughout the specimen and from test to test in order to ensure test results were due to the performance of the geosynthetic.

4.3.3 Moisture Content

To accurately determine the effects of using geosynthetics in pavement applications, the moisture content between control and geosynthetic-reinforced test sections must be similar. Because of the large volume of subgrade and GAB material required to build test specimens, several different moisture content checks were required. The moisture content of the layer is measured using a direct method, the microwave oven method, which is used to make a gravimetric moisture measurement during pavement construction. The advantage of using this method is the ease and relatively inexpensive cost.

To determine the moisture content of subgrade and GAB soils in this study, ASTM D4643 was followed. This test method outlines procedures for determining the

water content of soils by incrementally drying soil in a microwave oven and is used when more rapid results are desired to expedite other phases of testing.

4.3.4 Light Weight Deflectometer Test

While the DCP is commonly utilized to evaluate the strength of pavement layers, the LWD can be used to measure the stiffness of unbound layers. In practice, the LWD is often used to estimate compaction level and load-bearing capacity of subgrade and unbound aggregate layers. When evaluating the effects of geosynthetics on pavement layer stiffness, the LWD measurements can determine the permanent deformation characteristics of pavement structures (Reck, 2009). DCPs and LWDs are vital for the investigation in order to understand the complete effects that geosynthetics have on the stiffness and strength of pavement layers along the depth (Reck, 2009). There is an absence of studies that investigate the influence of geosynthetics on the post-trafficked stiffness and strength of pavement layers. Therefore, this study is designed to focus on the strength and stiffness differences in subgrade and aggregate base course layers with/without geosynthetics between post-construction and post-trafficking.

4.3.5 Preliminary Test Results and Discussion

The pretesting QC results shown in Table 4.3 were used to determine consistency between test specimens in order to attribute the differences in specimen performance exclusively to the geosynthetic. The pretest results concluded the repeatability of the large-scale test preparation and verified that pressure reduction in specimens was attributed solely to the inclusion of the geosynthetic.

TABLE 4.3
Pretesting Results

Test Number***	Subgrade			GAB		
	DCP Average mm/blow (in./blow)	Average LWD Modulus (psi/MPa)	Moisture Content (%)	DCP Average mm/blow (in./blow)	Average LWD Modulus (psi/MPa)	Moisture Content (%)
T6-CL-LCBR-CA-INT-S1	26.32 (1.04)	2,550/17.58	24.8	3.96 (0.16)	N/A	7.3
T7-GT-LCBR-CA-INT-S1	21.95 (0.86)		26.6	3.10 (0.12)		5.4
T5-GG-LCBR-CA-INT-S1	22.95 (0.90)		26.4	3.70 (0.15)		4.8
T4-CL-LCBR-GN-INT-S2	24.22 (0.95)	1,020/7.03	34.7	3.76 (0.15)	N/A	4.7
T8-GT-LCBR-GN-INT-S2	13.43 (0.53)		29.7	5.51 (0.22)		4.4
T3-GG-LCBR-GN-INT-S2	17.81 (0.70)		33.2	2.31 (0.09)		5.4
T12-CL-OMC-GN-MH-S3	8.46 (0.33)	2,170/14.96	19.6	4.07 (0.16)	N/A	4.9
T14-GT-OMC-GN-MH-S3	8.68 (0.42)		23.3	3.41 (0.13)		4.6
T13-GG-OMC-GN-MH-S3	8.47 (0.33)		19.6	3.07 (0.12)		5.0
T12-CL-OMC-GN-INT-S4	8.46 (0.33)	2,170/14.96	19.6	4.07 (0.16)	N/A	4.9
T17-GT-OMC-GN-INT-S4	8.10 (0.32)		21.6	3.52 (0.14)		5.8
T16-GG-OMC-GN-INT-S4	8.10 (0.32)		21.8	3.78 (0.15)		7.8
T23-CL-OMC-HL-INT-S5	14.17 (0.56)	2,560/ 17.65	14.6	2.89 (0.11)	11,245/77.5	7.7
T21-GT-OMC-HL-INT-S5	13.97 (0.55)		15.9	2.49 (0.10)		6.3
T18-GG-OMC-HL-INT-S5	12.00 (0.47)		17.4	3.99 (0.16)		6.3
T23-CL-OMC-HL-COM-S6	14.17 (0.56)	2,560/ 17.65	14.6	2.89 (0.11)	11,255/77.6	7.7
T22-GC-OMC-HL-INT-S6	14.25 (0.56)		14.4	3.57 (0.14)		6.2
T20-GG-OMC-HL-MH-S6	12.00 (0.47)		17.4	3.88 (0.15)		5.6

*** See “Testing Program Design” section for test number descriptions

Several field LWD measurements were conducted from an active roadway construction site of the same subgrade soil. These measurements verified that the modulus of the experimental test specimen was similar to field modulus values. Figure 4.7 shows both the average laboratory-compacted specimen's modulus and the field-compacted subgrade modulus measured by LWD. While the subgrade modulus of the cut sections is relatively higher than the laboratory-compacted specimens, the field fill sections are much closer to the laboratory modulus. The results prove that the test specimen's modulus is similar to field testing results, validating the compaction procedure.

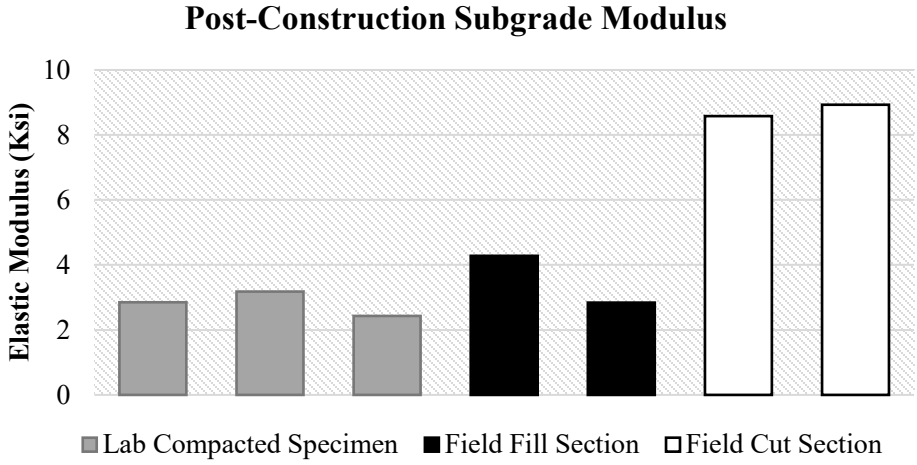

FIGURE 4.7

Validation of Subgrade Compaction Modulus

4.3.6 Confining Pressure at Steel Frame

It was confirmed through trial testing that the metal box walls do not exert any significant boundary confining effects at the stated 2,250-lb (10 kN) wheel testing load. A large-scale test specimen was prepared without the use of memory foam aligning the inside walls of the large-scale box. A load of 2,000 lb (8.9 kN) was exerted on the center of the specimen via the truck-sized wheel and slowly increased to 9,000 lb (40 kN) to measure the

horizontal pressures against the wall. Figures 4.8 and 4.9 illustrate the measured horizontal pressures at the center of each layer with the pressure cells placed against the wall closest to the loading plane.

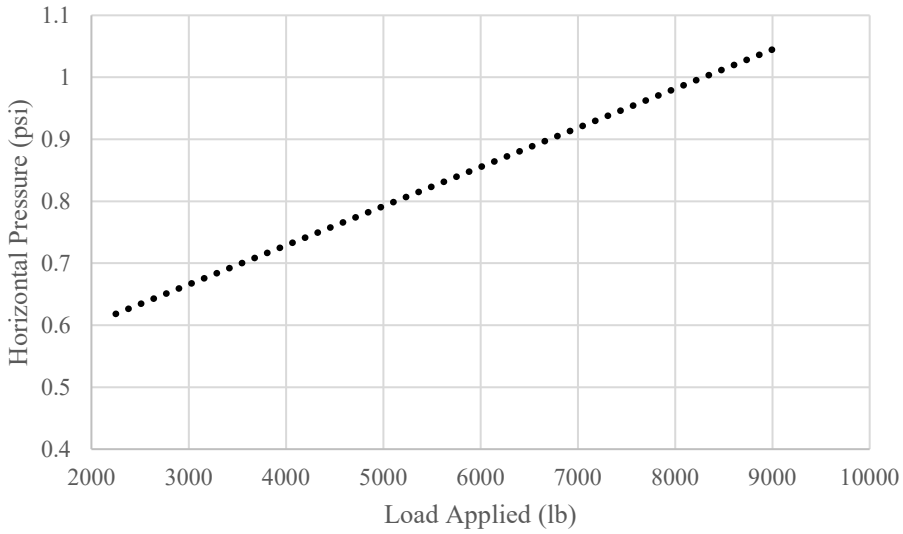

FIGURE 4.9

Preliminary Testing: Horizontal GAB Pressure at Wall of Large-Scale Box

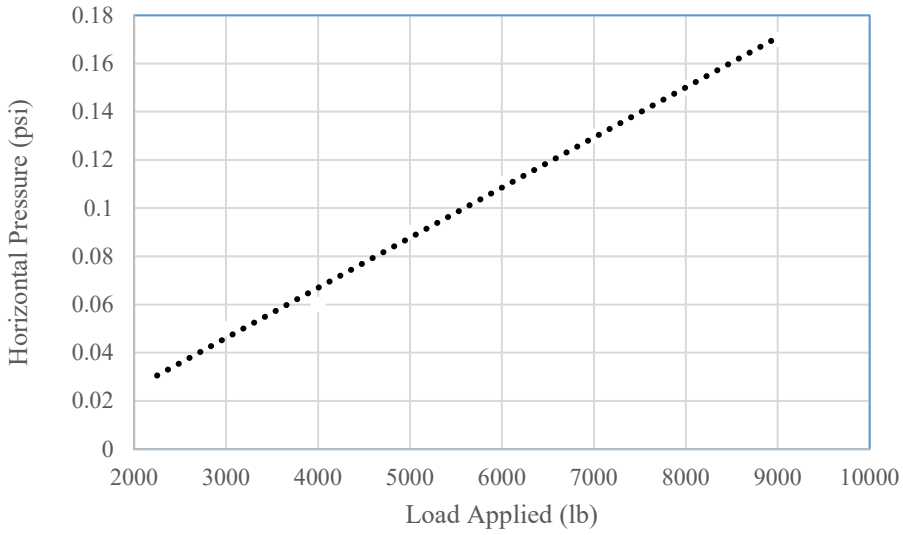

FIGURE 4.8

Preliminary Testing: Horizontal Subgrade Soil Pressure at Wall of Large-Scale Box

With an applied load of 2,250 lb (10 kN), the maximum amount of horizontal pressure felt by the outer walls of the large-scale box was approximately 0.6 psi (4.3 kPa). With the addition of 3-in.-thick (76 mm) memory foam, this small amount of pressure was considered insignificant. Because the simulated roadway was built in a steel container, specific adaptations were required at the boundary of the soil–container interface to prevent artificial boundaries that would not occur in full-scale pavement construction. Measurement errors in the data were possible from the pressure sensors absorbing readings from the reflection of waves at the boundary of the container. To minimize such erroneous data and minimize the edge confinement effect, a 4-in.-thick (102 mm) insulating foam was used to dampen the edges of the container. Figure 4.10 shows the testing apparatus during construction with the foam placed around the boundary of the box.

FIGURE 4.10

Memory Foam Installed Around the Edges of the Steel Container

4.4 Large-Scale Test Results

4.4.1 Pressure Measurements with Geosynthetic-Reinforced Pavement Foundation

In situ pressure cells help demonstrate the performance of geosynthetics by registering reduced stress in subgrade layers. Average pressure readings throughout the depth of each test specimen were measured (see Figure 4.11).

Figures 4.11 (a) and (b) show pressure measurements in both Coweta and Gordon County soils prepared with high moisture content. The weaker subgrade soil (Gordon County) creates higher pressures at the bottom of the GAB layer than the stronger Coweta County soils. As expected, the geogrid was observed to perform better than the geotextile, resulting in the reduction of stress in both the bottom of the GAB and top of the subgrade. Since the friction between GAB and subgrade soils reduces as subgrade condition becomes more wet and weaker, the load distribution capability of the geotextile through friction reduces. In this case, the dominant function of the geotextile at weak subgrade condition is separation to minimize the migration of fines.

On the other hand, the load distribution capability of the geotextile increases as the subgrade becomes stiffer and the friction at the interface increases. Specimen T5's vertical pressure at the top of the subgrade was not measured. Based on the decreasing trend of vertical pressure in other cases, it is expected that vertical pressure at the top of the subgrade with geogrid at the interlayer continues to decrease.

Figures 4.11 (c) and (d) show pressure distribution in Coweta and Gordon County soils prepared at optimum moisture content. The results allow for comparisons between geosynthetic products and various placement locations within pavement systems. The geosynthetics were placed at either the mid-height of the aggregate base layer or the interface of the subgrade and aggregate base. The geotextile performed better at the base–

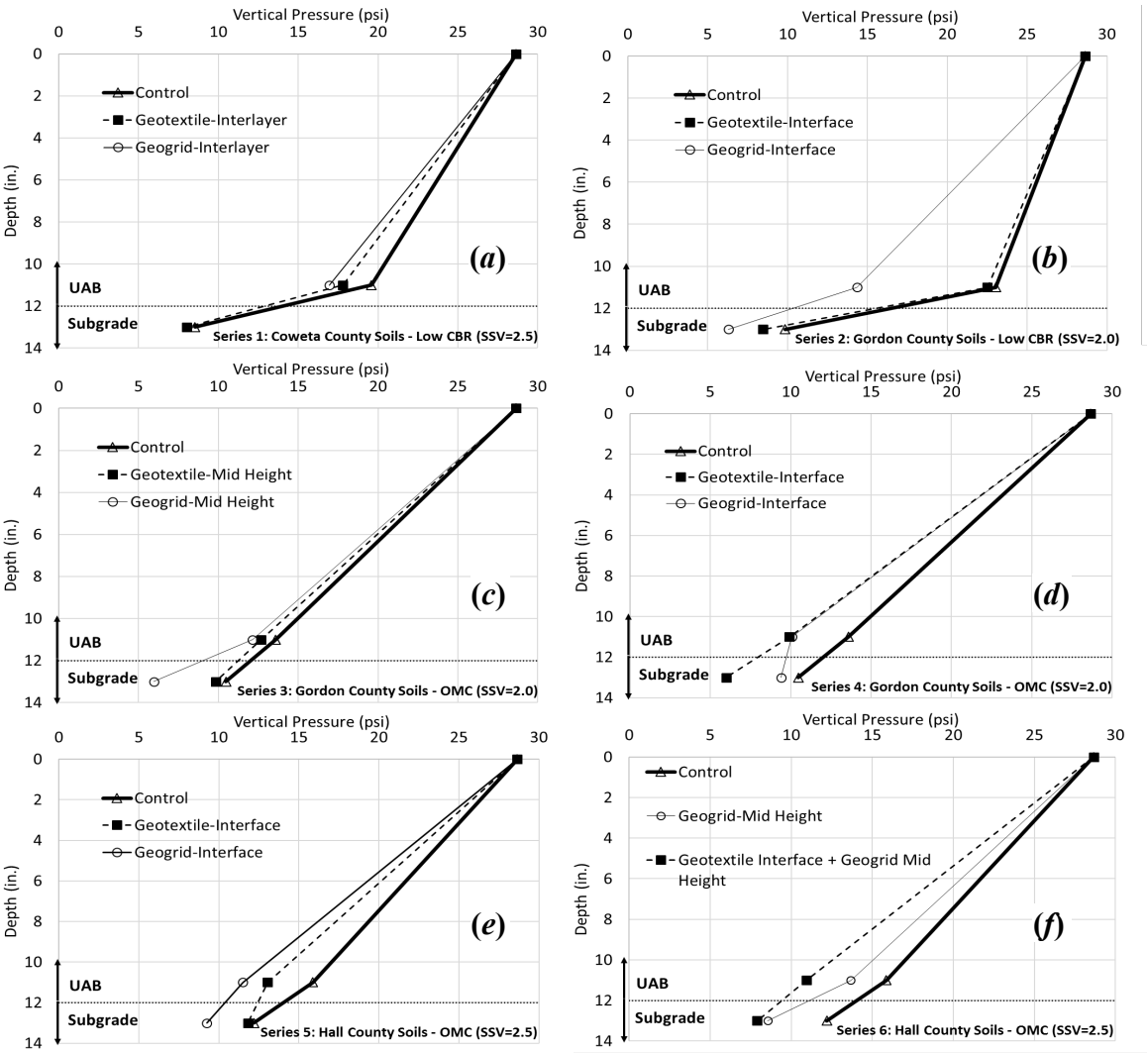

Test #	Subgrade	SSV	LCBR/OMC	Location	Geosynthetic	% Reduction in pressure (from the surface pressure)
T6	Coweta	2.5	LCBR	Control	None	Bot of GAB-30% / Top of Subg-70%
T7				Interface	GT	**37%** / 71%
T5				Interface	GG	**40%** / 70%
T4	Gordon	2.0	LCBR	Control	None	18% / 65%
T8				Interface	GT	**20%** / 70%
T3				Interface	GG	**49%** / 78%
T12	Gordon	2.0	OMC	Control	None	52% / 63%
T14				Mid-height	GT	**55%** / 65%
T13				Mid-height	GG	**57%** / 79%
T17	Gordon	2.0	OMC	Interface	GT	**65%** / 79%
T16				Interface	GG	64% / <-66%
T23	Hall	2.5	OMC	Control	None	**43%** / 57%
T21				Mid-height	GT	**53%** / 58%
T18				Mid-height	GG	**43%** / 67%
T23	Hall	2.5	OMC	Interface	GG	51% / 70%
T22				Interface/Mid-height	GG/GT	61% / 72%

(g)

Note: To convert PSI readings to kPa, divide value by 6.89.

FIGURE 4.11

Pressure Results: (a) Series 1, (b) Series 2, (c) Series 3, (d) Series 4, (e) Series 5, (f) Series 6, (g) % Vertical Pressure Reduction

subgrade interface than the mid-height of the GAB, resultingta in higher stress reductions than the geogrid placed at the interface. For subgrade soils prepared at OMC, the friction at the interface between geotextile and GAB increases and helps distribute the load better over a given area. A geotextile placed at the interface exhibits similar stress reductions as the geogrid placed at mid-height of the GAB layer. As shown in Table 4.3, DCP results indicate that this subgrade condition had the highest strength (lowest penetration rate) out of all the soil conditions.

Figures 4.11 (e) and (f) show the pressure distribution for Hall County subgrade soils with different locations of geosynthetics. The DCP results illustrate that the strength of the subgrade was higher than the low CBR conditions but lower than the Gordon County CBR results. Because the subgrade was weaker than the Gordon County OMC results, the results indicate the geogrid still performs better than the geotextile for weaker soils when placed at the interface. Geogrid placed at mid-height had higher pressure reductions at the top of the subgrade than when placed at the interface. The pressure reduction at the bottom of the GAB or the top of the subgrade is greatly influenced by the location of geosynthetics. When geotextile was placed at the interface between the GAB and the subgrade, higher pressure reduction was observed at the bottom of the GAB, while less pressure reduction was observed at the top of the subgrade. Higher pressure reduction at the top of the subgrade was observed when geogrid was placed at the middle of the GAB. The test that included both the geogrid at mid-height and geotextile at the interface, T22, exhibited high pressure reductions of the testing series. The T18 vertical pressure at the bottom of the GAB was not measured. Figure 4.11 (g) presents the percent pressure reductions in the

GAB and subgrade layers from the applied surface pressure. Specimen T17 shows the highest pressure reduction of all test specimens.

4.4.2 Strain Measurements with Geogrid-Reinforced Pavement Foundation

In this study, measurements were made in the geogrid test sections to investigate the load-induced strain during trafficking. The gages were placed on the geogrid directly under the wheel path in the center of the testing apparatus. Strain gages designated as 'MD' are placed parallel to the wheel path directly under the tire load in the middle of the testing apparatus. Strain gages designated as 'XMD' are placed transverse to the wheel path under the wheel load. Figure 4.12 shows the average recorded strain response of the geogrid at the end of trafficking. The strain readings ranged from 0.45% to 0.15%. The lower strain measurements may be attributed to the thick (12-in.) aggregate base layer on top of the geosynthetic.

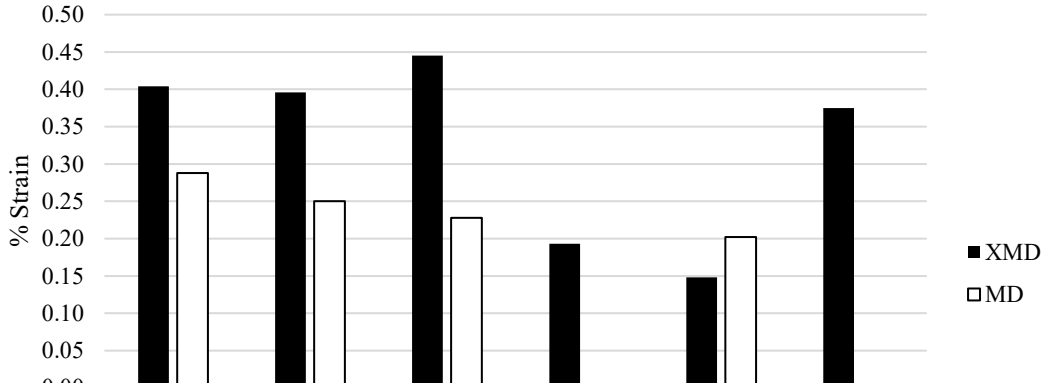

	T5-GG-LCBR-CA-INT-S1	T3-GG-LCBR-GN-INT-S2	T13-GG-OMC-GN-MH-S3	T16-GG-OMC-GN-INT-S4	T18-GG-OMC-HL-INT-S5	T20-GG-OMC-HL-MH-S6
XMD	0.404	0.396	0.445	0.193	0.148	0.375
MD	0.288	0.25	0.228		0.202	

FIGURE 4.12

Geogrid Strain Response

The geogrid accumulated strain as the number of traffic repetitions increased. All strain measurements started at a zero reading and increased as permanent deformation increased, indicating the utilization of the geogrid in the stress reduction. Several strain gages in the machine direction detached early during the traffic loadings, which prohibited measurements of strain in the longitudinal direction. Strain in the geotextile was not measured as noted in Section 2.2.2, Large-Scale Testing Instrumentation, of this report.

An analysis of the strain data results produces similar trends as previous geosynthetic studies. T5 and T3 have similar strain ra$_{NA}$ in both the XMD a$_{NA}$ MD readings. This similarity is likely due to the low CBR with high moisture content condition of subgrade soils. Due to the low support capabilities of the weak subgrade, more of the geogrid is mobilized, causing higher strain readings. T16 and T18 show that subgrade prepared at a higher strength can support the load better and therefore utilizes less of the geogrid strength shown with a smaller percent strain in the XMD. This upholds the findings of Bauer and Abd El Halim (2009). A comparison of T13 and T16 shows that geogrid placed at mid-height of GAB mobilizes more strength of the geogrid in the XMD due to the higher stress intensity at the mid-height than the bottom of the GAB. This trend is again found in the comparisons of T18 and T20. The strain measurement in the geogrid placed at mid-height is similar to the strain found in the low CBR test specimens.

4.5 Effect of Geosynthetics on Strength and Stiffness Improvement of Pavement Foundation Post-Trafficking

Post-test forensic investigations revealed that a majority of the permanent deformation was found in the top 4 in. (102 mm) of the aggregate base course before tension membrane effect is initiated. For the thick base course layer, therefore, it is deemed that the

deformation is not indicative of geosynthetic performance. As such, this study focuses on the stress reduction at the bottom of the aggregate base and top of the subgrade layers.

This portion of the study investigates the effect of geosynthetics on stiffness and strength variations after experiencing rolling wheel traffic loading by using a large-scale test apparatus. After trafficking on large-scale test specimens was completed, a series of post-tests was executed, involving a dynamic cone penetrometer and light wheel deflectometer to measure the changes of stiffness and strength of the pavement foundation. This allowed for an evaluation of the differences in support capabilities between the control and the geosynthetically reinforced test sections. Further, this analysis provides insight on the material behavior throughout the depth of the layers and helps form conclusions on why pressure and deformation reduction are commonly found in geosynthetically reinforced roadways.

Several significant large-scale geosynthetic studies have incorporated the use of the DCP testing to determine subgrade strength and ensure consistent compaction throughout the test area (Cuelho et al., 2011; Cuelho and Perkins, 2009; Tang et al., 2014; Al-Qadi et al., 2008). Cuelho and Perkins (2009) used the DCP to evaluate the subgrade conditions and found that the post-trafficking subgrade strength did not change dramatically from the pre-trafficking strength. A follow-up study by Cuelho et al. (2011) used the DCP to investigate the top 3 in. (76 mm) of subgrade material both post-construction and post-trafficking and observed a higher strength of subgrade in the post-trafficked test sections. Additionally, the report states that the increase in subgrade strength from the two measurements could have been a result of the extended period between measurements and the significant moisture loss of the subgrade during this time.

In addition to the evaluation of subgrade strength, the DCP can be used to measure strength changes in the aggregate base course due to the use of geosynthetics. Tingle and Jersey (2009) performed DCP tests both post-construction and post-trafficking to determine the changes in the strength of both the aggregate base course and subgrade layers. They found an increase in strength in the base course due to cementation during curing and over the test period. Figure 4.13 shows the capabilities of the DCP to show this increase in strength along the depth of the layer. The dashed lines indicate the post-trafficked measurements with higher strength readings than their post-construction counterparts. There were no significant changes in the strength of the subgrade. This test did not perform a control test section, thus no comparison can be made between the geosynthetic and control sections of DCP strength.

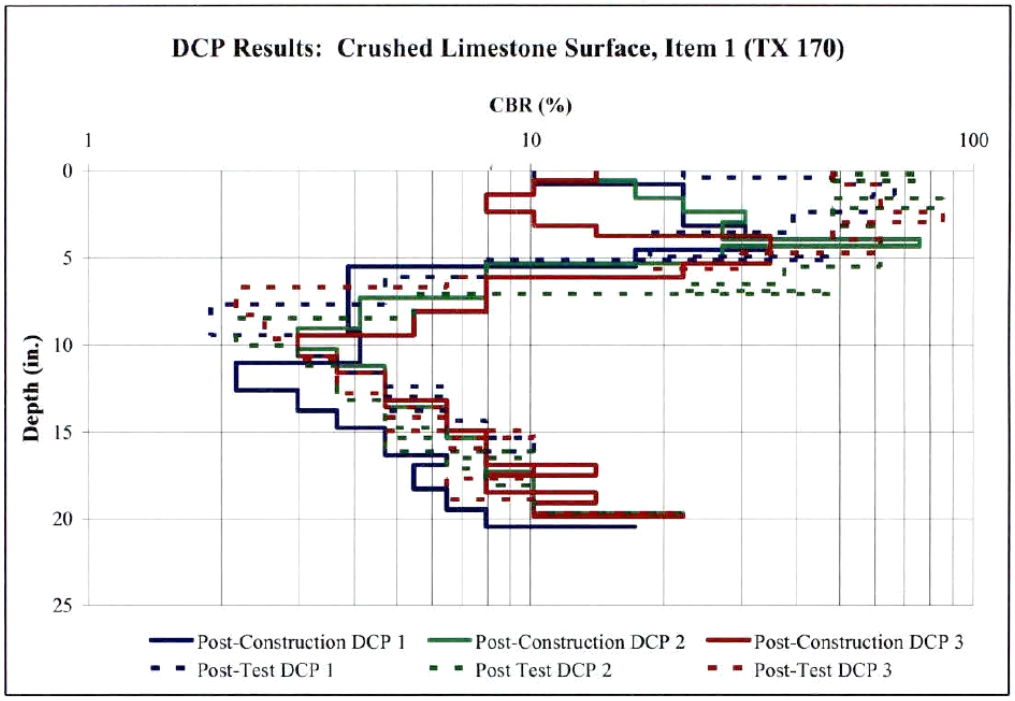

Note: To convert inches readings to centimeters, multiply value by 2.54.

FIGURE 4.13

DCP Test Results Along the Depth (Tingle and Jersey, 2009)

Geosynthetics used in pavement foundation layers help stiffen and strengthen the aggregate base layer. For geogrid, aggregate particles interlock within the geogrid, which creates confinement within the apertures. The depth of the aggregate base layer influences this interlock with higher confinement found closest to the geogrid (Cavanaugh et al., 2008). Figure 4.14 shows this confinement effect.

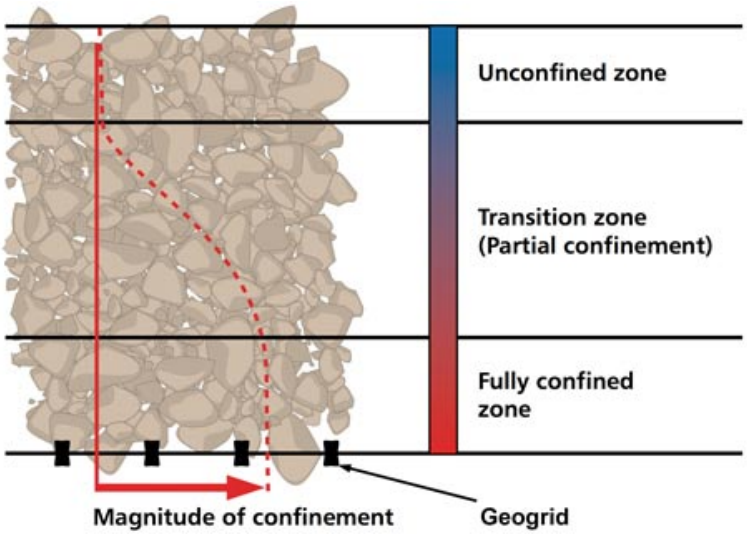

FIGURE 4.14

Zone of Influence of the Geogrid (Cavanaugh et al., 2008)

4.5.1 Test Methods

To determine the effects of the geosynthetics on the stiffness of the post-trafficked aggregate base and subgrade layers, three different individual unbound pavement test specimens were compared. This study was designed to focus on the effects of using a geotextile at the interface on the stiffness in pavement layers. To investigate this, a control and geotextile test specimen were planned to make comparisons. A third test specimen was included in this study to see how adding a second geosynthetic, a biaxial geogrid, in this case, would affect the pavement layers compared to the single geotextile reinforcement and

control test specimens. T23, identified as the control test section, had no geosynthetic reinforcement installed. T21 consisted of a woven geotextile placed at the base–subgrade interface. T22 included a woven geotextile at the interface and an extruded biaxial geogrid placed at the mid-height of the GAB. Table 4.4 shows a summarized testing matrix, while Figure 4.15 shows the locations of the geosynthetic for each test type in profile view.

TABLE 4.4
Testing Matrix

Test Type	Test Number
Control	T23
Geotextile at Interface	T21
Geotextile at Interface & Geogrid at Mid-Height of GAB	T22

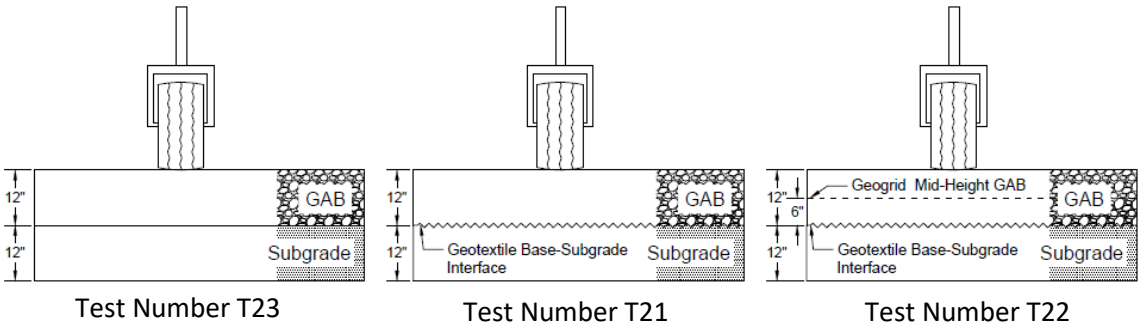

FIGURE 4.15
Profile View of Test Sections

DCP and LWD readings were split into two different categories. The post-construction readings gave an initial reading and were performed after compaction of each layer. The second category, the post-traffic readings, were taken after the test specimen had been trafficked by the wheel load. Because soil properties, such as moisture content, likely had changed between the post-construction and post-traffic time periods, measurements

both in the wheel path and outside the wheel path were compared to see the change due to trafficking. Since the measurements taken outside the wheel path had not been trafficked, they were designated as post-construction measurements.

The post-construction DCP test categories were taken with 12-in. (305 mm) penetration depths in both the GAB and subgrade layers. Several measurements were taken in various locations in the specimen and averaged together for a single DCP reading. The LWD was used after test specimen construction to determine the stiffness regarding an elastic modulus of the underlying layers. The post-construction measurements with the LWD were determined with a plate of approximately 6-in. (150 mm) diameter in the center of the GAB and subgrade layers due to the thin layer depths.

The second category denoted as post-traffic measurements required additional DCP and LWD readings. After trafficking, two DCP readings were taken inside the wheel path to determine the strength change along the depth of the aggregate base layer due to the traffic loading. LWD testing was performed in the wheel path post-traffic to determine the stiffness increase of the aggregate base and subgrade soils. Figure 4.16 illustrates the LWD testing on the subgrade layer post-construction.

FIGURE 4.16

LWD Measurements on the Subgrade Layer

4.5.2 Results and Analysis

The test results and data analysis shown herein are categorized into the two testing methods: LWD results, and DCP results. The mechanical properties (stiffness and strength) in pavement foundation are highly influential on pavement responses, and this analysis investigates how a geotextile and a geosynthetic combination affect these properties.

4.5.2.1 LWD Test Resuts

LWD results indicate the stiffness of the pavement foundation. The post-construction values illustrate that the modulus of the GAB layer is consistent with each test specimen. Figure 4.17 shows that the GAB elastic modulus increases after trafficking in all three test sections. The inclusion of the geosynthetic has little influence in the stiffness of the upper portions of the GAB layer post-construction because all three specimens had similar modulus values.

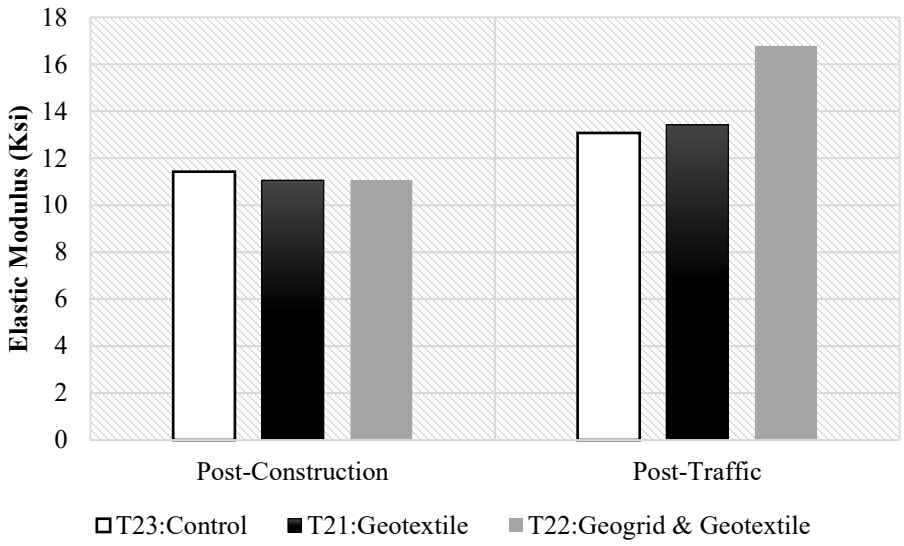

Note: To convert ksi readings to kPa, multiply value by 6894.

FIGURE 4.17

GAB Elastic Modulus LWD Readings

In all cases, the modulus of the GAB layer increases from the untrafficked (post-construction) to trafficked portions of the specimen due to the densification of the material from the rolling wheel loadings. The control case for the post-traffic section shows that it has the lowest modulus increase at 14.4%, which is likely the result of the absence of a geosynthetic to provide additional stiffness. The geotextile increased the modulus 7% over the control test specimen with a total modulus increase of 21.4%. Using the geogrid and geotextile in combination increased the modulus by 51.4%. Because the stiffness and strength of pavement layers correlate, these results corroborate the strength trends found by Tingle and Jersey (2009). In both studies, the geosynthetic increased the post-traffic modulus or strength of the aggregate base layer when compared to the post-construction modulus. This stiffening of the base course is likely one of the causes of reduction in pressure exhibited in geosynthetically reinforced pavements.

4.5.2.2 DCP Test Results

Measurements shown in Figure 4.18 represent the post-traffic DCP readings taken from inside the wheel path. The number of blows required to penetrate 1 in. (25 mm) of the pavement layers is presented as the circular data points. The black line indicates the base subgrade interface and the location where the geotextile was placed for Tests 2 and 3. DCP results show the strength of the pavement layers along the depth. The points farther to the right indicate a stronger layer because they require more blows to penetrate each inch. Conversely, the points further to the left indicate a weaker layer.

Several trends are found in the DCP results. Comparing the control (T23), and the geotextile-reinforced (T21) test specimen illustrates that the geotextile effectively strengthens about 4 in. (102 mm) of the GAB located directly on top of it with its friction. Both test sections show about the same strength at the 4-in. (102 mm) depth, but as the depth increases, the geosynthetic stiffens the base course shown with a line farther to the right for the geotextile specimen. This is determined by the higher number of blows required than the control. A GAB layer of 12 in. (305 mm) is considered a thick base material. While geotextiles do provide some benefit in strengthening the subgrade, their influence likely is unable to strengthen the entire depth of thick base course sections. These results provide some insight on why geotextiles can decrease the pressure distributed to subgrade material when placed at the base–subgrade interface.

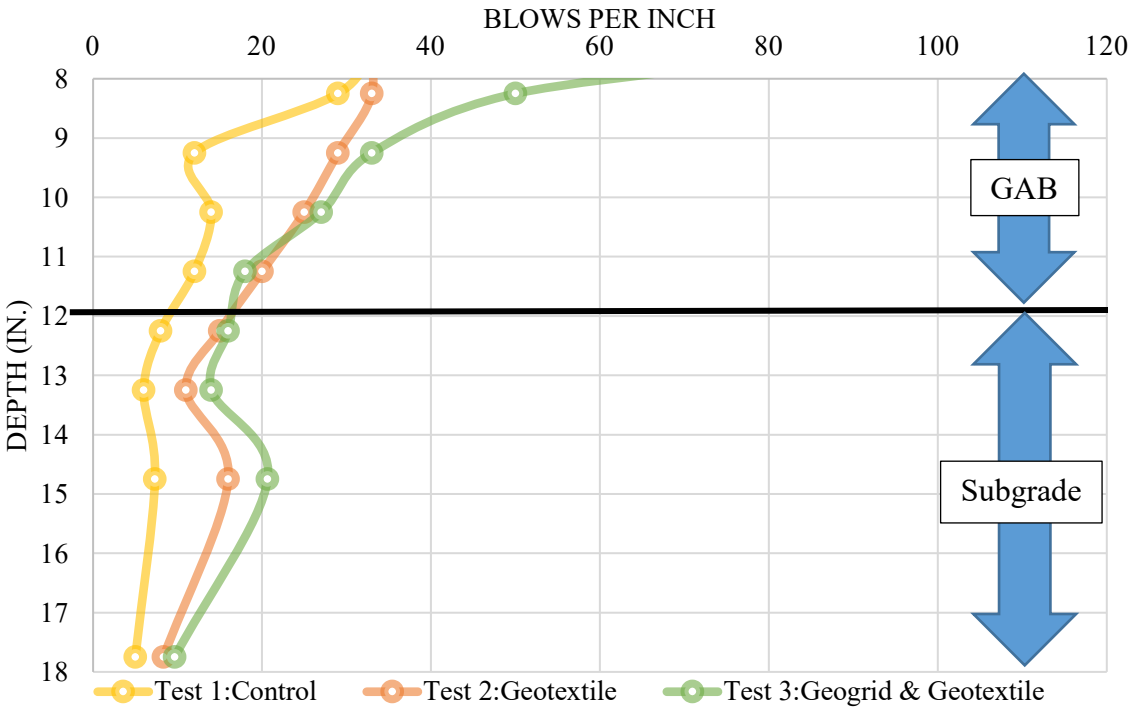

Note: To convert inches readings to centimeters, multiply value by 2.54.

FIGURE 4.18

DCP Post-Traffic Readings along the Depth of the Specimen

Comparisons are made between T22, the geogrid and geotextile combination, versus the control DCP measurements. Figure 4.18 shows that the aggregate base course is significantly stronger than the control readings. The area between the two geosynthetics shows a combination of interlock effect from the geogrid and friction effect from the geotextile, which creates a dual strengthening effect. This area has a higher strength than both the standalone geotextile and control test sections showing that the geogrid can strengthen the base material under it, creating an additive strengthening effect with the geotextile.

DCP and LWD measurements of the GAB layer have several similarities. For post-traffic readings, both the stiffness and strength of the layer were generally highest for the

geogrid and geotextile specimen (T22), second highest for the geotextile-reinforced specimen (T21), and lowest for the control test section (T23). While the general layer trends were similar, there were a few differences between the two measurements. Because the DCP was able to measure strength along the depth, it showed that for the geotextile-reinforced specimen, the strength was equal to the control at 8 in. (203 mm) below the surface with a 4-in. (102 mm) stiffened base above the geotextile. The LWD test for the base material only produced one measurement and showed that the layer as a whole was stiffer than the control test specimen.

4.6 Statistical Analysis of Pressure Results

Statistics is an invaluable tool to make conclusions regarding the trends found in geosynthetic-reinforced experimental test specimens. In this study, two different statistical analysis methods were performed to produce conclusions on geosynthetic-reinforced pavement performance.

4.6.1 Two-Sample t-Test between Mean Percent Pressure Reduction between Geogrid and Geotextile

A two-sample t-test was used to determine if two population means are equal. In the context of this study, the t-test helped evaluate if the percent pressure reduction in the subgrade layer was different between the geogrid and geotextile test specimens. The first step of a t-test was to define the parameters in context of the problem:

μGG = the mean percent of pressure reduced by using a geogrid

μGT = the mean percent of pressure reduced by using a geotextile

$H0$: μGG = μGT

Ha: μGG ≠ μGT

Independence, normality, and constant variance were all checked and determined to be satisfied. To continue the analysis, the t-test was computed with the JMP statistical software. Figure 4.19 shows a test statistic of 0.1571 and p-value of 0.8783. Since the p-value is greater than 0.05, the null hypothesis is rejected. There is not enough evidence to conclude the mean percent pressure reduction in the subgrade is different between geotextile and geogrid test specimens.

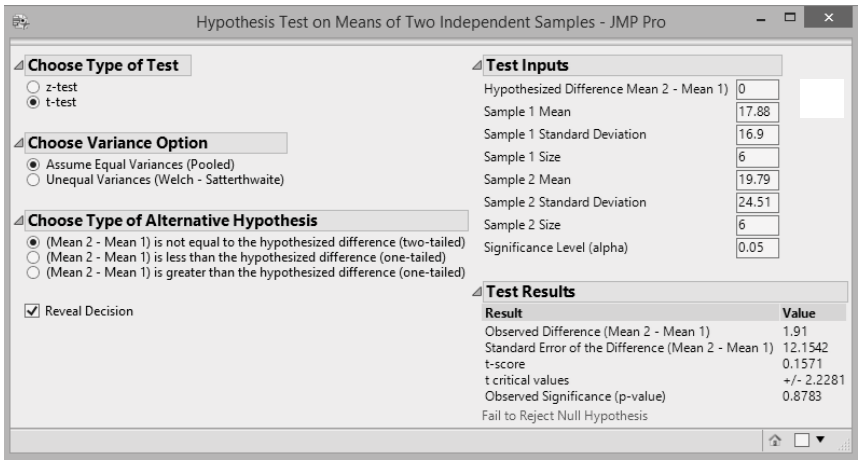

FIGURE 4.19

Two-Sample t-Test Results

4.6.2 Comparison of Two Means with Matched Pairs t-Tests

After showing that the pressure reduction was not statistically different between the two geosynthetic materials, it was acceptable to make comparisons of all geosynthetic-reinforced specimens to control values. To analyze the pressure data, a two matched pairs t-tests was conducted. These matched t-tests are valuable in that they can prove that the use of the geosynthetics in the test specimens definitively reduces pressure in the subgrade and aggregate base layer. The first test compared the percent reduction in pressure at 1 in. (25 mm) above the soil interface between the control and geosynthetic specimens. The

second test compared the percent reduction in pressure at 1 in. (25 mm) below the soil interface between the control and geosynthetic specimens. The normality and independence conditions were checked and determined that the test was valid.

The next step was to define the appropriate parameters in the context of the problem. Since this is a paired t-test, let μ_d be the mean percent reduction in pressure where the difference is defined as:

$$D = Control\ Pressure - Geosynthetic\ Pressure \tag{4.1}$$

$$\%\ Reduction = \frac{Control\ Pressure - Geosynthetic\ Pressure}{Control\ Pressure} \times 100 \tag{4.2}$$

The null and alternative hypotheses for these tests are:

$$H_0: \mu_d = 0$$
$$H_a: \mu_d > 0$$

A significance level of 0.05 was used for both comparison tests. For the 1-in.-above and 1-in.-below tests, the p-value was 0.0025 and 0.0078, respectively. Figures 4.20 (a) and (b) show the JMP outputs of the t-tests.

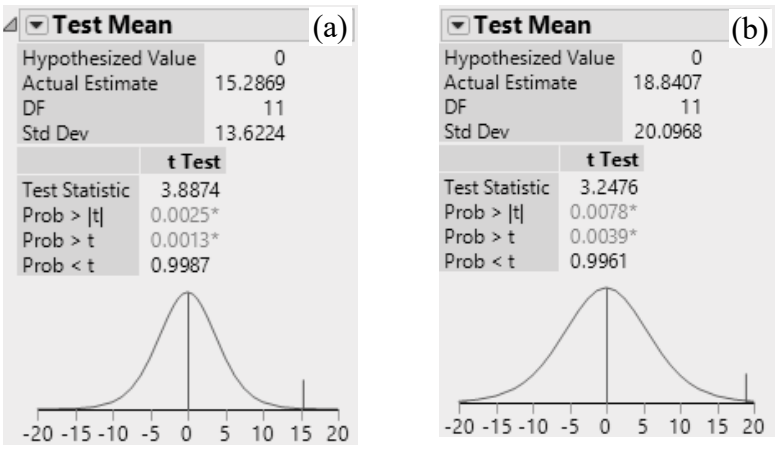

FIGURE 4.20

Statistical Analysis Results:
(a) JMP Output for t-Test 1 in. Above the Interface in the GAB and
(b) JMP Output for t-Test 1 in. Below the Interface in the Subgrade

Since the p-value is less than the level of significance, 0.05, the null hypothesis is rejected. There is enough evidence to conclude that the mean difference in the percent of pressure reduction 1 in. (25 mm) above in the aggregate base, and 1 in. (25 mm) below in the subgrade is greater than zero. Therefore, there is enough evidence to conclude that adding geosynthetic to soil reduces pressure 1 in. (25 mm) above and 1 in. (25 mm) below the interface. With 95% confidence, the mean difference in pressure at 1 in. (25 mm) above the interface is between 6.63% and 23.94% with an expected average value of 15.3% reduction. With 95% confidence, the mean difference in pressure 1 in. (25 mm) below the interface is between 6.07% and 31.61% with an expected average value of 18.8% reduction.

Statistically speaking, geosynthetics used for reinforcement and stabilization can reduce pressure in both the top of the subgrade and the bottom of the aggregate base layer. There is not enough evidence to determine the significant differences in the stress reduction

for geogrid and geotextile test specimen results to prove statistically that one product is more effective in reducing stress than the other.

4.7 Summary of Results

The large-scale experimental testing program performed in this study provides the necessary results to describe why geosynthetics are beneficial additions to flexible pavement structures.

4.7.1 Pressure

Several conclusions are drawn from the in situ stress measurements from the large-scale wheel trafficking tests. For thicker aggregate base layers, the optimal geogrid placement location is at the mid-height of the aggregate base layer. For a subgrade soil type with high fine contents, the use of geotextile provides a better long-term choice to improve pavement performance by minimizing migration of fine contents. Geotextile should only be placed at the base–subgrade interface and not the mid-height of the GAB (as recommended by manufacturers). Geotextile reduces the most pressure in the subgrade layer when the soil is prepared at OMC in the highest strength soils (SSV = 2.5 or greater) used in this study as measured by the DCP, as in Gordon County. When the subgrade soil is prepared at a high moisture content, the aggregate base layer experiences higher pressures than when prepared at OMC. Additionally, the high moisture content soil experiences less pressure than when prepared at OMC.

4.7.2 Strain

The strain experienced by the geogrid ranges from 0.15–0.45% in the transverse direction and 0.20–0.29% in the direction parallel to the wheel path. Geogrid placed on the weaker

subgrade specimens exhibits higher strain than when placed on subgrade compacted at optimum moisture content. Additionally, when the geogrid is placed at the mid-height of the aggregate base layer, it experiences more strain than when placed at the base–subgrade interface.

4.7.3 Post-traffic Testing DCP and LWD

The use of a geotextile at the interface and the geogrid at mid-height both stiffens and strengthens the aggregate base course after trafficking when compared to the control test specimen. This is likely one of the causes for the reduction of stress transferred to the subgrade and bottom of the aggregate base layer when using geosynthetics. The results of this testing plan have corroborated the findings of Tingle and Jersey (2009) in that the post-trafficked geosynthetic-reinforced test specimens are stronger than the post-construction values. The use of a woven geotextile at the interface and an extruded biaxial geogrid at the mid-height of the aggregate base course increased the stiffness of the post-trafficked aggregate base course 37% more than the control case. The single geotextile case increased the stiffness of the GAB 7% more than the control case. The DCP readings showed that the geogrid and geotextile case strengthened the base significantly more than the control and geotextile-alone case. The single geotextile case stiffened the bottom 4 in. (102 mm) of the base.

4.7.4 Statistical Analysis

By using a matched t-test statistical analysis, it was determined that the addition of a geosynthetic helps to reduce pressure in both the aggregate base course and in the subgrade layers. From the test results, a 95% confidence interval was created for both the expected reduction in the base and subgrade layers. A pressure reduction between 6.63% and 23.94%

is expected 1 in. (25 mm) above the interface in the aggregate base and between 6.07% and 31.61% at the top of the subgrade. The expected pressure reduction for when using a geosynthetic is 15.3% at the bottom of the base course and 18.8% for the top of the subgrade. The two-sample t-test shows that there is no difference found using the biaxial geogrid and woven geotextile in the pressure reduction in the base and subgrade materials.

This page is intentionally left blank.

5. BENCH-SCALE TEST

Studying the permanent deformation behavior of geosynthetics-reinforced pavement foundation systems prior to construction could be greatly beneficial to improve the long-term performance of pavements in soft-subgrade conditions. However, this problem is complex to study considering the multiple geo-materials involved in the system, the non-linearity in their engineering behavior under repeated traffic loading, and the difficulty of assessing the particle-scale interaction between the aggregates and geosynthetics. To sufficiently understand the behavior of such a composite system, a series of experiments simulating the various operational conditions is necessary. While the effect of geosynthetic stabilization on pavement performance is best assessed using full-scale sections to fully replicate the operational conditions, these procedures are labor-intensive. On the other hand, it is common practice to conduct laboratory tests like cyclic triaxial tests and repeated-load plate tests for measuring the resilient modulus of aggregates and soils, which is an important input parameter in the AASHTO *Mechanistic–Empirical Pavement Design Guide* (MEPDG) design framework. A disadvantage of these laboratory procedures is that they fail to accurately replicate field conditions such as moving wheel loading or geosynthetics' tension membrane effects, and therefore, are not ideal for studying the permanent deformation (rutting) behavior of the composite pavement system. Multiple researchers have observed that the performance of aggregate materials in the field cannot be predicted solely using resilient modulus tests ,and permanent deformation tests can be greatly beneficial to predict full-scale performance of geogrid-aggregate combinations (Thompson, 1998; Xiao et al., 2012; Mishra, 2012; Kim et al., 2017).

This chapter introduces a bench-scale pavement simulation apparatus used to measure permanent deformation and stress variations in the subgrade induced by a cyclic rolling-wheel load on pavement specimens. For a bench-scale test, the specimens are scaled down to mimic the geometry of a full-scale pavement, including subgrade and base layers whose thicknesses are proportional to the size of the loading wheel. The advantages of this system include short durations to prepare and test the specimens, requirements of low quantities of materials, and allowance for a high degree of control over specimen properties. For the current study with the bench-scale testing system, five geosynthetics are used to study their effects on pavement specimens composed of a soft silty subgrade soil and a well-graded aggregate base material. The performance of the pavement specimens is assessed using two performance criteria: 1) surface rutting and 2) stress changes in the subgrade.

5.1 Materials

As discussed in Chapter 3, three subgrade soils from Coweta, Gordon, and Hall Counties were identified as soft and problematic by GDOT and hence used as subgrade materials along with standard graded aggregate base material in the experimental study. Four geogrids of varying aperture sizes and one geotextile were chosen to assess their performance in the pavement tests, including the commercially available geogrid and woven geotextile, which were used in the large-scale testing program of this study. The additional three geogrids are of smaller aperture sizes and stiffness compared to the geogrid, and were incorporated into the bench-scale study to assess differences in performance due to the smaller scale of the bench-scale specimens. This is especially important with geogrids since geogrid interaction with aggregate particles is heavily dependent on particle

interlocking, which in turn is influenced by the number of ribs present in the given pavement specimen. The following section presents the properties of the subgrade soil, aggregate, and the geosynthetics used for the bench-scale tests.

5.1.1 Subgrade and Aggregate Materials

As already described in Chapter 3, three subgrade soils were used in the bench-scale tests. The particle size curves and the properties of these subgrade soils are already presented in Table 3.2 and Figure 3.1.

However, the GAB material was slightly modified for the bench-scale testing by scalping aggregate particles larger than 9.5 mm (3/8 in.) and compensating with additional particles of sizes between 4.76 (No. 4) and 9.5 mm (3/8 in.). This was done to ensure minimal boundary effects with lateral walls of the chamber, which measures 203 mm (8 in.) in width. The modified grain size distribution curve for the GAB is presented in Figure 5.1.

5.1.1 Geosynthetics

As stated, five geosynthetic products, including four geogrids and one geotextile, were used in the bench-scale study. In addition to the commercially available BX1200 geogrid (GG1000) and geotextile (GT) used in the large-scale study, three additional geogrids of smaller aperture sizes were selected to assess effects of geogrid opening size on rutting behavior. The tensile properties of the three new geogrids, referred to as GG500, GG250 and GG125 with opening sizes 0.5, 0.25, and 0.125 in. (12.7, 6.35, and 3.175 mm), respectively, were estimated using multi-rib tensile tests (ASTM D6637). It is worth noting that all these geogrids exhibit opening sizes that are larger than the mean particle size of the modified GAB (D_{50}) of 0.08 in. (2 mm), which is a typically accepted rule of thumb in

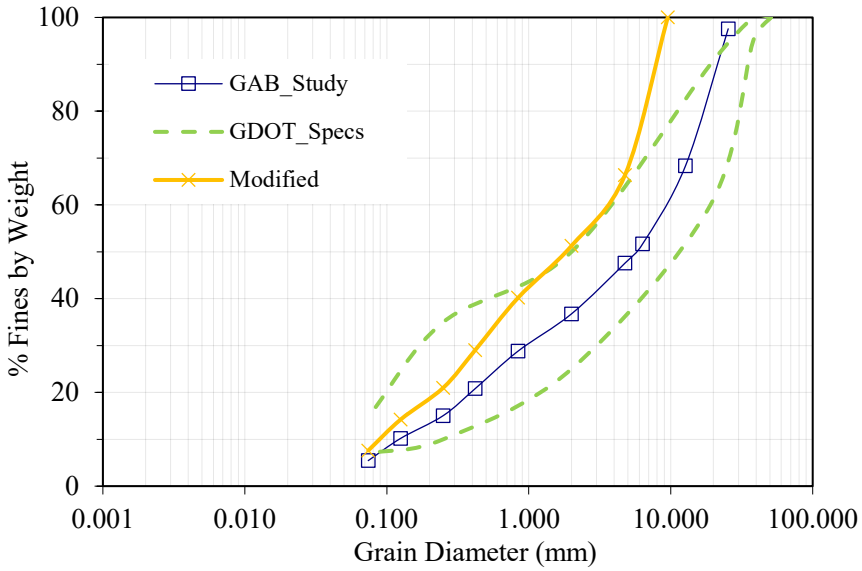

FIGURE 5.1

Modified Gradation of the Graded Aggregate Base Mix

practice as necessary for particle penetration and therefore, effective interlocking. In addition, the thickness of the geosynthetic and the tensile stiffness are properties that are known to influence the aggregate–geosynthetic interaction and are important for pavement design in practice. A summary of properties of the geosynthetics used is presented in Table 5.1. Figure 5.2 shows specimens of all five geosynthetic materials. In terms of rib thickness, GG500 has the highest rib thickness of all the geogrids, followed by GG1000, GG250 and GG125. The stiffness of the geotextile is almost double that of the GG1000 geogrid, while the remaining three geogrids exhibit much lower stiffness values. While the GG500 and GG250 are composed of medium-density polyethylene, the GG125 is composed of low-density polyethylene, which explains its low stiffness. These properties of the geosynthetics could play a crucial role in their interaction with the aggregate layer and must be considered in the assessment of results from the experiments.

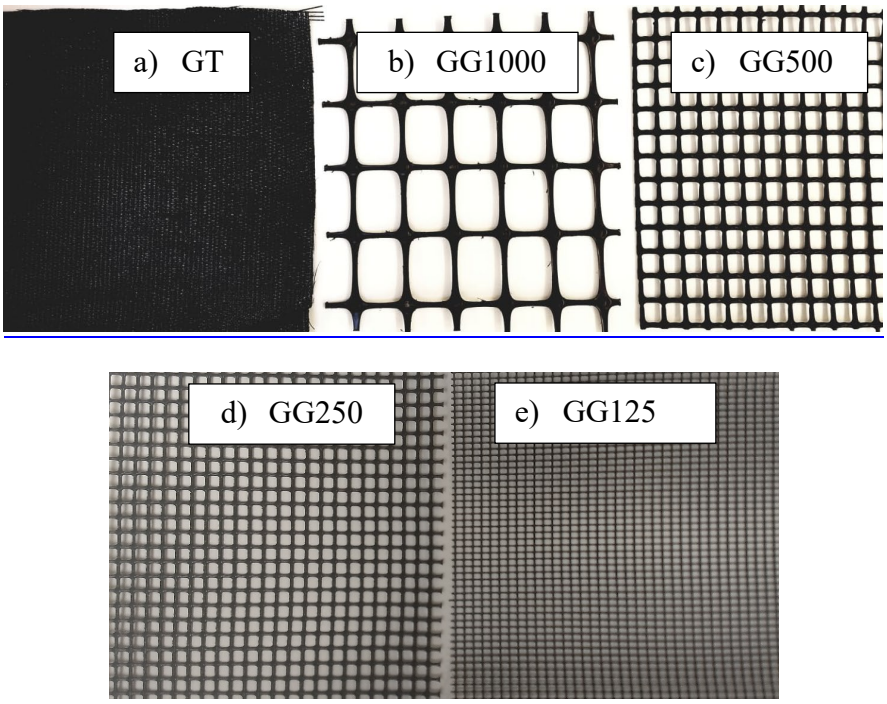

FIGURE 5.2

Geosynthetics Used for Bench-Scale Test

TABLE 5.1
Geosynthetic Properties for Bench-Scale Test

		GG1000*	GG500	GG250	GG125	GT*
Opening Size, in. (mm)		1.0 (25.4)	0.5 (12.7)	0.25 (6.35)	0.125 (3.18)	0.024 (0.6)
Minimum Rib Thickness, in. (mm)		0.05 (1.27)	0.08 (1.95)	0.05 (1.30)	0.03 (0.74)	–
Tensile Strength @ 2% strain, lb/ft (kN/m)	MD	410 (6.0)	292 (4.26)	209 (3.05)	132 (1.93)	–
	XMD	620 (9.0)	347 (5.06)	249 (3.63)	163 (2.38)	–
Tensile Strength @ 5% strain, lb/ft (kN/m)	MD	810 (11.8)	402 (5.87)	286 (4.18)	169 (2.46)	1,274 (18.6)
	XMD	1340 (19.6)	492 (7.18)	363 (5.3)	206 (3.02)	1,439 (21.0)
Ultimate Tensile Strength, lb/ft (kN/m)	MD	1310 (19.2)	410 (5.99)	292 (4.26)	169 (2.46)	2,640 (38.5)
	XMD	1,970 (28.8)	504 (7.36)	405 (5.91)	206 (3.02)	2,460 (35.9)

*Supplied by manufacturer

5.2 Bench-Scale Testing System

In the presented study, the bench-scale rutting system is used to conduct a parametric assessment of the influence of geosynthetics in flexible pavement systems at various subgrade stiffness conditions. The results facilitate a relative comparison of the behavior of the stabilized pavement system compared to the unstabilized specimens, therefore allowing quantification of the benefits of geosynthetics.

The rutting assembly, shown in Figure 5.3, comprises three components: the specimen chamber, the wheel propagation system, and the loading suspension system. The chamber, measuring 36-in. (914 mm) × 8-in. (203 mm) × 6-in. (152 mm), is used to prepare the specimen. A computer-controlled track actuator system installed over the chamber connects to a wheel that is 3-in. (76 mm) diameter and 1-in. (25 mm) wide, forming the wheel propagation system. The wheel is loaded using the dead-load suspension system (refer to Figure 5.3) to simulate stresses imposed by a loaded truck. A constant stress of 27.6 psi (190.3 kPa) was applied over a contact area of 0.8 $in.^2$ (522.6 mm^2) with the specimen, corresponding to a circular diameter of 1 in. (25 mm). The wheel assembly is then programmed to cycle between two user-defined points along the length of the specimen at a constant speed, typically set to 1.2 in./sec. Each specimen was then individually tested for a minimum of 250 loading cycles and a maximum of 500 cycles. A loading cycle is defined as the sequence of wheel passes from the start of the test section to the end and back, covering a total distance of 16 in. (406 mm). Typically, the rutting curves showed little change in vertical deformations, indicating stabilization, after 250 loading cycles.

Instrumentation of the specimen includes linear variable differential transformers (LVDTs) to continuously monitor rutting deformations, as well as pressure sensors to

record stresses experienced in the subgrade. The following section briefly explains the test methodology and subsequent stages for data processing.

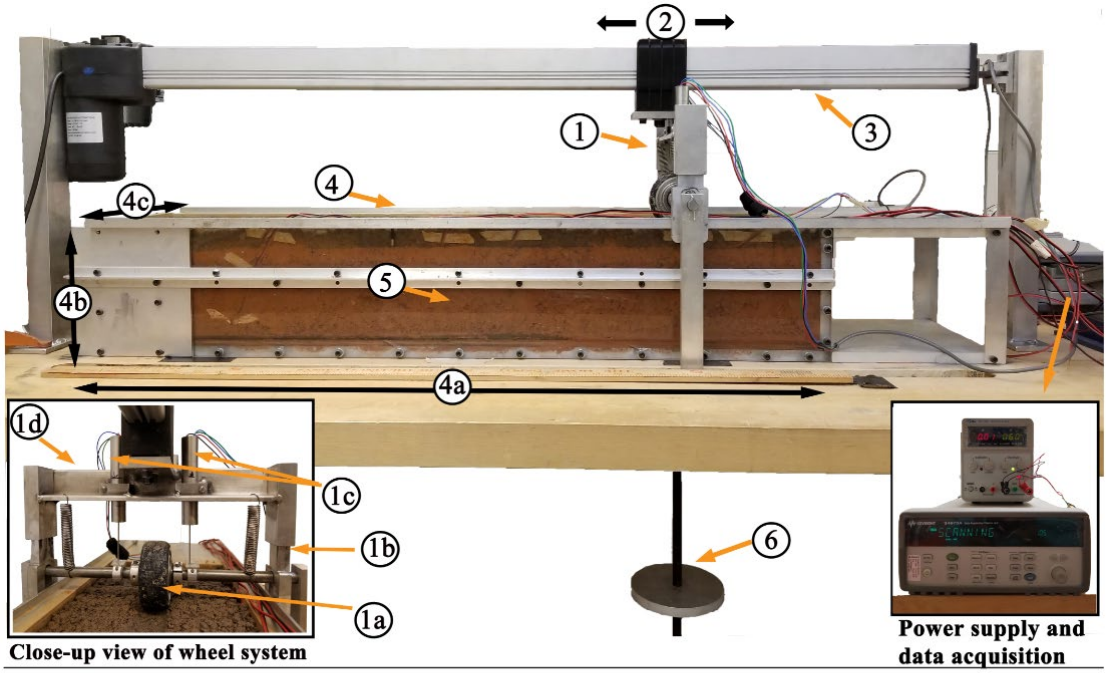

FIGURE 5.3

Schematic Showing the Rutting Apparatus

5.2.1 Specimen Fabrications

The geometry of the specimen was designed based on full-scale specimen proportions with respect to the lane width, tire width, and layer thicknesses. This is schematically presented in Figure 5.4. The testing specimen is prepared to comprise a subgrade layer and base layer of thicknesses of 5 in. (127 mm) and 1 in. (25 mm), respectively. This was based on the following reasoning. Typically, field pavement sections are constructed with an 8- to 12-in.-thick (203 to 305 mm) base layer, and the width of a full-size truck wheel ranges

between 10 and 12 in. (refer to Figure 5.4). This proportion was approximated to be 1:1 and replicated in the experimental specimen with a 1-in.-thick (25 mm) base layer for the 1-in.-wide (25 mm) loading wheel.

One of the main advantages of this system is the high rate of testing possible due to the smaller size of the specimen, compared to full- or large-scale testing, which reduces the specimen preparation as well as testing times. Additionally, to further accelerate the testing rates as well as ensure uniformity in specimen properties for future comparison of performances, the length of the chamber was designed to accommodate multiple tests with the same prepared specimen. Thus, the overall length of the chamber of 36 in. (914 mm) was divided into three subsections, allowing three test sections of 8 in. each. This test-specimen size encompasses a sufficient sample size to study the rutting behavior, along with adequate buffer spacing of 3 in. (76 mm) between the test sections. Trial tests were conducted with the three-specimen and single-specimen arrangement to make sure results were repeatable.

In preparing the specimens, a constant compaction energy was used for each lift of the subgrade layer. The subgrade soil was prepared at the prescribed water content to simulate CBR values ranging between 1 and 15, while the GAB was compacted at optimum water content to 95% of its maximum dry density, representing a CBR greater than 20. The geosynthetic material was placed at the interface between the two layers. Upon completion of the specimen preparation, it was allowed to equilibrate for a minimum duration of 12 hours before the loading stage was started with the rolling wheel. No human intervention is required during the test until the target number of loading cycle is reached. Figure 5.5 presents photographs taken at various stages of testing.

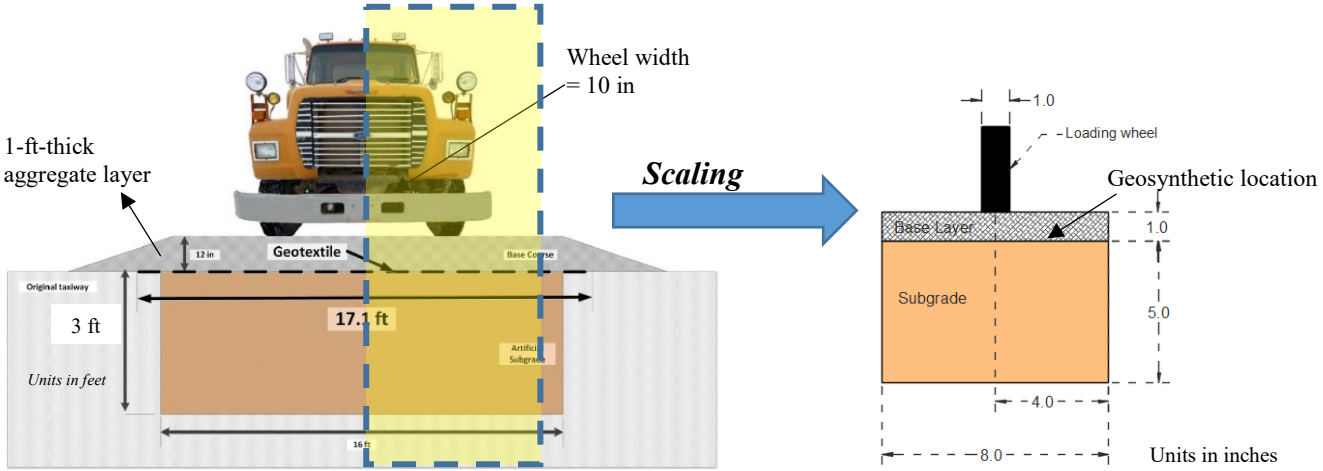

FIGURE 5.4

Schematic Showing Cross-sections of Full-Scale (after BSI et al., 2014) and Bench-Scale Specimens

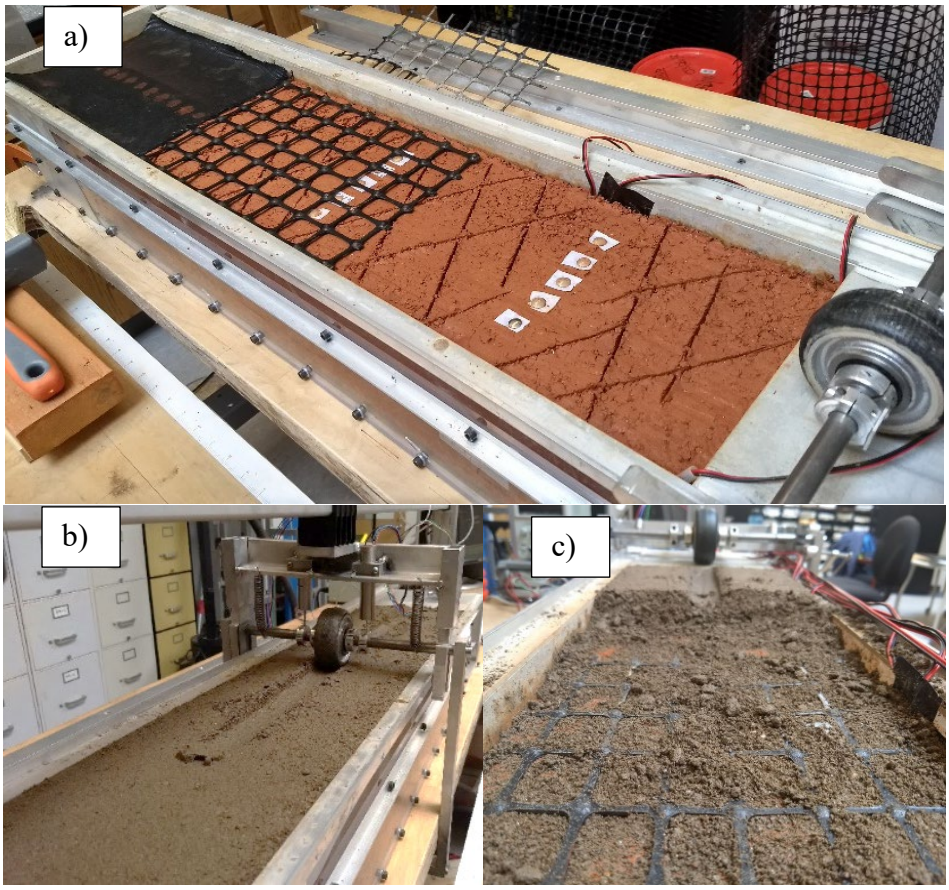

FIGURE 5.5

Various Bench-Scale Testing Stages:
(a) Placement of Geosynthetic over Subgrade, (b) Wheel Loading Cycles in Progress, and (c) Exhumed Aggregate Layer upon Completion of Test

5.2.2 Data Processing

After the loading sequence is completed, the data are processed using a custom algorithm to segment the dataset into cycles based on the associated wheel position data. Figure 5.6 shows a plot of the wheel position along the 8-in. (203 mm) length of the specimen for the first few scan readings and subsequent segmentation into cycles. Figure 5.7 (a) shows the LVDT readings for the first few cycles and Figure 5.7 (b) shows the LVDT readings at the end of the test. Using these data, the mean rut depth along the length of the specimen is

identified for each cycle. Since the specimens were carefully prepared in the laboratory, uniform rut depths were observed along the test section. Some tests showed marginally greater rut depths at the end-points of the test sections, owing to the abrupt stopping of the wheel before changing direction. Therefore, measurements made at the extreme 1 in. (25 mm) of the specimen section were not used in further analysis.

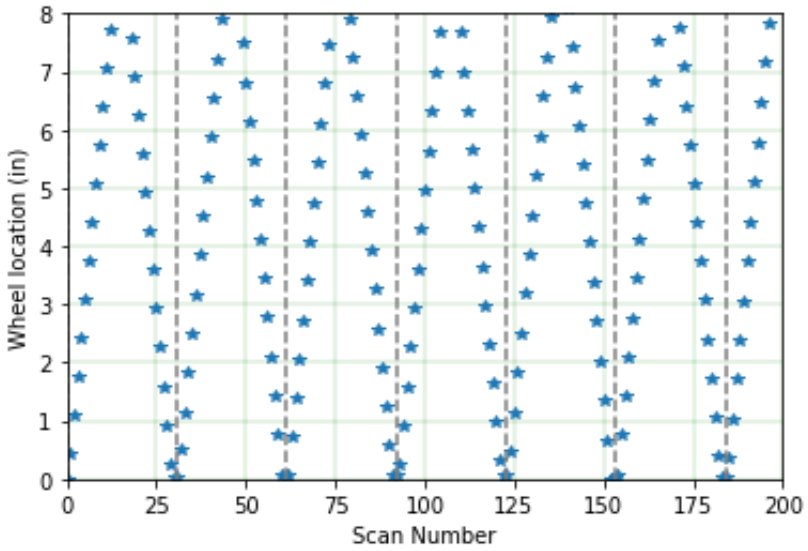

FIGURE 5.6

Wheel Position Readings Showing Bi-directional Cyclic Nature and Segmentation into Cycles

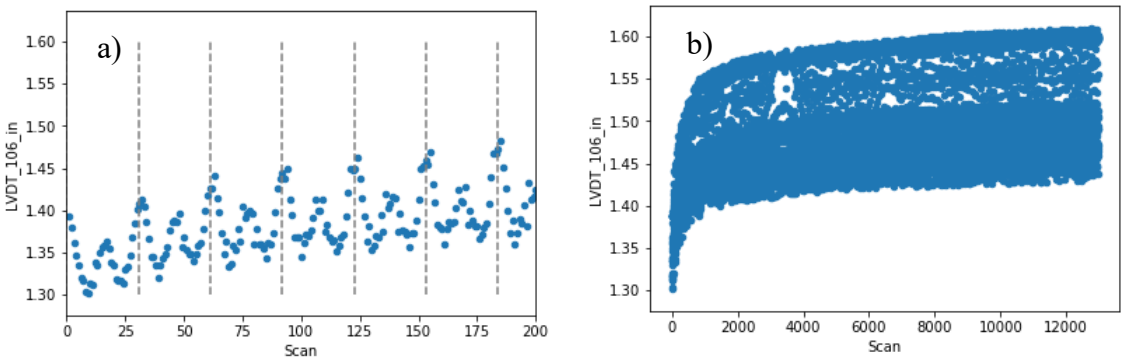

FIGURE 5.7

Plot Showing Typical LVDT Readings Collected
(a) For the First Few Cycles and (b) For the Entire Test

In addition to vertical deformation, flexible pressure sensors, with a sensing diameter of 0.6 in. (15.2 mm), were placed under the wheel path at two locations, at the base layer–subgrade interface and at a depth of 1 in. (25 mm) below the top of the subgrade. This geometry of sensor location should provide a three-point stress distribution profile under the wheel, including surface stress of 27.6 psi (190.3 kPa), and two pressure sensors at the surface of the subgrade (bottom of the base layer) and 1 in. (25 mm) below the top of subgrade. Figure 5.8 (a) shows a typical pressure sensor response when the wheel passes over the surface, while Figure 5.8 (b) shows the collected data over the entire test. As before, the maximum pressure per cycle is picked and plotted for further analysis.

5.2.3 Experimental Program

All three subgrade soils, namely, Coweta, Gordon, and Hall Counties, were used as the subgrade at two conditions: 1) high stiffness (CBR > 10) when placed at optimum water content, and 2) low stiffness (CBR < 2.5) when placed at higher water contents. Rutting tests were conducted for the unstabilized case at both subgrade conditions and stabilized

cases with all five geosynthetics. The geosynthetic was placed at the interface of the base and subgrade layers in all tests.

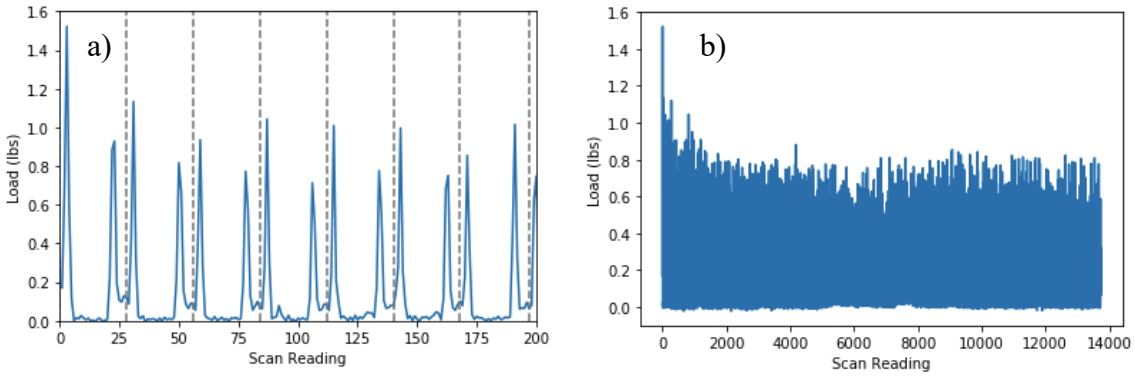

FIGURE 5.8

Plot Showing Typical Pressure Sensor Readings Collected (a) For the First Few Cycles and (b) For the Entire Test

5.3 Bench-Scale Testing Results

Generally, following the development of a new laboratory testing system, it is desirable to conduct multiple tests at different scenarios to ascertain the functionality and validity of the procedure. If the observed behavior matches expected trends, it can then be used to meet the objectives of the study. In this study, the bench-scale procedure was first validated based on multiple tests that were used for establishing repeatability of results, comparing stress measurements in the specimen to expected values and assessing the rutting behavior for various loading stresses and stabilization. Following this, the tests comparing unstabilized and stabilized specimens were conducted. These results are presented in the following sections.

5.3.1 Typical Rutting Behavior

The rutting curve obtained after the data processing steps described in the previous section followed a typical exponential pattern, with the majority of the deformations occurring in the initial 50 cycles and stabilizing in subsequent cycles. The typical rutting depths in the base layer at the end of the test ranged between 0.1 and 0.5 in. (2.5 and 12.7 mm), which represents permanent strains of 10% to 50% of the base layer thickness. The rutting curves were in close conformance with the exponential rutting model proposed by Tseng and Lytton (1989), as shown in Equation 5.1.

$$\epsilon_a = a.e^{-(\frac{b}{N^c})} \quad (5.1)$$

where

ϵ_a is the axial permanent strain;

N is the number of load cycles; and

a, b, and c are the fitting parameters.

To demonstrate the exponential nature of the rutting curves and justify 250 loading cycles for the test duration, the results from a sample test were used to form three datasets, each comprising the first 100, 250, and 500 cycles. The first two datasets with 100 and 250 loading cycles were fitted to the rutting model shown in Equation 5.1, as shown in Figures 5.9 (a) and 5.9 (b). The fitted models were then extrapolated to 500 cycles and plotted along with the laboratory-obtained dataset for all 500 cycles, as shown in Figure 5.9 (c). Clearly, the predicted curve based on 100 cycles overestimates the rutting. However, there is negligible variation in the predicted curve using 250 cycles and the 500-cycle laboratory curve, thus justifying the selected test duration of 250 loading cycles.

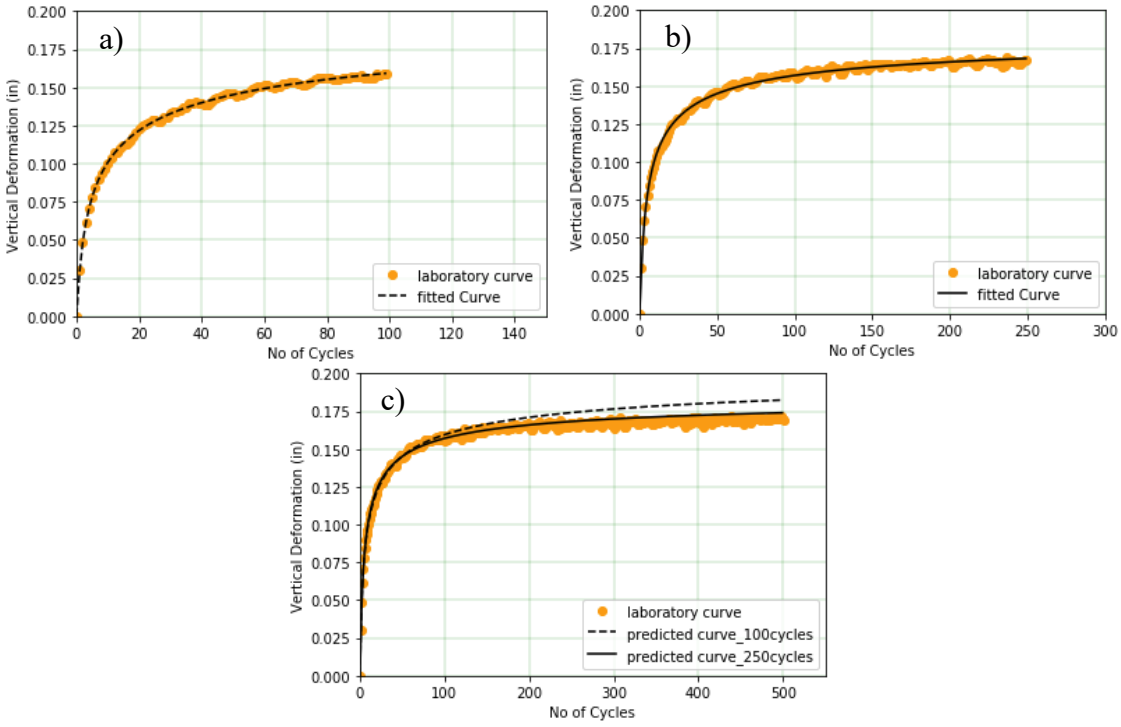

FIGURE 5.9

Rutting Curves Fitted to Exponential Model for (a) First 100 Loading Cycles, (b) First 250 Loading Cycles, and (c) Comparison of Laboratory Curve over 500 Cycles and Predicted Curves from (a) and (b)

5.3.2 Typical Stress Behavior

While the surface rutting behavior is most commonly used to evaluate the performance of pavements, the pattern of stresses in the subgrade can also be critical in gaining useful insights into the influence of the geosynthetics. Figure 5.10 presents a comparison of the theoretical stress distribution under a circularly loaded area (shown in Equation 5.2) for a surface stress of 27.6 psi (190.3 kPa), and the measured stresses at various depths under the wheel using the sensors. In this figure, the depth z/R is normalized with the loading radius, which is 0.5 in. (12.7 mm). Therefore, z/R of 2 is the bottom of the base layer (top of the subgrade) while z/R of 4 is at depth 1 in. (25 mm) below the top of the subgrade.

The measured stresses match reasonably closely with the expected distribution, even for the moving wheel loads.

$$p = q\left[1 - \frac{1}{\left[\left(\frac{R}{z}\right)^2 + 1\right]^{\frac{3}{2}}}\right] \tag{5.2}$$

where,

q is the surface stress of 27.6 psi (190.3 kPa),

p is the vertical stress at depth z, and

R is the radius of the loading area.

In addition to stress measurements under the wheel, stresses were also recorded at the wall to establish the absence of boundary effects. Figure 5.11 presents test results showing sensor measurements at the top of the subgrade and at the wall of the box at a depth of 2 in. (51 mm) below the surface. No stresses are recorded at the wall, indicating a lack of boundary effects influencing the rutting behavior of the specimens.

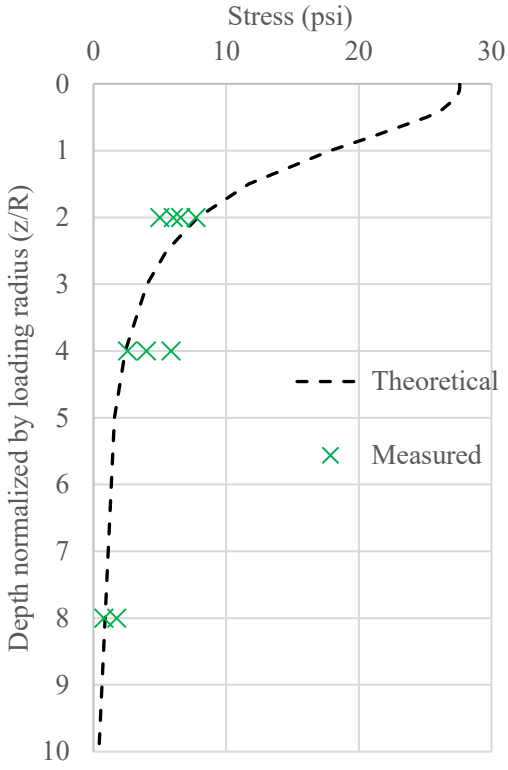

FIGURE 5.10

Stress Distribution Below Center of Circularly Loaded Area

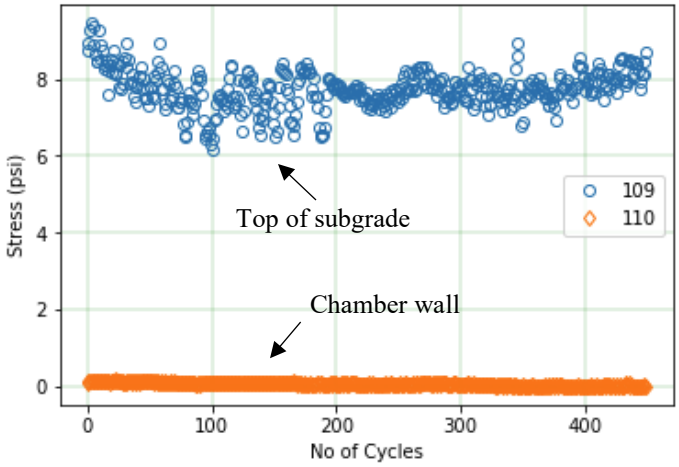

FIGURE 5.11

Stress Measurements Made at Bottom of Base Layer and Side Wall of Box

5.3.3 Repeatability of Rutting Behavior

Multiple tests were repeated during the testing program to establish repeatability of results and gain confidence in the laboratory apparatus and procedure. A sample of these results, which includes unstabilized and stabilized cases for Gordon and Coweta County subgrade soils, are presented in Figure 5.12. It can be concluded that the repeated curves matched the previous test trial, thus establishing repeatability.

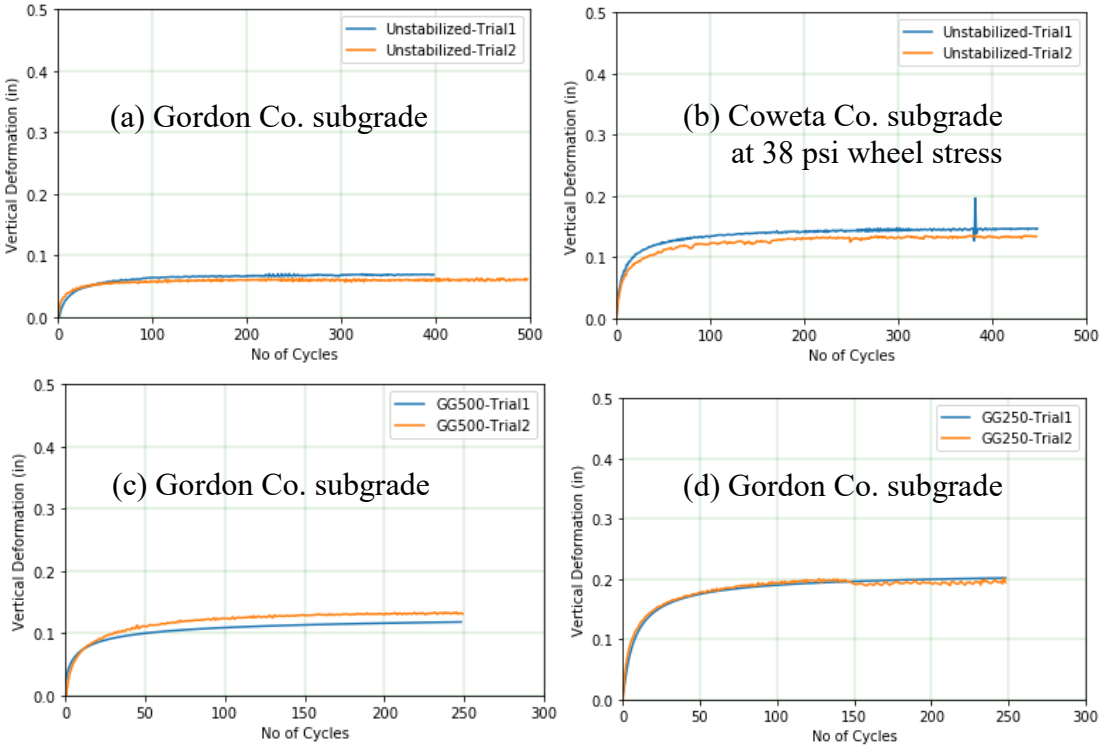

FIGURE 5.12

Repeatability of Rutting Performance for Tests with a) Unstabilized Specimens Using Gordon Co. Soil at 20% Water Content, b) Unstabilized Specimens Using Coweta Co. Soil at 15% Water Content, and c) Stabilized Specimens with Geogrid GG500 over Gordon Co. Soil

The rutting tests shown in Figure 5.12 (b) for Coweta County soils at 15% water content were conducted at a higher wheel stress of 38 psi (262 kPa), since these tests were

part of initial iterations to identify study parameters. This explains the greater rutting compared to curves shown in Figure 12 (a) with Gordon County soil at 20% water content.

5.3.4 Effect of Loading Stress

The effect of loading stress was studied by testing the same combination of materials at three stresses, namely, 10 psi (69 kPa), 15 psi (103 kPa), and 27.6 psi (190.3 kPa). The specimens were prepared using Coweta County soil at 27% water content (CBR~2.5) with no stabilization incorporated. Figures 5.13 (a) and 5.13 (b) show the corresponding rutting curves and the obtained trend of rut depth after 400 loading cycles versus wheel stress, respectively. There is a significant effect that applied stress has on rutting. As expected, the rutting depth increases from 0.08 in. (2.03 mm) at 10 psi (69 kPa) to 0.5 in. (12.7 mm) at 27.6 psi (190.3 kPa).

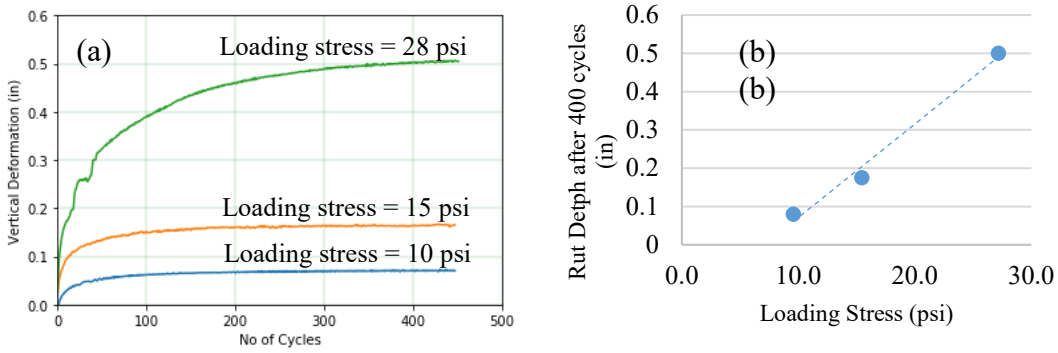

FIGURE 5.13

Effect of Loading Stress on Rutting of Unstabilized Specimens Using Coweta County Subgrade with CBR<2.5

Similarly, a comparable set of tests were conducted using the same specimen conditions at 20 psi (138 kPa) and 27.6 psi (190.3 kPa), but using the GG125, GG250, and GG500 geogrids. These are shown in Figures 5.14 (a) and 5.14 (b), respectively. The

objective of these tests was to assess the individual rutting depths of the stabilized specimens, as well as the effect of increased stress on the stabilized specimens. Firstly, compared to unstabilized rutting depths of 0.3 in. (7.6 mm) and 0.5 in. (12.7 mm) from Figure 5.13 (b) after 400 cycles at 20 psi (138 kPa) and 27.6 psi (190.3 kPa), respectively, the geogrids are evidently showing reduced rutting by about 50%. Additionally, from Figure 5.14 (a), it is seen that a stress of 20 psi (138 kPa) does not induce any significant difference in rutting behavior among the three geogrids, but at 27.6 psi (190.3 kPa) in Figure 5.14 (b), the rutting curves are farther apart from each other. This shows that the effects of the individual geogrids are all favorable compared to the unstabilized case, and vary relative to each other depending on the specimen and loading conditions. Among the three tested grids, GG250 shows the best performance, followed by GG500 and GG125.

This observation is noted here to establish the effectiveness of geogrids compared to the unstabilized scenario, as well as potentially close behavior of geogrid-stabilized specimens depending on the subgrade/stress conditions.

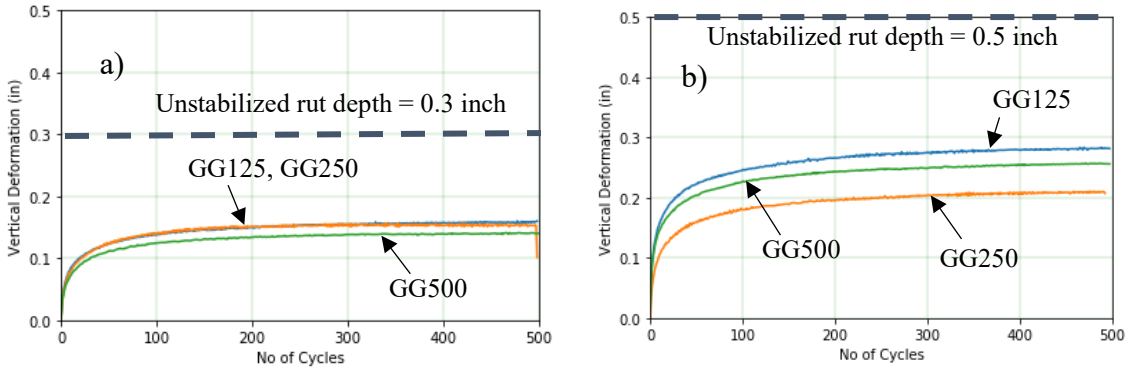

FIGURE 5.14

Effect of Loading Stress on Rutting of Stabilized Specimens at Loading Stress of a) 20 psi and b) 27.6 psi Using Coweta County Subgrade Soil with CBR of 2.5

5.3.5 Effect of Subgrade Stiffness

Subgrade stiffness is a critical parameter since it influences the behavior of the overlying base layer. A stiff subgrade acts as a strong foundation, which provides structural support to the base layer and helps transmit traffic loads into the soil media. On the other hand, soft subgrades are prone to rutting and lack confinement due to their low stiffness. Figure 5.15 presents photographs from two sets of rutting tests conducted on a stiff and soft Gordon County subgrade soil, after 300 cycles. The rut developed in the base layer over stiff subgrade (CBR > 10) is significantly lower than the rut over soft subgrade (CBR > 2.5).

As mentioned, unstabilized rutting tests were conducted for at least two subgrade stiffness conditions for all three soils, corresponding to water contents between 15–20% and 27–33%. Two additional rutting tests were conducted with Gordon County soil to obtain a trend of rutting behavior. The GAB material was consistent for all the tests, with 6% water content and placed at 95% relative compaction. These results are presented in Figure 5.16. As mentioned earlier, the rutting test on the Coweta County soil specimen at

optimum water content was conducted at 38 psi (262 kPa) as indicated in Figure 5.16 (a), and all other tests were conducted at 27.6 psi (190.3 kPa).

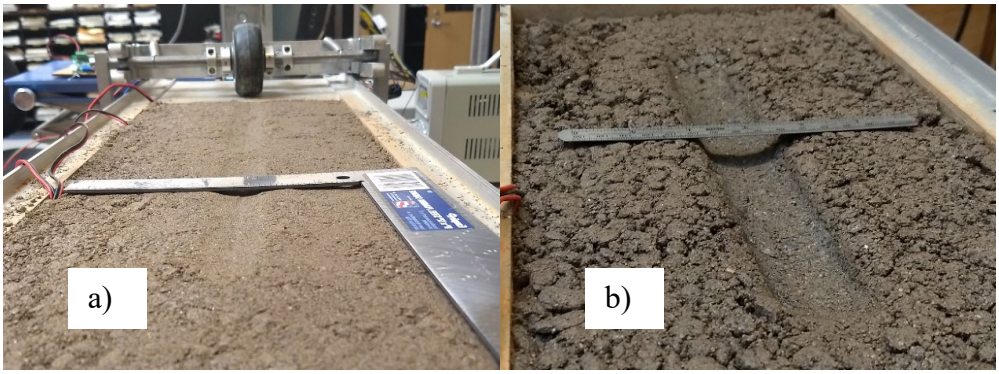

FIGURE 5.15

Photos Showing Rutting Depths for (a) Stiff and (b) Soft Subgrade Conditions

As expected, increasing subgrade water contents result in degradation in the rutting behavior. At subgrade water contents close to optimum, the layer was stiff enough to support the base layer under the imposed traffic loads and resulted in rut depths between 0.05 and 0.15 in. (1.27 to 3.81 mm) after 250 loading cycles. These values of vertical permanent strains of 5–15% are below the accepted limits of 30% in practice. However, soft subgrade conditions with CBR below 2.5 were observed to result in rut depths of around 0.4 in. (10.2 mm) after 250 loading cycles, which represents a significantly high vertical strain of 40% in the base layer. This indicates a need for geosynthetic stabilization. In the case of the set of tests with Gordon County soils shown in Figure 5.16 (c) and Figure 5.17, the decrease in rutting resistance is clearly visible at four subgrade water contents (20, 25, 27, and 33%). Importantly, the steep slope of the trend line establishes the influence of subgrade water content on surface rutting in the base layer.

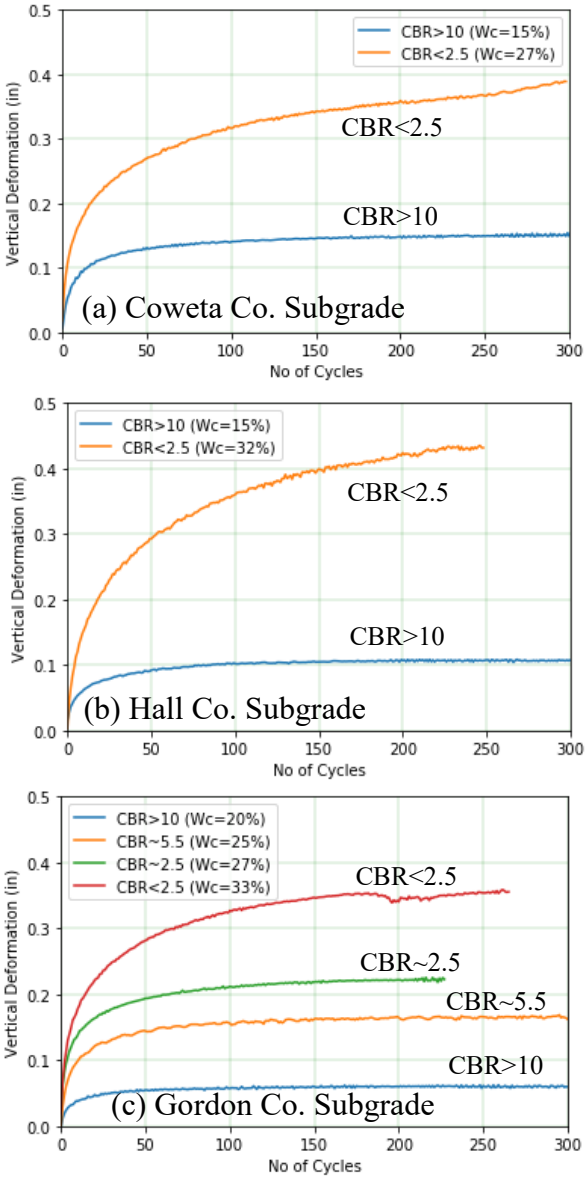

FIGURE 5.16

Rutting Behavior for Unstabilized Specimens with a) Coweta Co., b) Hall Co., and c) Gordon Co. Soils at Various Stiffness Conditions

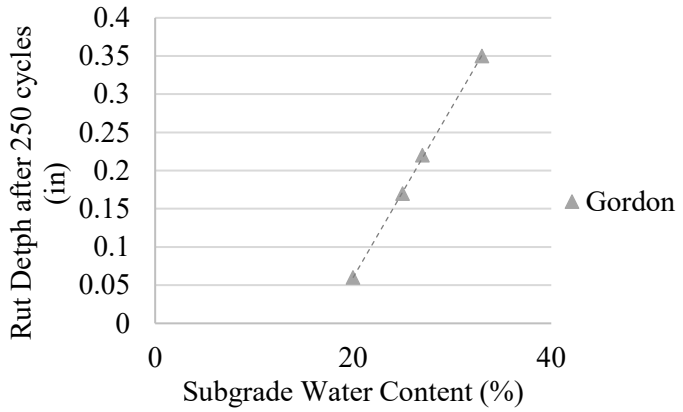

FIGURE 5.17

Rut Depths after 250 Cycles for the Three Subgrade Soils with No Stabilization

5.3.6 Effect of Geosynthetic Stabilization

As reported in multiple studies (Barksdale, 1989), geosynthetic stabilization shows the greatest improvement over soft subgrade soils with CBR below 2.5 or 3.0. This pattern was clear in the bench-scale rutting experiments.

5.3.6.1 Rutting with Stiff Subgrades at CBR>2.5

Rutting tests were conducted on Gordon and Hall County soils over relatively stiff subgrades with a CBR of 5 or greater, to assess the benefits of geosynthetics in stiff-subgrade conditions. The Gordon County specimen was prepared at a subgrade water content of 25% (CBR~5.5) and the Hall County specimen was prepared at 15% water content (CBR > 10). The rutting curves for each set of tests are presented in Figure 5.18, and the following observations can be made. Firstly, as noted before, the rutting for the unstabilized specimens is low with both subgrades, approximately 0.15 in. (3.81 mm) over Gordon County subgrade and 0.1 inch (2.5 mm) over Hall County subgrade, after 300 loading cycles. In the case of the Gordon County subgrade, shown in Figure 5.19 (a),

GG500 cause a reduction in rutting while GG250 showed a higher rutting of 0.2 in. (5.1 mm). In the case of the Hall County subgrade, shown in Figure 5.19 (b), the geogrids (GG1000, GG500, GG125) and geotextile did not show any further reduction in rutting, but instead showed a slightly greater rutting between 0.10 and 0.18 in. (2.5 and 7.1 mm). This anomalous behavior can be explained as follows: in stiff granular and soil media, the particles are closely packed, which allows the stresses to be efficiently transmitted through the pavement system with minimal lateral movement of the aggregate particles. This degree of lateral spreading is not sufficient to show any benefits of interlocking in geogrid apertures or frictional interaction with the geotextile. To the contrary, the presence of the geosynthetic material probably results in lower mobilized interface friction compared to the aggregate and the subgrade.

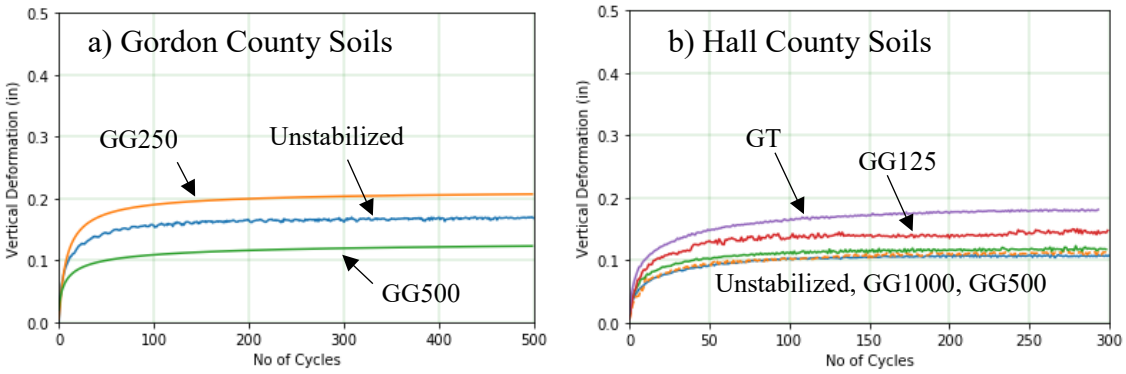

FIGURE 5.18

Effect of Geosynthetic Stabilization on (a) Gordon and (b) Hall County Subgrades with CBR>2.5

Upon establishing the low rutting deformations over stiff subgrade and considering that the focus of the bench-scale study was to establish the effectiveness of geosynthetic stabilization over soft subgrades, further tests were conducted on wetter subgrade soils with CBR less than 2.5. These results are discussed below.

5.3.6.2 Rutting with Stiff Subgrades at CBR<2.5

The stabilization effects of the geosynthetics were much more apparent in rutting tests over soft subgrade soils. Over soft subgrades, the larger magnitudes of rut depths induce significantly greater aggregate deformations, and the presence of a geosynthetic is helpful in arresting these movements, as demonstrated in the following results. Figures 5.19 to 5.21 present the rutting curves using low-stiffness (CBR<2.5) Coweta, Gordon, and Hall County subgrade soils, respectively. Among the three soils at CBR<2.5, Gordon County soil showed the least rutting of 0.35 in. (8.9 mm) after 250 loading cycles, followed by Hall County and Coweta County soils, which showed 0.43 and 0.48 in. (10.92 and 12.19 mm), respectively. While the unstabilized rutting is significantly greater compared to stiff subgrade condition, geosynthetic stabilization reduces the rutting by 28%, 31%, and 27% after 300 loading cycles for the three subgrade soils. This is a significant improvement and emphasizes the effectiveness of stabilization. There is no consistent trend observed among the individual geosynthetics and three subgrade cases, which probably is due to a combination of factors, including variations in soil properties and testing water contents.

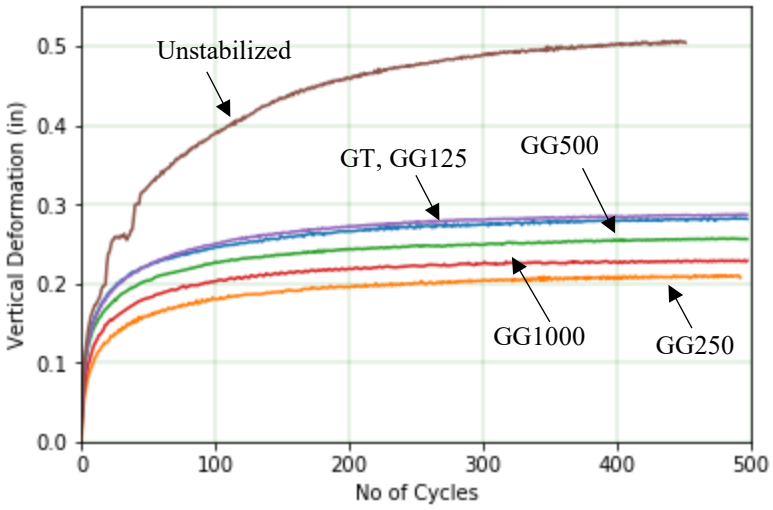

FIGURE 5.19

Effect of Geosynthetic Stabilization on Soft Coweta County Subgrade at 27% Water Content

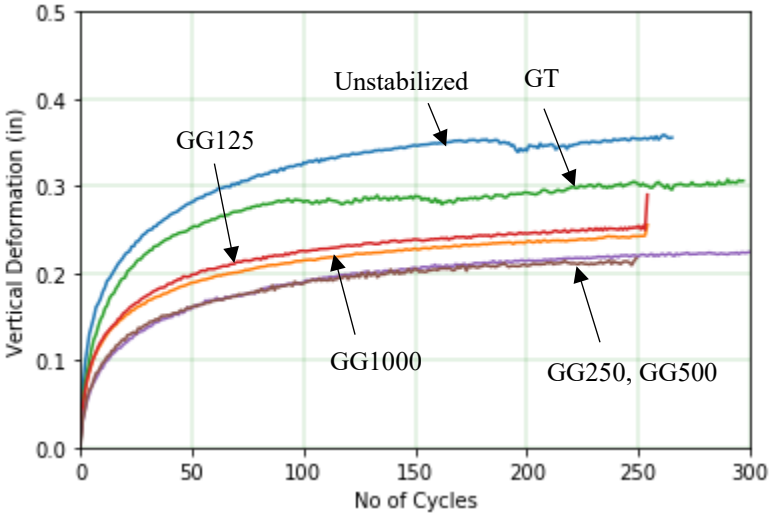

FIGURE 5.20

Effect of Geosynthetic Stabilization on Soft Gordon County Subgrade at 32% Water Content

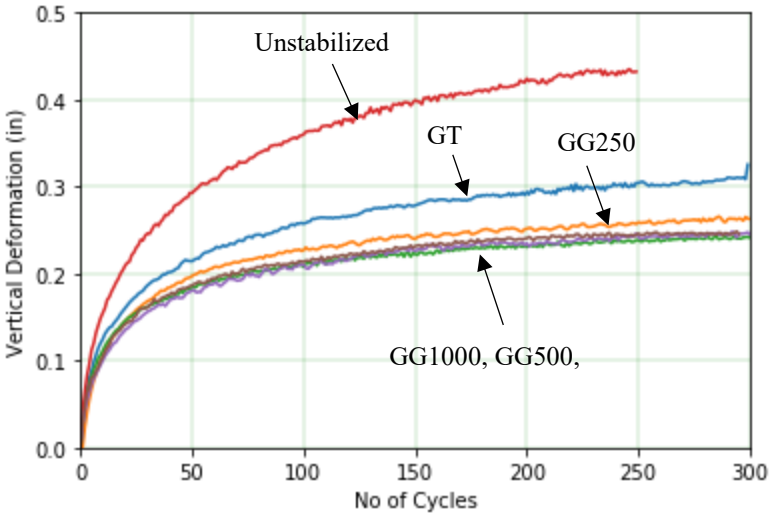

FIGURE 5.21

Effect of Geosynthetic Stabilization on Soft Hall County Subgrade at 32% Water Content

As stated before, the performance of the geosynthetics are a function of a multitude of factors, including interaction mechanism, geometry, rib thickness, and tensile stiffness. Owing to this fact, it is difficult to attribute the rutting depths to a specific parameter. Figures 5.10 through 5.21 clearly demonstrate the difference in mechanisms of aggregate–geogrid and aggregate–geotextile interactions, based on the consistent superior performance of the geogrids compared to the geotextile. The interlocking of aggregates achieved with geogrids is clearly more efficient than the solely frictional resistance that is mobilized with the geotextile, even though the geotextile has the higher tensile strengths among all geosynthetics.

The other useful observation is based on the performance of the commercially available GG1000 and the three scaled-down geogrids. First, GG1000 and GG500 are comparable in terms of the 2% tensile strength and rib thicknesses and are fairly close to each other in the rutting performance in all three subgrade cases. Secondly, GG250 shows

an equally good or improved rutting behavior despite its inferior tensile properties. This indicates that these geogrids fall within the range of optimal opening size for highest interlocking with the aggregate particles. Lastly, the performance of GG125, which is the least stiff of the five geosynthetics used in the study, is in the proximity of the geogrids and geotextile based on the rutting curves in Figures 5.10 through 5.21. However, as presented in the subsequent section, stress measurements in the subgrade showed that this aspect has an adverse impact on the subgrade, which is not seen with other geosynthetics.

5.3.7 Stress Distribution in Subgrade

The stabilizing potential of geosynthetics was assessed in terms of their influence on stress variations in the subgrade.

5.3.7.1 Effect of Subgrade Stiffness

The rutting curves over stiff subgrade were similar for both stabilized and unstabilized tests. Figure 5.22 presents stresses measured during the test in (a) an unstabilized specimen and (b) a GG250-stabilized specimen over Gordon County subgrade at 20% water content (CBR>10). Each subplot presents stress measurements made at the surface of the subgrade and at a depth of 1 in. (25 mm) below the surface of the subgrade. The latter set of measurements inside the subgrade should clearly reflect the influence of the overlying geosynthetic, if any.

The mean stresses in the case of the unstabilized rutting test were 8 psi (55 kPa) at the top of the subgrade and 2.6 psi (17.9 kPa) at a depth of 1 in. (25 mm) below the top of the subgrade, as in Figure 5.22 (a). The corresponding values in the case of the GG250-stablized rutting test were 7 psi (48 kPa) and 2 psi (14 kPa), respectively, as in Figure 22 (b). The corresponding rut curves are very similar for the two test cases, as in

Figure 22 (c). Although it is expected that the impact of geogrid is going to be minimal in stiff subgrade conditions, the slight reduction in stress is encouraging. The pattern of stress reduction as the test progresses as shown in Figure 5.22 (b) is unique, and probably indicates the improving capability of the geogrid to laterally distribute the vertical loads upon stabilization of the base layer.

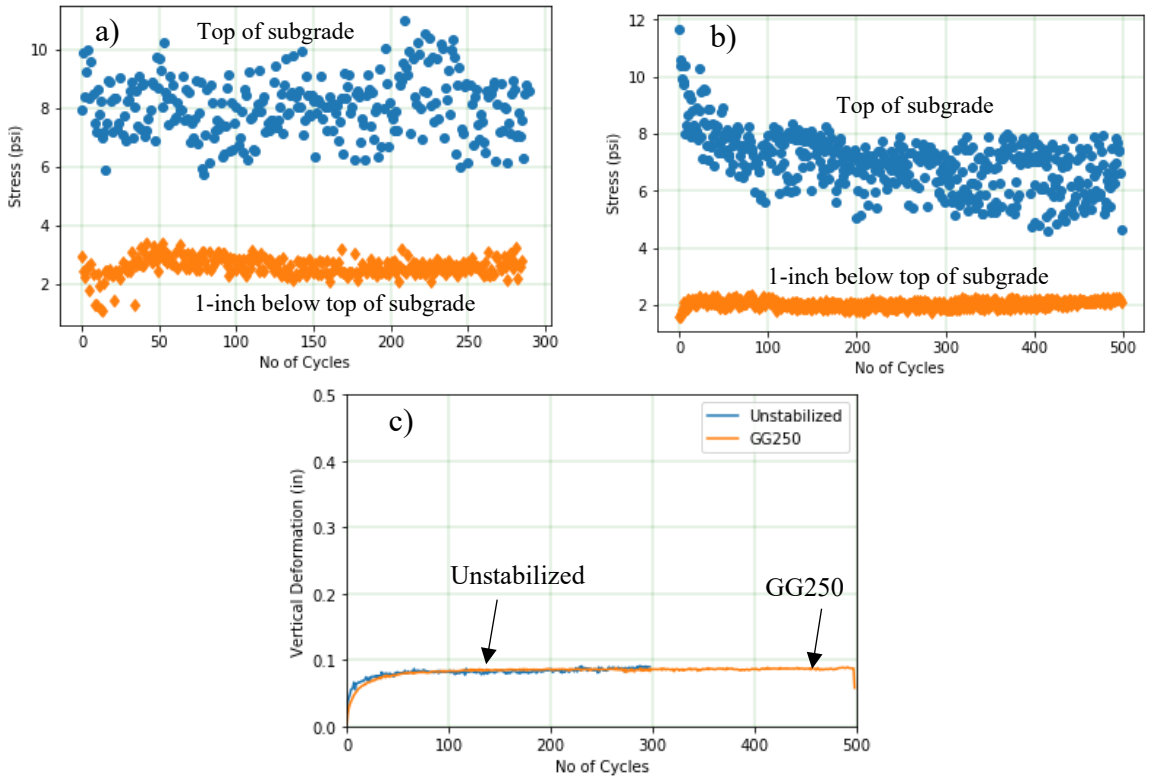

FIGURE 5.22

Stress Measurements in a) Unstabilized and b) GG250-Stabilized Specimens with Stiff Gordon County Subgrade and c) Corresponding Rutting Curves

Figure 5.23 shows stress measurements made in the Gordon County subgrade layer for various unstabilized and stabilized scenarios. The top-of-subgrade stresses vary initially and stabilize between 4 and 6 psi (25 and 41 kPa) in all cases. However, the stress measured

at depth 1 in. (25 mm) below the surface of the subgrade shows different behavior for the unstabilized and stabilized cases. As seen in Figure 5.23 (a), the stresses measured inside the subgrade increase to 4 psi (25 kPa) at the end of 300 cycles of loading. This indicates deterioration of the base layer, leading to higher stresses being transmitted to the subgrade

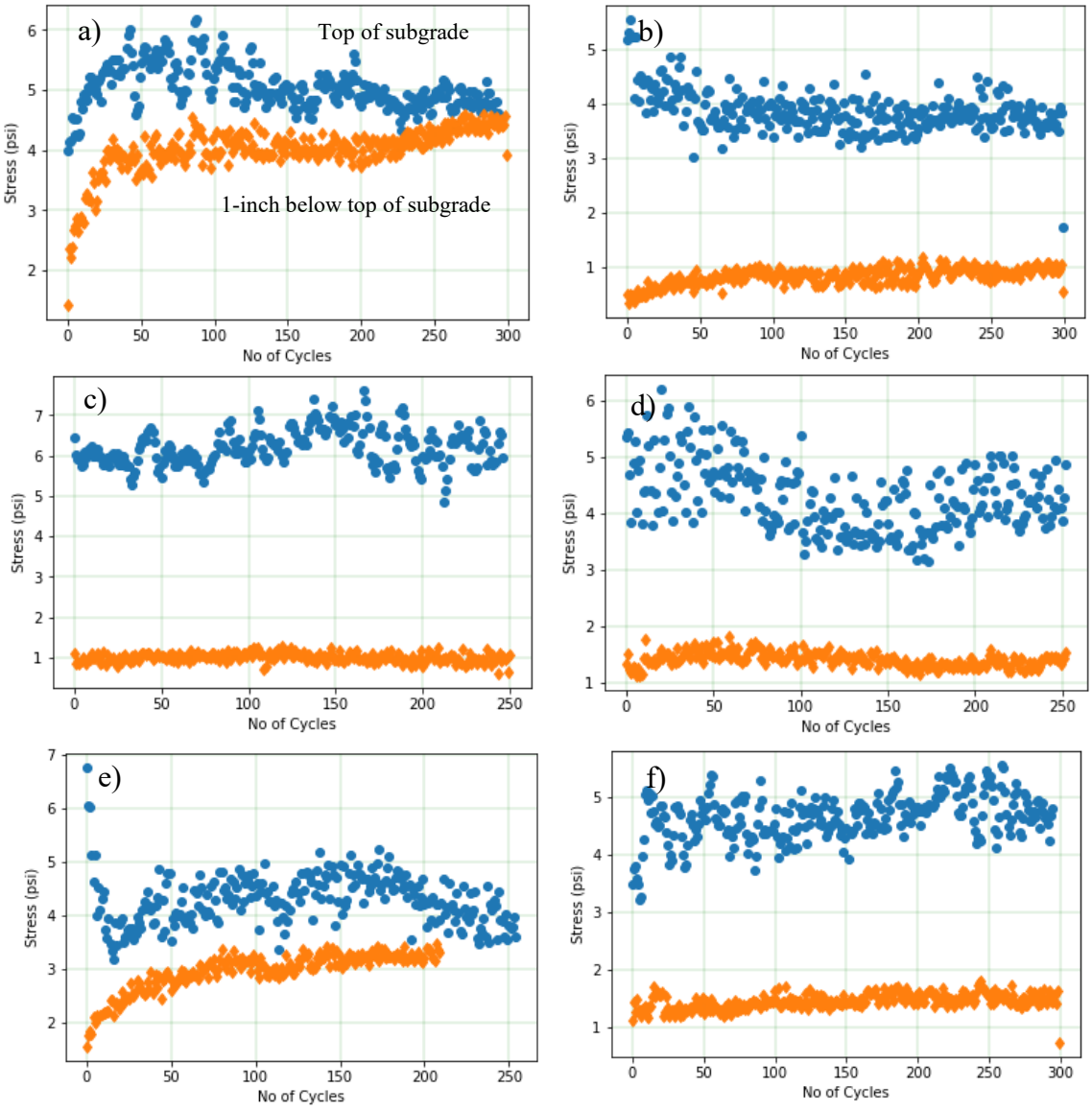

FIGURE 5.23

Stress Variation in Top 1 in. of Subgrade for a) the Unstabilized Case and the Stabilized Cases with b) GG1000, c) GG500, d) GG250, e) GG125 and f) GT

as the test progresses. Meanwhile, all other subplots in Figures 5.23 (b) to (f), except Figure 23 (e), show significantly lower magnitudes of stresses, of about 2 psi (14 kPa) being experienced in the subgrade. This observation clearly demonstrates that the geosynthetics are able to distribute the traffic loads laterally, which is crucial in maintaining the structural integrity of the pavement.

However, Figure 5.23 (e) shows a different behavior compared to the other geosynthetic cases. As noted in Figure 5.20, the rutting curve corresponding to GG125 lies between the remaining geogrids and the unstabilized case. Rutting with GG125 was lower than the GT-stabilized test. However, Figure 5.23 (e) shows the top-of-subgrade stresses to be increasing as the test progresses and thus, not efficiently distributing the loads laterally. Interestingly, this observation is complemented with a similar pattern in magnitudes of subgrade rutting. These measurements were made after completion of a test and exhuming the aggregate layer by manually placing a ruler horizontally across the specimen and measuring the depth of the center point under the wheel path using calipers. The subgrade rut was recorded at three locations along the wheel path to get an accurate estimate of subgrade rutting. The values of subgrade rutting for the tests corresponding to Figures 5.23 (a) through (f) were 0.231 (unstabilized), 0.153 (GG1000), 0.099 (GG500), 0.099 (GG250), 0.157 (GG125), and 0.184 (GT) in., respectively. As stated before, the GG125 is the lowest stiffness material of all the geosynthetics. The above-stated observations regarding the lack of load distribution and increased subgrade rutting with the GG125 could be caused by its low stiffness.

Another observation along similar lines concerns the GT-stabilized test results. Even though the rutting with the GT case is higher than all the geogrid-stabilized cases, the

stresses are comparatively smaller, as seen in Figure 5.23 (f). Again, this could be caused by the high stiffness of the geotextile, which distributes the load to a larger area over the subgrade. So, in spite of the high surface and subgrade rutting, the stress experienced over the stress sensor is smaller.

Interestingly, the top-of-subgrade stress measurements in Figures 5.23 (b) to (d), corresponding to the geogrids, show an initial decrease before stabilizing after about 50 loading cycles. This is probably the phase where aggregate particles are interlocking in against each other and the geogrid apertures, after which strong particle contacts are better able to distribute lateral forces, consequently reducing the vertical stress. The same phenomenon was observed with the large-scale testing.

A clear variation in the stress measurements was observed at low and high subgrade stiffnesses. Figure 5.24 presents the mean stresses measured in Gordon County subgrade over a range of stiffness conditions, including subgrade water contents of (a) 20%, (b) 27%, and (c) through (e) 33% water content. In subplots (a)–(e) in Figure 5.24, a comparison has been presented between measurements from unstabilized and stabilized cases, at both locations in the specimen, i.e., the top of the subgrade and 1 in. (25 mm) below the top of the subgrade. Figure 5.24 (f) presents the same comparison using geogrids GG500, GG250, and GG125. The following observations can be made from Figure 5.24.

Comparing the unstabilized cases in Figures 5.24 (a) through (d), the effect of subgrade stiffness can be observed. At 20% water content, seen in Figure 5.24 (a), there is a significant drop of 6 psi (41 kPa) in measured stresses from the top of the subgrade to 1 in. below the top. However, at greater water contents this gap is reduced to about 1 psi

or lower. These observations match expected behavior relating to high stiffness and low stiffness subgrade soils.

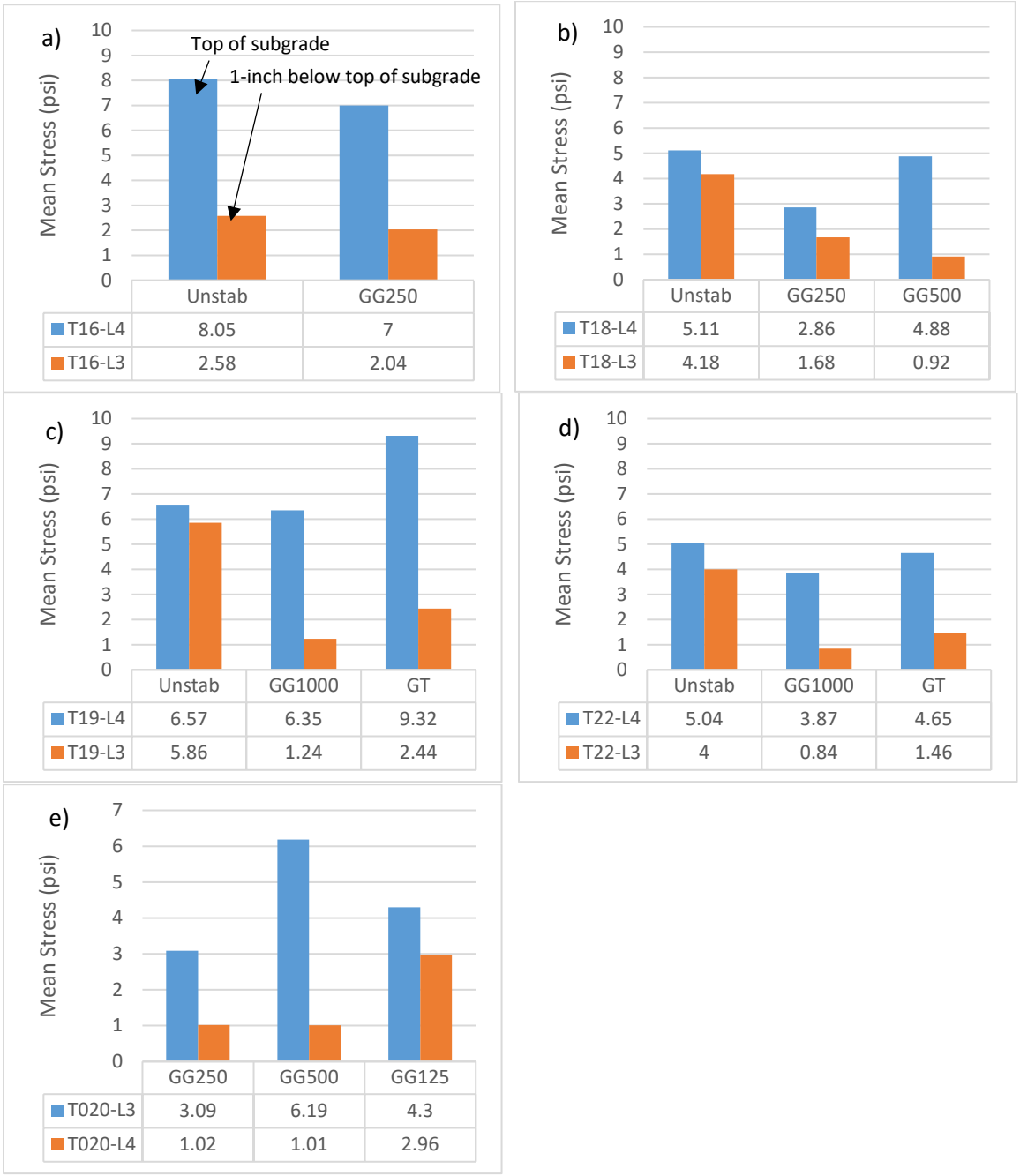

FIGURE 5.24

Mean Stress Measured for Various Scenarios of Stabilization Using Gordon Co. Subgrade at Water Contents of a) 20%, b) 25%, c) 27%, and d) and e) at 32%

The effect of inclusion of geosynthetic is also clearly observed from these plots. In Figure 5.24 (a) in stiff subgrade conditions, the stabilized test shows slightly lower stress values than the unstabilized test, and, more generally, follows the pattern shown by the unstabilized test. This is similar to the observations made with the rutting curves, where the effect of stabilization on the rutting curves was negligible. Even at greater water contents, as in Figures 5.24 (b) to (d), the stresses measured in the stabilized case at the top of the subgrade is still generally slightly lower than the unstabilized case. However, the influence of the geosynthetic can be witnessed by the significant difference in the values recorded 1 in. (25 mm) inside the subgrade. As stated earlier, in the unstabilized tests at higher water contents, as in Figures 5.24 (b) to (d), the gap in the stress magnitudes from the top of the subgrade to 1 in. (25 mm) below is greatly reduced. The stress measured 1 in. (25 mm) below the top of the subgrade is very close to the measurement at the top of the subgrade, due to the inability of the soft soil to distribute the applied load. Interestingly, the stabilized tests exhibit a much lower stress inside the subgrade compared to the unstabilized test measurements. This shows that the geosynthetics are able to distribute the loads laterally, and thereby reduce the intensity of the stress that is transmitted into the subgrade.

In summary, the geosynthetics are significantly more influential in stabilizing soft soils, which is the trend that was observed in the case of the surface rutting depth measurements. Figure 5.24 (e) shows a comparison of the performance of the GG500 and GG250, which are stiff geogrids, and GG125, which exhibits the least stiffness. In fact, GG125 can also be torn by hand, which gives a sense of its low stiffness. As explained earlier in Figure 5.23 (e), the low stiffness of GG125 causes higher stress to be transmitted

into the subgrade, while the GG1000, as well as GT, shows remarkably improved performance.

6. DISCRETE ELEMENT MODELING

Discrete element modeling facilitates the simulation of complex physical processes by modeling the behavior of individual particles. These particles interact with each other based on linear-elastic forces and Coulomb friction (Cundall and Strack, 1979). For this study, discrete element modeling (DEM) was used to numerically simulate a repeated-load test over an aggregate specimen, with and without a geogrid. The change in porosity and surface vertical deformation under the loading cylinder are recorded, since they reflect the interactions between the individual aggregate particles as well as aggregate-geogrid particles. By studying the differences in behavior between the unstabilized and geogrid-stabilized specimens, the benefits of particle interlocking in geogrid openings can be estimated. The three-dimensional (3D) numerical model was developed using the Yade discrete element framework, which is open-source and actively developed by academicians across the world (Smilauer et al., 2015). The following section details the procedure and properties for the model design and calibration.

6.1 Geogrid and Aggregate Modeling

The geogrid and aggregate materials were first modeled individually based on available experimental data. The geogrid geometry was modeled to simulate the BX1200 properties, such as biaxial geometry, aperture opening size of 1 in. (25 mm) × 1.3 inch (33.0 mm), and rib thickness of 0.03 in. (0.76 mm). The tensile stiffness was calibrated based on the tensile strength value of 280 lb/ft (417 kg/m) at 2% axial strain. For this study, the aggregate material was modeled as mono-sized mixture of spherical particles of diameter equal to half the geogrid aperture opening (i.e., 0.5 in. or 12.7 mm).

6.2 Specimen Modeling

The goal of this exercise for the current study is to provide a glimpse into the particle-level information available using the DEM technique. The scale of the model was chosen to achieve a balance between incorporating a sufficiently sized geogrid to observe benefits, as well as reduce computation time. The geogrid was placed in the middle of the specimen. Figures 6.1 (a) and (b) show the generated specimen without and with a geogrid, respectively.

The aggregate and geogrid particles are generated and assembled in a chamber measuring 10 in. (254 mm) × 8 in. (203 mm) in area and 10 in. (254 mm) in height. These values were chosen to limit simulation time since the DEM process is a computation- and time-intensive exercise. Next, the chamber is cyclically constricted and expanded in thickness to simulate the compaction process, which results in rearrangement of the particles to a more dense state. If the geogrid is present in the specimen, this ensures interlocking between the aggregate particles and geogrid openings. While the thickness of the specimen was chosen to be approximately 10 in. (254 mm) prior to compaction, the thickness reduced to 5 in. (127 mm) after the compaction stage. The loading cylinder, measuring 4 in. (102 mm) in diameter, is made to cyclically impact-load the specimen, applying a predefined stress for 400 cycles. The performance of the specimen was assessed at multiple loading stresses, including 7.0, 13.8, and 27.6 psi (48, 95.1, and 190.3 kPa).

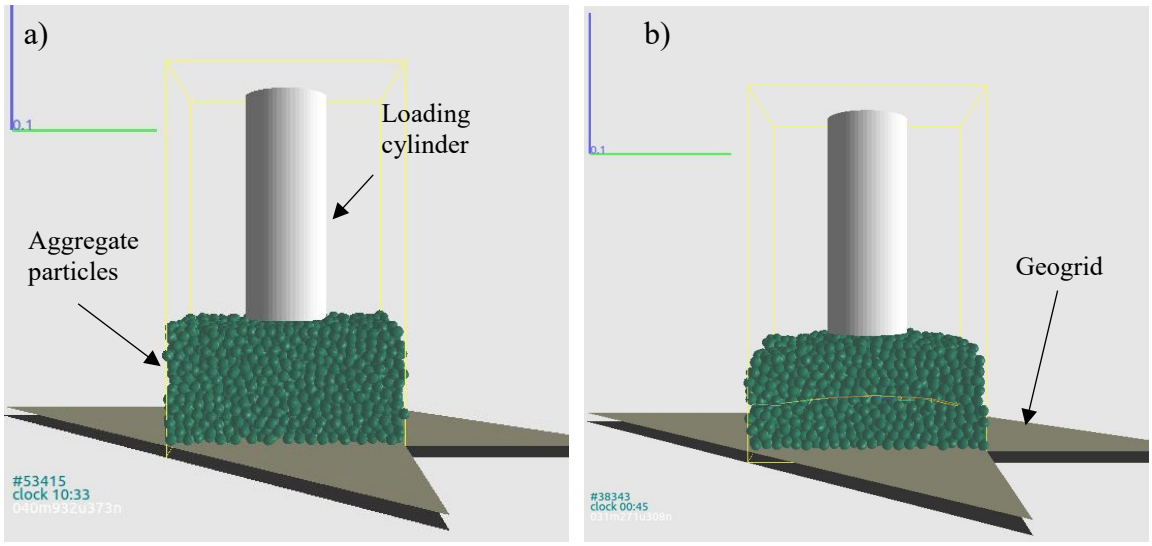

FIGURE 6.1

Generated Specimens: (a) Unstabilized Test Case and (b) Geogrid-Stabilized Test Cases

The generated specimens were subjected to cyclic loading for multiple hundreds of cycles, and the surface vertical deformation (rutting) and the specimen porosity were continually recorded. The rutting curves for the three loading stresses are presented in Figure 6.2. At a low stress value of 7 psi (48 kPa), the unstabilized curve is similar to the stabilized curve. At 13.8 psi (95.1 kPa), the stabilized curve shows an improvement in performance compared to the unstabilized curve, while at 27.6 psi (190.3 kPa), this improvement is even higher. This, again, proves that the effect of geogrid stabilization is evident at extremely unfavorable conditions.

Figures 6.3 (a) and (b) present the variation of porosity of the specimen for unstabilized and stabilized tests, respectively. In Figure 6.3 (a), the porosity initially decreases instantly with all three loading stresses, and stabilizes for the 7-psi (48 kPa) test case but increases again at higher stresses. This increase is steeper at 27.6 psi (190.3 kPa) compared to 13.8 psi (95.1 kPa). This is an interesting observation, and follows the

behavior of dilation effects observed in dense soils. A plateau in the porosity indicates the specimen is able to sustain the applied loads, while a continuous increase probably indicates it requires stabilization. In Figure 6.3 (b), there is the initial decrease in porosity as expected with the first few cycles of loading, but the increase of porosity is much less pronounced than in the unstabilized tests. In addition, this proves the stabilization potential of geogrids.

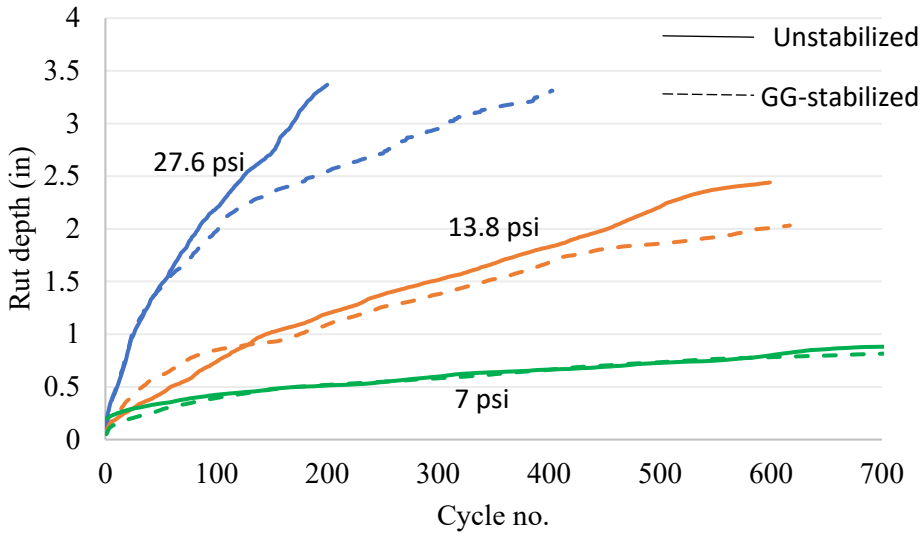

FIGURE 6.2

Rutting Depths for Repeated Cyclic Loading of Unstabilized and Geogrid-Stabilized Specimens at 27.6 psi, 13.8 psi, and 7 psi

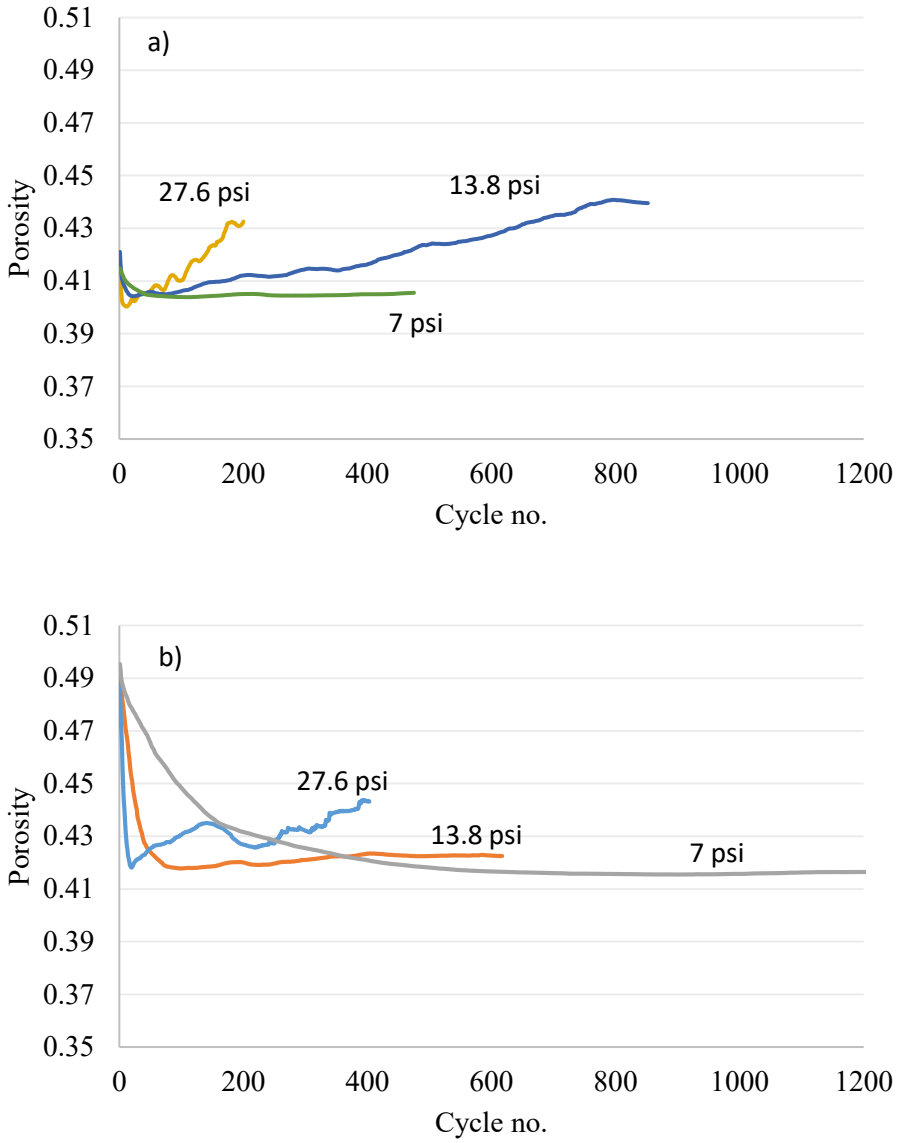

FIGURE 6.3

Porosity Variation for (a) Unstabilized and (b) Geogrid-Stabilized Specimens at Loading Stresses of 27.6 psi, 13.8 psi, and 7 psi

Beyond these measurements, there are several added advantages of computational modeling that are extremely difficult to achieve in the laboratory environment. These benefits, although all are not implemented for this study but form potential topics of further study, include 1) measurement of lateral displacements of individual particles under the loaded area to track confining effects induced by geogrids, 2) measurement of vertical and

lateral stresses on selected particles, and 3) visualization of the tensile forces in the ribs of the geogrid at various stages of the test. A glimpse of the usefulness of one such insight, concerning the deformation pattern of the geogrid inside the specimen, is presented in Figure 6.4. At the start of the test, the geogrid is only deformed by the compaction of the specimen, and indicates conformance to the aggregate packing, as shown in Figure 6.4 (a). Figures 6.4 (b) to (d) show the deformed geogrid after 400 loading cycles at 7, 13.8, and 27.6 psi (48, 95.1, and 190.3 kPa), respectively.

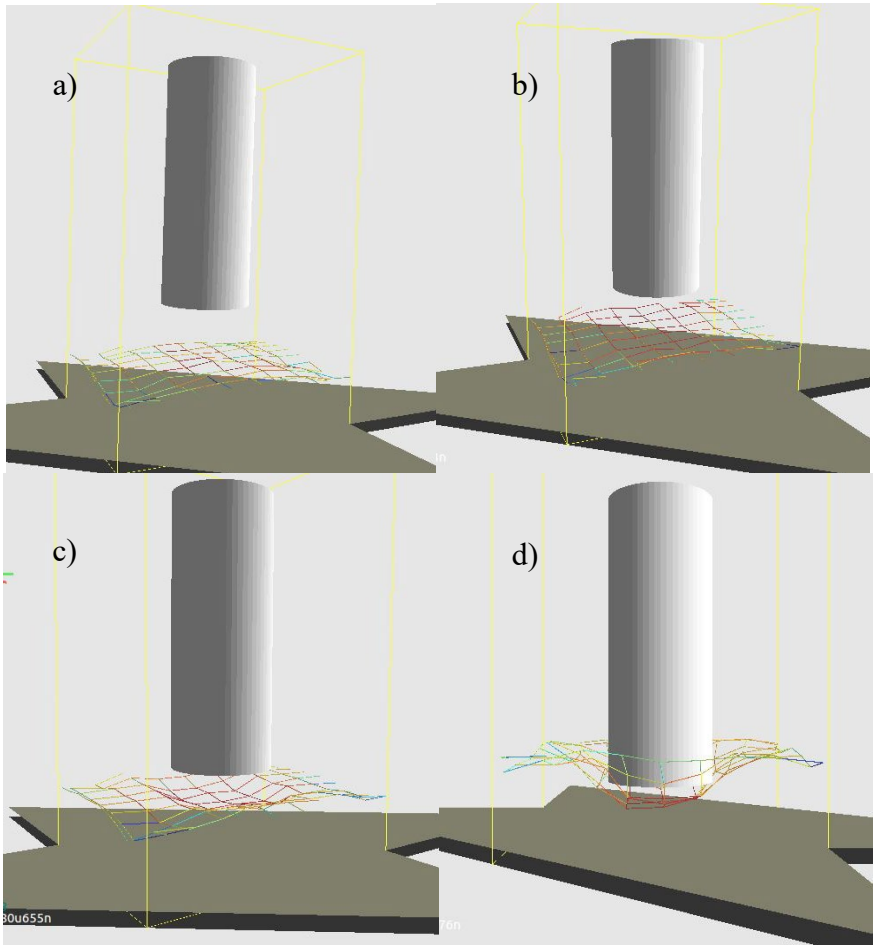

FIGURE 6.4

Geogrid Conditions at: (a) Cycle 1 of Testing Stage, (b) Cycle 400 with 7 psi, (c) Cycle 400 with 13.8 psi, and (d) Cycle 400 with 27.6 psi

7. CONCLUSIONS AND RECOMMENDATIONS

This study investigated the effects of geosynthetic stabilization of pavement systems using both bench-scale and large-scale moving wheel load systems. The results presented confirm the effectiveness of geosynthetics using performance metrics of surface rutting and vertical stresses at the bottom of the graded aggregate base and the top of the subgrade. The following conclusions can be made:

- For thicker aggregate base layers (greater than 10 in. or 254 mm), the optimal geogrid placement location is at the mid-height of the aggregate base layer as long as the migration of subgrade fines is not a concern. For a subgrade soil type with high fine contents (greater than 50% passing No. 200 sieve size), the use of geotextile at the subgrade and GAB interface is highly recommended to enhance long-term performance of pavement by minimizing migration of fine contents.
- Geotextile is able to provide the greatest pressure reduction in the subgrade layer when the soil is prepared at optimum moisture content in the highest strength soils (SSV = 2.5 or greater).
- When the subgrade soil is prepared at a high moisture content, the aggregate base layer experiences higher vertical pressures than when prepared at OMC. At this subgrade condition with high moisture content, geogrid generally performs only in reducing pressure.
- Comparing the light wheel deflectometer results to pressure results of a weak subgrade soil compacted at OMC brings forth an important relationship. Higher measured stiffness in the aggregate base layer correlated with a lower pressure

at the top of the subgrade. When geosynthetics are utilized, a higher GAB post-traffic modulus was observed. This results in a significant vertical pressure reduction in both the base and subgrade, which is beneficial for long-term pavement performance.

- The effect of geosynthetic stabilization was negligible at high subgrade-stiffness conditions but evident at low-stiffness conditions. For all geogrid-stabilized cases in the bench-scale tests, the observed rutting was at least 28% lower than the unstabilized case, while the geotextile achieved a minimum rut reduction of 14%.
- Stress measurements were very beneficial in gaining more complementary insights to surface rutting measurements. In high stiffness conditions, stresses measured 1 in. (25 mm) into the subgrade were significantly lower (about 5 psi or 34.5 kPa) than the top of the subgrade, irrespective of the stabilization condition. However, at lower subgrade stiffnesses, the unstabilized tests showed a reduction of less than 1 psi (7 kPa) and more than 4 psi (28 kPa) in subgrade, while the stabilized tests continued to show significant reductions that reduced the stress to below 2 psi (14 kPa).
- A discrete element modeling technique was used to demonstrate the effectiveness of geogrid stabilization, as well as the further added particle-level insights available with such techniques.
- Ultimately, the experimental study presented in this report presents compelling evidence establishing the usefulness of geogrids and geotextiles over soft subgrades. By combining insights from the evolution of rutting and stresses in

the specimens, the understanding of the complex response of aggregate–geosynthetic–subgrade systems can be improved.

Based on this study, a "Quick Selection Guide of Geosynthetics" was developed and included in the Appendix. The research team recommends use of the guide as a condition-specific guidance to effectively incorporate geosynthetics in flexible pavement construction in North Georgia. This guide will allow users to consider subgrade soil conditions and other properties to select the optimal geosynthetic type and installation location to help extend the service life of the roadway.

This page is intentionally left blank.

8. REFERENCES

1. Abdalla, M. (2008). Effect of Subgrade Properties on Pavement Performance. *Gulf Conference on Transportation*.

2. Al-Qadi, L. L., Dessouky, S. H., & Tutumluer, E. (2008). Geogrid-reinforced low-volume flexible pavement response to loadings by various tire configurations. In *Efficient Transportation and Pavement Systems: Characterization, Mechanisms, Simulation, and Modeling - Proceedings of the 4th International Gulf Conference on Roads* (pp. 741-751)

3. ASTM D1140 Standard Test Methods for Determining the Amount of Material Finer than 75-µm (No. 200) Sieve in Soils by Washing, ASTM International, West Conshohocken, PA, 2017

4. ASTM D1556/D1556M-15e1 Standard Test Method for Density and Unit Weight of Soil in Place by Sand-Cone Method, ASTM International, West Conshohocken, PA, 2015, https://doi.org/10.1520/D1556_D1556M-15E01.

5. ASTM D1557 Standard Test Methods for Laboratory Compaction of Soil using Modified Effort (56,000 ft-lbf/ft3 (2,700 kN-m/m3)), ASTM International, West Conshohocken, PA, 2012

6. ASTM D1557-12e1 Standard Test Methods for Laboratory Compaction Characteristics of Soil Using Modified Effort (56,000 ft-lbf/ft^3 (2,700 kN-m/m^3)), ASTM International, West Conshohocken, PA, 2012, https://doi.org/10.1520/D1557-12E01.

7. ASTM D1883 Standard Test Method for California Bearing Ratio (CBR) of Laboratory-Compacted Soils, ASTM International, West Conshohocken, PA, 2016

8. ASTM D4221-18 Standard Test Method for Dispersive Characteristics of Clay Soil by Double Hydrometer, ASTM International, West Conshohocken, PA, 2018, https://doi.org/10.1520/D4221-18.

9. ASTM D4318-17e1 Standard Test Methods for Liquid Limit, Plastic Limit, and Plasticity Index of Soils, ASTM International, West Conshohocken, PA, 2017, https://doi.org/10.1520/D4318-17E01.

10. ASTM 4439-18 Standard Terminology for Geosynthetics, ASTM International, West Conshohocken, PA, 2018

11. ASTM D4643-17 Standard Test Method for Determination of Water Content of Soil and Rock by Microwave Oven Heating, ASTM International, West Conshohocken, PA, 2017, https://doi.org/10.1520/D4643-17.

12. ASTM D6637 Standard Test Method for Determining Tensile Properties of Geogrids by the Single or Multi-Rib Tensile Method, ASTM International, West Conshohocken, PA, 2015

13. ASTM D6913 Standard Test Methods for Particle-Size Distribution (Gradation) of Soils Using Sieve Analysis, ASTM International, West Conshohocken, PA, 2017

14. ASTM D6951/D6951M-18 Standard Test Method for Use of the Dynamic Cone Penetrometer in Shallow Pavement Applications, ASTM International, West Conshohocken, PA, 2018, https://doi.org/10.1520/D6951_D6951M-18.

15. Bagshaw, S. A., Herrington, P. R., Kathirgamanathan, P., & Cook-Opus International Consultants LTD, S. R. (2015). *Research Report 574 Geosynthetics in basecourse stablisation* (Rep. No. 574). Wellington, NZ: NZ Transportation Agency.

16. Barksdale, R. D. (1972, September). Laboratory evaluation of rutting in base course materials. In *Presented at the Third International Conference on the Structural Design of Asphalt Pavements, Grosvenor House, Park Lane, London, England, Sept. 11-15, 1972.* (Vol. 1, No. Proceeding).

17. Barksdale, R.D.; Brown, S. F.; and Chan, F. (1989). Potential Benefits of Geosynthetics in Flexible Pavement Systems, National Cooperative Highway Research Program Report No. 315, Transportation Research Board, National Research Council, Washington, D.C., 56 p.

18. Bauer, G. E., and A. O. Abdelhalim. The Performance of Geogrid Reinforced Road Bases. *Construction & Building Materials,* Vol. 1, No. 2, 1987, pp. 71–75.

19. Berg, R. R., Christopher, B. R., & Perkins, S. (2000). *Geosynthetic reinforcement of the aggregate base/subbase courses of pavement structures* (No. GMA White Paper II).

20. Bilodeau, J. P., Dore, G., & Pierre, P. (2009). Pavement base unbound granular materials gradation optimization. In *Bearing Capacity of Roads, Railways and Airfields. 8th International Conference (BCR2A'09)*.

21. Boussinesq, J. (1885). Discussed in Theory of Elasticity.

22. BSI (British Standards Institution). (1990). Methods of test for soils for soils for civil engineering purposes. BS 1377, London.

23. Burmister, D. M. (1945). The General Theory of Stresses and Displacements in Layered Systems. I. Journal of Applied Physics, 16(2), 89-94. doi:10.1063/1.1707558

24. Cavanaugh, J., Kwon, J. (2008). Developing Mechanistic-Empirical Design Methods. CE News, 20(9).

25. Chen, F.H. (1973). The basic physical property of expansive soils. Proc. 3rd Int. Conf. Expansive Soils, Haifa, Israel 1:17-25

26. Christopher, B. R., Perkins, S. W., Lacina, B. A., & Marr, W. A. (2009, February). Pore water pressure influence on geosynthetic stabilized subgrade performance. In *Proceedings, 2009 Geosynthetics Conference*.

27. Cuelho, E. V., Perkins, S. W., & von Maubeuge, K. (2011). Full-scale field study of geosynthetics used as subgrade stabilization. In *Geo-Frontiers 2011: Advances in Geotechnical Engineering* (pp. 4703-4712).

28. Cuelho, E. and Perkins, S. (2009). *Field investigation of geosynthetics used for subgrade stabilization* (No. FHWA/MT-09-003/8193). Montana Department of Transportation.

29. Cuelho, E., Perkins, S., and Morris, Z. (2014), Relative Operational Performance of Geosynthetics Used as Subgrade Stabilization, Final Project Report to the Montana Department of Transportation, FHWA/MT-14-002/7712-251, 313 pp.

30. Cundall, P.A. and Strack, O.D.L. (1979). A discrete numerical model for granular assemblies, Géotechnique, 29, 47–65.

31. Dantu, P., Contribution a l'Etude Mechanique et Geometrique des Milieux Pulverulents, Proceedings, 4th International Conference on Soil Mechanics, Vol. 1, London, U.K., 1957.

32. Department of the Army. (1994). Planning and Design of Roads, Airfields, and Heliports in the Theater of Operations-Airfield and Heliport Design (FM 5-430-00-2). Washington, DC. Retrieved from https://chetaero.files.wordpress.com/2016/11/fm5-430-vol2-entire.pdf

33. GDOT Office of Materials and Research. (2013). *Georgia Department of Transportation Pavement Design Manual*. Atlanta, GA: GDOT.

34. Greene, J., Kim, S., & Choubane, B. (2011). Accelerated pavement testing and gradation-based performance evaluation method. *Transportation Research Record: Journal of the Transportation Research Board*, (2225), 119-127.

35. Holtz, R. D., Christopher, B. R., & Berg, R. R. (2008). *Geosynthetic Design & Construction Guidelines: Reference Manual*. US Department of Transportation, Federal Highway Administration, National Highway Institute.

36. Huang, Y. H. (2012). Pavement analysis and design (2nd ed.). Upper Saddle River, NJ: Pearson/Prentice Hall.

37. IDOT Bureau of Bridges and Structures. (2005). Subgrade Stability Manual, Illinois Department of Transportation.

38. Kim, S., Tutumluer, E., Little, D., and Kim, N. (2007). Effect of gradation on nonlinear stress-dependent behavior of a sandy flexible pavement subgrade. *Journal of Transportation Engineering*, *133*(10), 582-589.

39. Koerner, G. R. (2005). Update on GSI's Geotextile Highway Separation Study. In *Geosynthetics Research and Development in Progress* (pp. 1-6).

40. Kim, S., Yang, J., and Kwon, J. (2017). Effects of using screening materials in the graded aggregate base layer of flexible pavements, International Journal of Pavement Engineering, Vol., 18, Issue 2, 97-107

41. Koerner, R. *Designing with Geosynthetics,* 5th ed. Prentice Hall, Englewood Cliffs, N.J., 2005.

42. Lacina, B. A. (2011). Functions of Geotextiles Used in Roadway Base Course Construction: The benefits of using geotextiles in roadway construction include separation and stabilization. *AATCC Review: the magazine of the textile dyeing, printing, and finishing industry*, *11*(5), 37.

43. Lacina, B. A., P.E. and Dull, F. S., P.E. (2013). Flexible Pavement Performance with and Without Geosynthetics: Nine Year Follow-Up. In *Geosynthetics Conference 2013* (pp. 321-331). Long Veach, CA.

44. Lacina, B. A., Sack, R. L., & Odgers, B. O. (2015). Flexible Pavement Reinforcement using Geotextiles. *Geosynthetics Conference 2015*.

45. Luo, R., Gu, F., Luo, X., Lytton, R. L., Hajj, E. Y., Siddharthan, R. V., & Pournoman, S. (2017). *Quantifying the Influence of Geosynthetics on Pavement Performance* (No. NCHRP Project 01-50).

46. Metcalf, J. B. (1996). *Application of full-scale accelerated pavement testing* (Vol. 235). Transportation Research Board.

47. Milligan, G. W. E., Jewell, R. A., Houlsby, G. T., and Burd, H. J. (1989). A New Approach to the Design of Unpaved Roads – Part 1. *Ground Engineering*, *22*(3).

48. Mishra, G. (2016, December 04). Flexible Pavement Composition & Structure - Layers of Flexible Pavement. Retrieved November 13, 2017, from https://theconstructor.org/transportation/flexible-pavement-composition-and-structure/5499/

49. Mishra, D. and Tutumluer, E. (2012). Aggregate Physical Properties Affecting Modulus and Deformation Characteristics of Unsurfaced Pavements, Journal of Materials in Civil Engineering, 24(9), 1144-1152.

50. Nelson, J., and Miller, D. J. (1997). *Expansive soils: problems and practice in foundation and pavement engineering*. John Wiley & Sons.

51. Partl, M. N., Raab, C., & Arraigada, M. (2015). Innovative asphalt research using accelerated pavement testing. *Journal of Marine Science and Technology*, *23*(3), 269-280.

52. Pavement Interactive | Subgrade. (2012). Retrieved November 15, 2017, from http://www.pavementinteractive.org/

53. Perkins, S. W., Bowders, J. J., Christopher, B. R., and Berg, R. R. (2005). Geosynthetic reinforcement for pavement systems: US perspectives. In *International Perspectives on Soil Reinforcement Applications* (pp. 1-13).

54. Powell, R. B. (2012). A history of modern accelerated performance testing of pavement structures. *Advances in Pavement Design through Full-scale Accelerated Pavement Testing*, 3-12.

55. TenCate Geo (2018). Product Specification for Mirafi HP-270. https://www.tencategeo.us/en-us/products/woven-geotextiles/mirafi-hp. Accessed July 11, 2018.

56. Reck, N. C. (2009). Mechanistic empirical design of geogrid reinforced paved flexible pavements. In *Jubilee symposium on Polymer Grid Reinforcement, Institute of Civil Engineers, London, England*.

57. Saghebfar, M., Mustaque, H., Lacina, B. A., & Odgers, B. (2013). Investigation of Bearing Capacity of Geotextile-Reinforced Paved Roads. In *Mid-Continent Transportation Research Symposium*.

58. Saunders, C.H., Increasing the Single Lift Thickness for Aggregate Base: Base Placement and Compaction of Increased Lift Thickness of Aggregate Base on Test Projects, Paper Presented at the 5th Annual Symposium of the International Center for Aggregate Research (ICAR), 1997.

59. Smilauer, V. (2015), Yade Documentation 2nd ed. The Yade Project. DOI 10.5281/zenodo.34073 (http://yade-dem.org/doc/)

60. Steyn, W. J., Monismith, C. L., Nokes, W. A., Harvey, J. T., Holland, T. J., & Burmas, N. (2012). Challenges confronting road freight transport and the use of vehicle-pavement interaction analysis in addressing these challenges. *Journal of the South African Institution of Civil Engineering*, *54*(1), 14-21.

61. Tang, X., Abu-Farsakh, M., Hanandeh, S., & Chen, Q. (2014). Evaluation of Geosynthetics in Unpaved Roads Built over Natural Soft Subgrade Using Full-Scale Accelerated Pavement Testing. *Geo-Congress 2014 Technical Papers*. doi:10.1061/9780784413272.295

62. Tensar Biaxial BX Geogrid Product Specification. Tensar International Corporation. http://www.tensarcorp.com/Systems-and-Products/Tensar-Biaxial-BX-geogrids. Accessed July 11, 2018.

63. Thompson, M.R. (1998). State-of-the-art: unbound base performance. Proceedings of the 6th annual symposium of International Center for Aggregate Research (ICAR). Austin, TX.

64. Tingle, J. S., and S. R. Jersey. Full-Scale Evaluation of Geosynthetic-Reinforced Aggregate Roads. In *Transportation Research Record: Journal of the Transportation Research Board, No. 2116*, Transportation Research Board of the National Academies, Washington, D.C., 2009, pp. 96-107.

65. Transportation Research Board & SHRP (1986). *Final Report for Strategic Highway Research Program Research Plans*. NCHRP Project 20-20.

66. Tseng, K.H. and Lytton, R.L. Prediction of Permanent Deformation in Flexible Pavement Materials, ASTM STP, 1989. 1016, 154-172.

67. Tutumluer, E. (2013). Practices for Unbound Aggregate Pavement Layers. Synthesis, NCHRP, ed.

68. Tutumluer, E., Little, D., & Kim, S. (2003). Validated model for predicting field performance of aggregate base courses. *Transportation Research Record: Journal of the Transportation Research Board*, (1837), 41-49.

69. Wu, S., and Sargand, S. M. (2007). *Use of dynamic cone penetrometer in subgrade and base acceptance* (No. FHWA/ODOT-2007/01).

70. Xiao, Y., Tutumluer, E., Qian, Y. and Siekmeier, J.A. (2012). Gradation Effects Influencing Mechanical Properties of Aggregate Base-Granular Subbase Materials in Minnesota, Transportation Research Record: Journal of the Transportation Research Board, No 2267

71. Yoder, E. J., & Witczak, M. W. (1975). Principles of pavement design. New York, NY: Wiley.

APPENDIX A: QUICK SELECTION GUIDE OF GEOSYNTHETICS FOR PAVEMENT CONSTRUCTION IN NORTH GEORGIA

I. INTRODUCTION

Geosynthetics have become a popular alternative to traditional soil-improvement techniques for unsuitable subgrade soils. This manual serves as a quick guide when Georgia DOT engineers consider using geosynthetics for pavement construction projects located in or around North Georgia. This quick guide can provide answers for the following questions:

1) When (or in what soil condition) should geosynthetics be used?
2) What type of geosynthetics should be used for a given soil condition and graded-aggregate-base (GAB) thickness?
3) Where is the optimal geosynthetic placement location in the pavement structure?

Currently, GDOT has special provisions for Geogrid Reinforcement and Fabrics in Sections 457 and 881, respectively. Once a geosynthetic is selected from Figure A.3, users should refer to the appropriate special provision for installation procedures and other important information. Sections 457 and 881 are attached at the end of this document. Geosynthetics have functions including reinforcement, separation, filtration, drainage, fluid barrier, and protection. However, GDOT provisions only include information related to the geosynthetic functions of separation and reinforcement. As such, this guide primarily focuses on the separation and reinforcement functions.

The *separation* of aggregate base course and subgrade layers is important to maintain structural support of flexible pavement system. Geosynthetics, specifically geotextiles, can be used in-between the two layers to provide this separation. The second function emphasized in this quick guide is *reinforcement*, which adds tensile strength to the flexible pavement soil matrix (Holtz, Christopher, and Berg, 2008). Geotextiles and geogrids are both used for reinforcement, which allows for embankments to be constructed over the problematic fine-grained soils commonly found in North Georgia. Geosynthetics typically are used in design for a specific “primary” function but often have one or more secondary

functions that provide additional benefit to flexible pavements and further promote their use.

II. BACKGROUND

Subgrade soil is the foundational material underneath pavement structures. Pavement resilience can be dependent on the subgrade soil's support, so it is vital to maintain subgrade strength to ensure stability. For finished subgrade to be stable, it must have specific strength and deformation properties that impact pavement construction activities. High moisture content and high silt content of subgrade materials indicate a higher likelihood of instability and excessive rutting (IDOT, 2005). Different solutions have been developed to combat weak subgrades including removal of unsuitable soils, remediation techniques including mixing of soil and cement for strength, and placement of geosynthetics in the pavement system.

GDOT uses soil support values (SSVs) ranging from 2.0 to 4.5 for pavement design. Figure A.1 shows GDOT's SSV Map. A lower SSV indicates a soil with less ability to support the overlying pavement structure. Areas in North Georgia are well-known for having subgrade soil with SSVs ranging from 2.0 to 3.0, which commonly consist of fine-grained soils. In general, soils found above the fall line (see Figure A.2) typically fit into this category. Below the fall line, SSVs range from 3.0 to 4.5 (GDOT, 2013).

Subgrade soil found in North Georgia has lower support capabilities due to its physical composition. The soil in this area commonly contains high fines content (material passing the No. 200 sieve) and is commonly classified as high plasticity silt or clay. This high fines content is problematic for several reasons. As the fine material migrates upward with the change in water content and mixes with the base course, a decrease in the structurally sound base course thickness occurs, in addition to a lower density of the subgrade, and thereby decreases the pavement structural number (SN). High fines subgrades are also problematic due to their susceptibility to excessive deflections making compaction difficult, and their vulnerability to frost impacting long-term performance (Holtz et al., 2008).

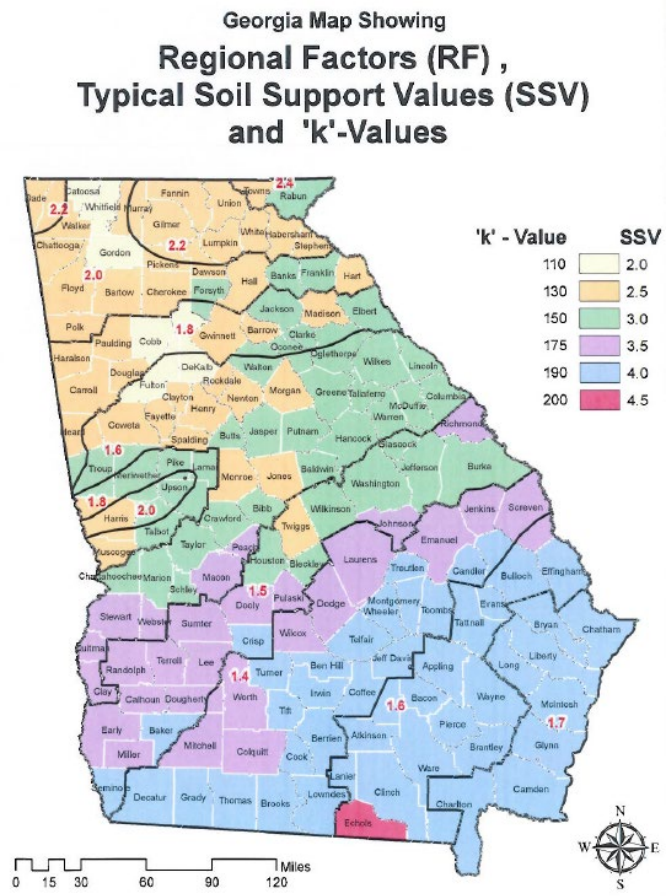

FIGURE A.1

GDOT Soil Support Value Map (GDOT, 2013)

III. GEOSYNTHETIC SELECTION

Since the majority of subgrade soil below the fall line in Georgia has higher SSVs and specific soil improvement procedures, it is suggested that this geosynthetic selection guide only incorporate projects North of the fall line. Figure A.2 provides geographical information to determine the applicability of the selection guide in relation to the fall line.

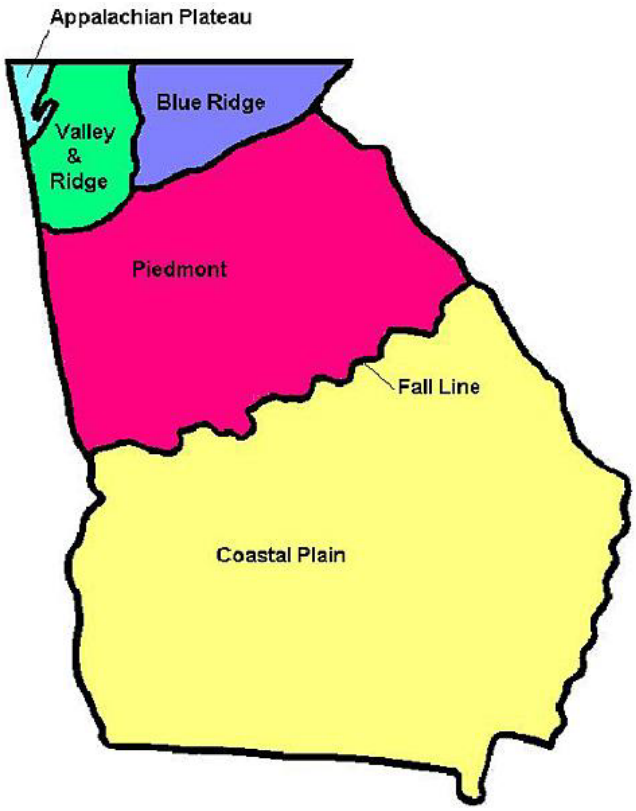

FIGURE A.2

Georgia Fall Line Location
(Georgia Humanities and the University of Georgia Press, 2018)

Figure A.3 shows the geosynthetic selection guide based on large-scale testing results from the GDOT RP 16-11 study. The chart is intended to help designers who are working with subgrade soils with GDOT SSVs <3.0 to select an appropriate geosynthetic to improve flexible pavement performance.

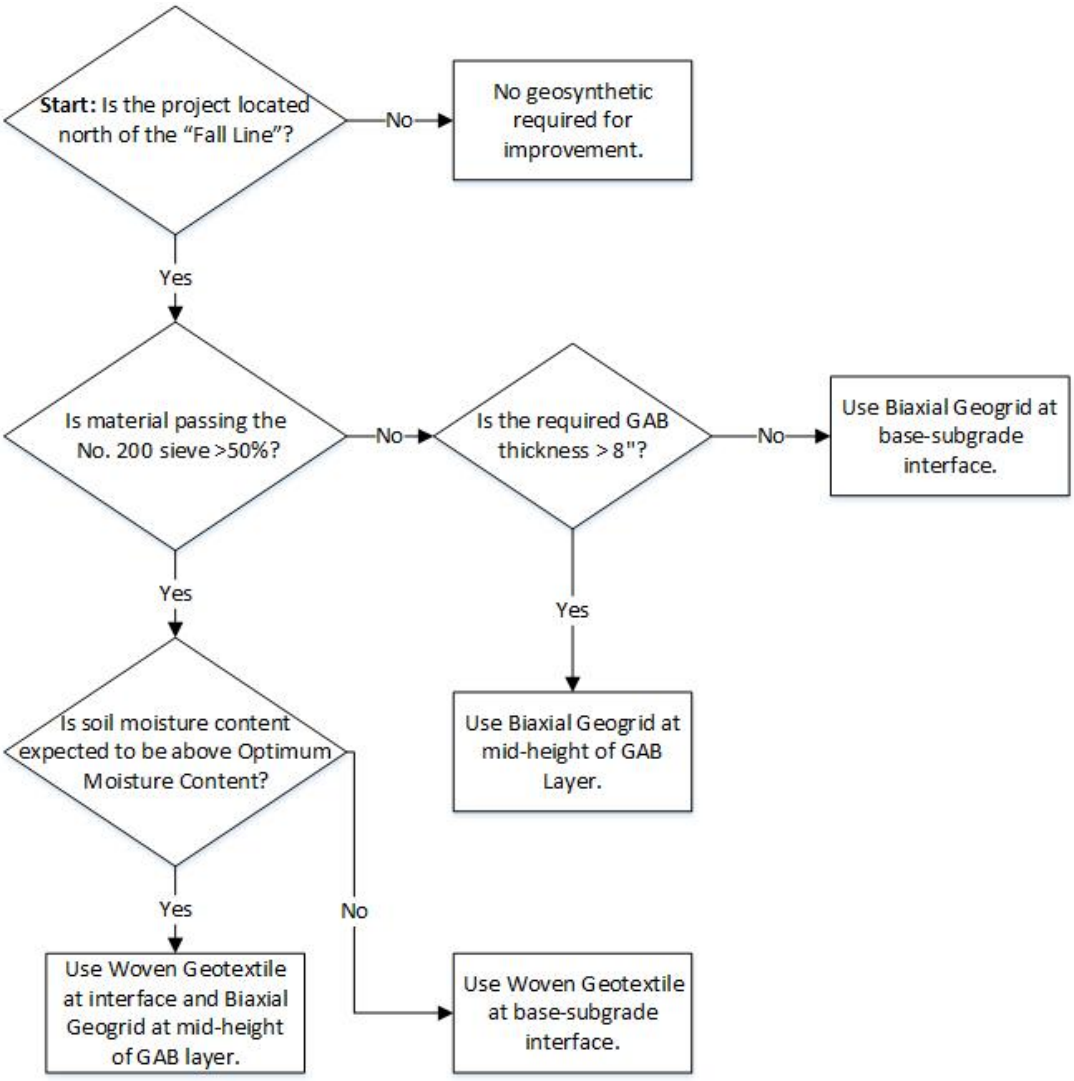

FIGURE A.3

Geosynthetic Selection Decision Flowchart

Geosynthetics must have certain strength and survivability properties to be effective for reinforcement. Table A.1 identifies minimum *geotextile* strength properties, while Table A.2 identifies minimum *geogrid* strength properties. Values are listed for both the machine direction (MD) and the cross-machine direction (CD) in the table. These values are the tensile capacity for the geotextile in the parallel direction of the roadway (MD) and the perpendicular direction of the roadway (CD) and are different due to the manufacturing processes.

TABLE A.1
Geotextile Minimum Strength Requirements

Mechanical Properties	Test Method	Unit	Minimum Average Roll Value	
			MD	CD
Tensile Strength (at Ultimate)	ASTM D4595	lb/ft (kN/m)	2,640 (38.5)	2,460 (35.9)
Tensile Strength (at 2% Strain)	ASTM D4595	lb/ft (kN/m)	504 (7.4)	600 (8.8)
Tensile Strength (at 5% Strain)	ASTM D4595	lb/ft (kN/m)	1,272 (18.6)	1,440 (21.0)
			Minimum Roll Value	
Flow Rate	ASTM D4491	gal/min/ft^2(l/min/m^2)	40 (1,630)	
Permittivity	ASTM D4491	sec^{-1}	0.6	
			Maximum Opening Size	
Apparent Opening Size (AOS)	ASTM D4751	U.S. Sieve (mm)	30 (0.60)	

TABLE A.2
Geogrid Minimum Strength Requirements

Index Properties	Units	Minimum Average Roll Value	
		MD	CD
Tensile Strength @ 2% Strain	lb/ft (kN/m)	410 (6.0)	620 (9.0)
Tensile Strength @ 5% Strain	lb/ft (kN/m)	810 (11.8)	1,340 (19.6)
Ultimate Tensile Strength	lb/ft (kN/m)	1,310 (19.2)	1,970 (28.8)

IV. GEOSYNTHETIC SELECTION EXAMPLE

Definition of Design Example:

A two-lane state highway is scheduled for construction in Gordon County, Georgia. The subgrade is expected to be prepared at optimum moisture content. The top of the subgrade elevation is sufficiently above the ground water table so that high moisture contents are not expected during its design life. A sample of the subgrade is taken and analyzed with a sieve analysis. It is determined that soil is classified as A-7-5, MH, or IIB3 and contains 53% fines.

Selection:

This simplified example problem is planned for Gordon County. Since the location is above the fall line, the selection guide in Figure A.3 is applicable. A sieve analysis found that 53% of the material passed the No. 200 sieve, therefore fines migration is a concern. The next step in the decision flowchart is to determine if the soil moisture content is expected to be above OMC. Because the subgrade is sufficiently above the ground water table, high moisture contents are not expected. After the relevant project properties are input into the selection guide, it is determined that a woven geotextile should be placed at the base–subgrade interface to prevent migration of fines and extend the performance period of the roadway.

V. CONSTRUCTION

Please refer to GDOT Specification Section 457 for Geogrid Reinforcement, and Section 881 for Fabrics.

VI. REFERENCES

GDOT (Georgia Department of Transportation). (2013). Standard Specifications: Construction of Transportation Systems.

GDOT Office of Materials and Research. (2013). Georgia Department of Transportation *Pavement Design Manual*. Atlanta, GA: GDOT.

Holtz, R. D., Christopher, B. R., and Berg, R. R. (2008). *Geosynthetic Design & Construction Guidelines: Reference Manual*. U.S. Department of Transportation, Federal Highway Administration, National Highway Institute.

IDOT Bureau of Bridges and Structures. (2005). *Subgrade Stability Manual*. Retrieved October 16, 2017.

Georgia Humanities and the University of Georgia Press. (2018). "Geologic Regions of Georgia: Overview." Retrieved October 9, 2018, from https://www.georgiaencyclopedia.org/articles/science-medicine/geologic-regions-georgia-overview

GDOT Special Provision 457 – Biaxial Grid Under GAB.

GDOT Special Provision 881 – Fabrics.

APPENDIX B: GDOT SPECIAL PROVISION SECTION 457 GEOGRID REINFORCEMENT

DEPARTMENT OF TRANSPORTATION
STATE OF GEORGIA

SPECIAL PROVISION

PROJECT No.
P. I. NO.

SECTION 457 – GEOGRID REINFORCMENT

457.1 Description

This Work consists of placing geogrid reinforcement under new embankments at the locations and to the elevations or depths indicated on the Plans or as directed by the Engineer.

457.2 Materials

Use geogrid materials that meet the requirements of Special Provision Section 809– Geogrid Materials.

457.3 Construction

Place the geogrid reinforcement in accordance with the following requirements:

1. Preparation For Placement:

    a. Clearing and Grubbing: Clear and grub the areas of the proposed reinforcement in accordance with the applicable portions of Section 201.

    b. Embankments: Construct embankments in accordance with the applicable sections of Section 208.

2. Placement of Geogrids: Place geogrids in a manner and at the locations shown on the Plans. Place the geogrids level or sloping away from the existing embankment at an inclination that is no greater than 5°. Spread the geogrids out free of wrinkles, bends or undulation and hold the geogrids taut by stakes or other mechanical means while the embankment material is being placed.

3. Fill Placement Over Geogrid: Place fill over the geogrid in accordance with the Plans and applicable portions of Section 208. Maintain at least 4-inch (102 mm) of soil between the grid and any rubber-tired construction equipment. Maintain at least 8-inch (203 mm) of soil between the grid and any track construction equipment.

4. Degree of Compaction: Compact embankment fills to at least 100 percent of the maximum laboratory dry density for the full depth of the embankment, unless otherwise specified. The Engineer may adjust compaction requirements for initial lifts of fill over unstable soils until a stable mat is formed. Determine the maximum laboratory dry density and in place density of the compacted fill in accordance with Sub-Section 208.3.05.B.2.

5. Joints or Splices: Place grids in continuous strips in the direction of main reinforcement. Do not use joints or splices in the machine direction unless the joint or splice can be shown by laboratory tests to carry 100% of the required ultimate tensile strength of the grid.

6. Damaged Material: Remove any geogrid material damaged in shipping, storage or placement from the project and replace it at no additional expense to the Department.

457.4 Measurement

Geogrid reinforcement is measured for payment in square yards (meters) of accepted geogrid materials in place for Type B. Measurement is to the nearest square yard (meters).

457.5 Payment

Geogrid reinforcement is paid for at the Contract Price per square yard (meters), for geogrid Type B, complete and in place. Payment is full compensation for furnishing materials, placing materials, and for all labor, equipment, tools and incidentals necessary to perform the Work.

Payment for work under Section 457 will be made under:

Item No. 457-1010. Geogrid Reinforcement, Type B……. Per Square Yard (Meters)

APPENDIX C: GDOT SPECIAL PROVISION SECTION 881 FABRICS

DEPARTMENT OF TRANSPORTATION
STATE OF GEORGIA

SPECIAL PROVISION

PROJECT NO. ,County
P.I. NO.

SECTION 881 – FABRICS

Add the following to Sub-Section 881.2.05A:

Use woven filter fabric for embankment stabilization. Sew fabric with a lock stitch using high strength polypropylene or nylon thread. Obtain approval of the stitch and sewing method from the Engineer prior to use.

Delete Sub-Section 881.2.05.A.4 as written and substitute the following:

Use filter fabric for embankment stabilization with the following minimum tensile strength requirements:

Fabric Type	**Tensile Strengths in lb./in.(kN/m) width**			
	Warp Direction		**Fill Direction**	
	5% Strain	**Ultimate**	**5% Strain**	**Ultimate**

Polyester				
Polypropylene				

Minimum Seam Strength = lb./in. (kN/m) width

The ultimate strengths shown are based on reduction factors of 0.4 for polyester and 0.25 for polypropylene from the tensile strengths at 5% strain. The use of reduction factors other than those shown will be allowed only if verified by laboratory tests acceptable to the Department.

Delete Sub-Section 881.2.05.A.6. in its entirety.

Delete Sub-Section 881.2.05.C as written and substitute the following:

Test the filter fabric using the following methods:

Tensile Strength, Elongation	ASTM D-4595 Wide Strip Test
Seam Strength	ASTM D-4884 Wide Strip Test

Run the tests at a strain rate of 10% per minute. Use a pre-tensioning load of 10 pounds per inch (1.75 kN/m) or 3%, whichever is less.

Supply a certification from the manufacturer showing the physical properties of the fabric used and conformance with the Specification in accordance with Sub-Section 106.05 of the current Specifications.